



**INDIAN INSTITUTE OF TECHNOLOGY, GUWAHATI**  
North Guwahati, Guwahati - 781031

---

### Certificate

It is certified that the work contained in the thesis entitled "OXIDATIVE TRANSFORMATIONS OF SOME ACTIVATED AROMATIC COMPOUNDS MEDIATED BY COBALT(II) AND COPPER(II) COMPLEXES", by Amrit Puzari, a student in the department of Chemistry, Indian Institute of Technology, Guwahati for the award of the degree of Doctor of Philosophy has been carried out under my supervision and that this work has not been submitted for any other degree or diploma anywhere else.

Date:

Dr. JUBARAJ BIKASH BARUAH

Associate Professor  
Department of Chemistry  
IIT - Guwahati



## ACKNOWLEDGEMENT

At the very outset I would like to take the opportunity to express my heartiest gratitude to Dr. Jubaraj Bikash Baruah, my research supervisor. It is due to his endeavour, guidance and invaluable criticism which lead to a successful completion of the thesis. I would also like to acknowledge with honour the kind pursuance of all the faculty members of the Department of Chemistry as well as Dr. A. Srinivasan of the Department of Physics, IIT Guwahati. I am grateful to Director, I.I.T. Guwahati and Head, Department of Chemistry for their kind permission to carryout research work.

I sincerely acknowledge Prof. K. Osakada of Tokyo Institute of Technology, Japan for the GPC analysis ; CDRI, Lucknow for the elemental analysis ; RSIC, Madras for the esr spectra, S. I. F. Bangalore for NMR spectra and Prof. P. Balaraman of Indian Institute of Science, Bangalore for the MALDI spectra. Additionally I would also like to acknowledge Council of Scientific and Industrial Research, New Delhi for financial support.

I also acknowledge the research scholars of the Department of Chemistry and other fellow friends as well as the staff members of our Department and Department of Physics for their suggestions and help. Finally I take pride in expressing my gratitude to my parents and to my wife for their encouragement and support.

I.I.T.Guwahati.

Amrit Puzari

September 2001



# Contents

ACKNOWLEDGEMENT	ii
ABSTRACT	iii
<b>1. INTRODUCTION</b>	
1.1 General Introduction .....	1
1.2 Classification of oxidation reactions.....	2
1.2.1 Classification based on phase.....	3
1.2.2 Classification based on products.....	4
1.2.2(a) Dehydrogenation .....	4
1.2.2(b) Epoxidation reactions.....	6
1.2.2(c) Hydroxylation reaction.....	9
1.2.2(d) Oxidative coupling reaction.....	12
1.2.2(e) Oxidative addition reaction.....	17
1.2.2(f) Oxygenation reaction.....	18
1.2.3 Classification based on stoichiometry.....	19
1.2.4 Bio-chemical oxidation.....	19
1.3 Metal catalysed oxidation reactions.....	28

1.4 Classification based on the method of oxidation.....	42
CONTENTS	
<hr/>	
1.4.1 Electrochemical oxidation.....	42
1.4.2 Photochemical oxidation.....	44
1.5 Scope of the study.....	45
<b>2. COBALT CATALYSED OXIDATIVE REACTIONS</b>	
2.1 Background.....	47
2.2 Synthesis and characterization of cobalt-dionemoxime complexes.....	50
2.3 Oxidative reactions of 2.V and 2.VI with aromatic compounds...	58
2.3.1 Oxidation of toluene.....	59
2.3.2 Reactions of phenols.....	61
2.3.3 Oxidative polymerisation of aniline .....	82
2.3.4 Reactions of diaminobenzenes.....	90
2.4 Mechanistic study of the reactions.....	95
2.4.1 Recycling of oxygen from hydrogen peroxide during cobalt catalysed oxidative reactions.....	95
2.4.2 Kinetic of the oxidation reactions by visible spectroscopy.....	99
2.4.3 Study on metal content and ESR studies of the oligomers....	103
2.5 Electrical properties of the oligomer.....	106
2.6 Electrochemical properties of the oligomers.....	109

2.7 Experimental.....	111
2.7.1 General.....	111
2.7.2 Reagent and starting material.....	116

## CONTENTS

---

### **3. COPPER(II) CATALYSED REACTIONS OF ACTIVATED AROMATICS WITH HYDROGEN PEROXIDE**

3.1 Background.....	124
3.2 Hydroxylation of phenols.....	127
3.3 Oligomerisation of aniline and 1,4-phenylenediamine.....	132
3.4 Quinhydrone from hydroquinone.....	142
3.5 Oxidative reactions of oxime.....	142
3.6 UV-visible study on the reactions of phenol with <i>cis</i> -bis glycinato copper(II) monohydrate.....	143
3.7 Attempted reaction on copper tyrosinato complex.....	146
3.8 Mechanism of <i>cis</i> -bis glycinato copper(II) catalysed oxidative reactions.....	148
3.9 Electrical and thermal properties of hydroquinone aggregate, polyaniline and related compounds.....	152
3.10 Comparison of copper(II) and cobalt(II) catalysed oxidation reactions.....	161

3.11 Experimental.....	162
<b>REFERENCES .....</b>	<b>172</b>

**OXIDATIVE TRANSFORMATIONS OF SOME  
ACTIVATED AROMATIC COMPOUNDS MEDIATED BY  
COBALT(II) AND COPPER(II) COMPLEXES**

*By*

AMRIT PUZARI



**DEPARTMENT OF CHEMISTRY**  
**INDIAN INSTITUTE OF TECHNOLOGY, GUWAHATI**  
**AUGUST, 2001**

**OXIDATIVE TRANSFORMATIONS OF SOME ACTIVATED  
AROMATIC COMPOUNDS MEDIATED BY COBALT(II) AND  
COPPER(II) COMPLEXES**

A thesis submitted  
for the award of the degree of  
DOCTOR OF PHILOSOPHY

*By*

AMRIT PUZARI

*to the*

DEPARTMENT OF CHEMISTRY  
INDIAN INSTITUTE OF TECHNOLOGY, GUWAHATI  
AUGUST , 2001



# CHAPTER 1

## INTRODUCTION

### 1.1 General Introduction

The elimination of hydrogen from inorganic or organic substrate/s, replacement of hydrogen atom from a C-H bond with a more electronegative element in a chemical reaction is referred as oxidation reaction<sup>1</sup>. The oxidation reactions are one those involve loss of electron/s. The substrate losing the electron/s gets oxidised and the reagent causing oxidation is called as an oxidant or an oxidising agent.

Before the advent of sophisticated spectroscopic techniques the oxidation reactions were used as one of the tool for structure elucidation of organic molecules. Such procedure for structure elucidation included degradation of an organic compound into small molecules. The small molecules thus formed by oxidative degradation are comparatively easy to characterise. When sufficient evidence has been accumulated from the information of the degraded products, a tentative structure that fits to the facts is accepted. These degradative oxidations had been the most powerful tool for structure elucidation of many natural products such as terpenoids.

Some of the usual oxidizing agents used for these purpose are ozone, permanganates, chromates and hypobromides etc. An illustrative example of such a structure illucidation is of monoterpenoid myrcene<sup>2</sup>. Myrcene is a monoterpenoid having structure shown as **(1)**. The ozonolysis of myrcene **(1)** gives acetone, formaldehyde and a ketodialdehyde**(2)** (scheme1.1). The

ketodialdehyde **(2)** on further oxidation with chromic acid gives ketoglutaric acid and carbon dioxide. These oxidative degradation processes can be explained by the structure**(1)** (scheme 1.1). However, due to the easy access to more accurate spectroscopic techniques, in recent days such processes are of seldom in use.

### **1.2 Classification of oxidation reactions**

The oxidation reactions can be classified into number of broad categories based on the substrates, products, reagents, mechanism of oxidation etc. A schematic representation of such classification of organic oxidation reactions is shown in scheme 1.2. It is important to note that the classification of such a crucial and important reaction to delineate each reaction is difficult.

There is overlapping between different classification. For example when we refer to the classification based on mechanism the reaction may fall in the category of the classification based on products. On the otherhand a

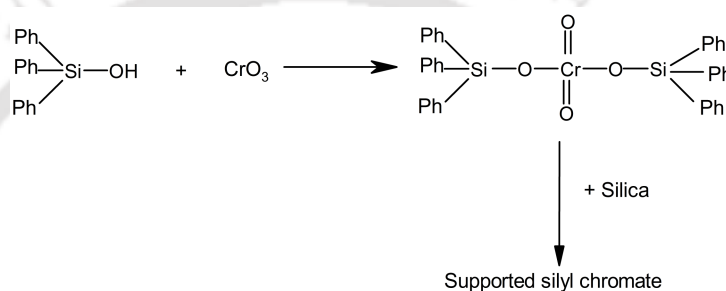


photochemical oxidation reaction or an electrochemical reaction may be homogeneous or heterogeneous.

### **1.2.1 Classification based on phase**

Based on the number of phases involved in an oxidation reactions, they can be broadly classified into three categories<sup>3</sup>. They are homogeneous, heterogeneous and phase transfer oxidation reactions. As the name implies, the homogeneous oxidation means an oxidation reaction/s carried out in one phase. In heterogeneous reactions the reactions are carried out in more than one phase<sup>4</sup>. The phase transfer reactions involve multiple phases, and in order to make uniform distribution over the two phases mediator/s are also used<sup>5</sup>.

Based on the nature of the phases involved there is another class of oxidation reaction i.e. oxidation reaction in a micelle. Homogeneous oxidations are commonly used in oxidation reactions and these reactions ensure repeatability and are versatile. Heterogeneous reactions give ways for easy separation of products and cause selective transformations. The oxidizing agents can be modified by polymer supports. Highly efficient modified



Scheme 1.3

reagents are developed of which chromates are one of the best examples<sup>6</sup>

(Scheme 1.3). Chromium pillared montmorillonite is a catalyst used in selective oxidation of alcohols<sup>7</sup>.

### 1.2.2 Classification based on products

Oxidation reactions can also be classified on the basis of the product formed from an oxidation reaction. This classification includes dehydrogenation reactions, epoxidation reactions, hydroxylation reactions, oxidative coupling reactions, oxygenation reactions, oxidative addition

reactions etc. Each of these reactions is discussed under separate sub-headings.

### **1.2.2(a) Dehydrogenation reaction**

As the name signifies, dehydrogenation reaction is the elimination of hydrogen atoms from a substrate molecule. The reactions may be stoichiometric or catalytic. It may also occur in a biological system with the help of an enzyme.

Dehydrogenation reactions are well studied in heterogeneous conditions. Absorption of alkane molecules on metal surfaces used as catalyst gives alkyl radicals<sup>8</sup>. Such radicals on subsequent desorption at high temperature leads to the dehydrogenation of alkanes. Dehydrocyclisation of long chain alkanes such as C<sub>6</sub>-alkanes leads to aromatic hydrocarbons<sup>8</sup>. Silver is generally employed as the catalyst for the production of formaldehyde from methanol by dehydrogenation<sup>9</sup> (Equation 1.1). Dehydrogenation of cholesterol with selenium as catalyst

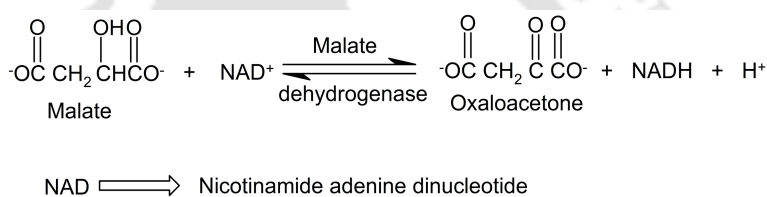
at 250°C gives chrysene(3)<sup>10</sup> (equation 1.2). In this reaction the hydrogen is removed as hydrogen selenide and skeletal rearrangement takes place.

The above example shows that carbon atoms may be removed from a complex molecule during such reactions. Particularly the angular methyl groups are degraded in the reaction depicted in equation 1.2. Platinum, iridium, palladium complexes are commonly used in catalytic



reactions<sup>8</sup>. Enzymes that are capable of catalysing oxidation reactions by removal of hydrogen from substrates are called dehydrogenase.

Enzymatic dehydrogenation of fatty acids takes place in the presence of dioxygen and such reactions are stereospecific. For example malate dehydrogenase catalyses the dehydrogenation of malate compounds to oxalacetone<sup>10</sup> (equation 1.3).



Equation 1.3

### 1.2.2(b) Epoxidation reactions

Oxidation of alkene with peroxyacid gives epoxides (oxiranes). However, if proper precautions are not taken the epoxide/s formed may be converted to monoacyl derivatives of 1,2-diol. The best reagent for preparation of epoxide is *m*-chloroperbenzoic acid<sup>11</sup>. The *m*-chloroperbenzoic acid is thermally stable than other peroxy acids. Epoxidation with *m*-chloroperbenzoic acid are highly stereoselective and the addition generally takes place *cis* to the double bond of the alkene. Besides peroxyacids, other

reagents like  $t$ -butylhydroperoxide in the presence of molybdenum or vanadium catalyst causes selective epoxidation. Jacobsen epoxidation is an important method for asymmetric oxidation of unfunctionalised olefins (equation 1.4)<sup>12</sup>. Best results on selectivities are obtained with the reaction of *cis* disubstituted alkenes. High enantioselectivity of the reactions is the most important feature of Jacobsen's epoxidation. Polymer bound chiral cobalt (salen) complexes<sup>13</sup> (where salen is schiff base of the condensation product of salicylaldehyde with ethylenediamine) are found to be more effective in selectivity. Incorporation of the salen ligands in a heterogeneous support like zeolites, clays as a mean to recycle the chiral catalyst were found to be successful in the case of asymmetric epoxidation<sup>14</sup>.

It is observed that the

oxidising power of the oxidant can be enhanced by adding additives. One such example is the addition of an N-oxide to *m*-chloroperbenzoic acid in epoxidation reaction. Out of the different compositions of N-oxide and peracids, *m*-chloroperbenzoic acid and N-methylmorpholine N-oxide as additive has shown to be highly enantioselective (scheme 1.4). Recently epoxidation reactions carried out with manganese(III) salen complexes as catalyst<sup>15</sup> has shown enantiomeric excess in the product epoxide. The titanium alkoxide are good catalyst for epoxidation reactions.

The composition of catalytic precursor in titanium catalysed epoxidation reaction plays an important role in asymmetric epoxidation of allylic alcohols. The appropriate ratios of titanium, ethyltartrate and water have been used in making enantioselective oxidation of a number of



thioethers<sup>16</sup>. In all these cases ee diastereomers were the predominant products (equation 1.5)

When such reaction is carried out with allylic alcohol by catalyst generated *in situ* from titanium tetraisopropoxide, (+) or (-) diethyltartrate

and *tert*-butyl hydroperoxide<sup>17</sup>. The asymmetric epoxidation of allylic alcohols results in high enantiomeric excess (>90%ee) The most notable feature of this asymmetric epoxidation is high asymmetric induction.

Irrespective of the nature of the substrate enantiomer the method gives the epoxide oxygen on the same enantiomeric face of the olefin. Although these are few important reactions large number of such epoxidation reaction are emerging everyday<sup>18</sup>. However in most cases the focus is on the look for selectivity and efficient catalyst systems.

### 1.2.2(c) Hydroxylation reaction


As the name implies in hydroxylation reaction a saturated or an unsaturated compound gets hydroxylated. The nature of the products from such reactions depends on the nature of the reagent/s used. The reaction of ferrous ion along with hydrogen peroxide on saturated hydrocarbons to give alcohols is of historic importance. This reaction has opened up the scope for metal catalysed hydroxylation reactions having close analogy to biological

systems<sup>19</sup>. For example when ferrous sulphate and hydrogen peroxide is used as oxidant of *t*-butylalcohol it produces 2,5-dimethyl 2,5-hexanediol, while the same reaction in the presence of small amount of copper(II) ion leads to 2-methyl propanediol through hydroxylation. The

role of copper(II) in the later case is to intercept the resulting radical to give C-C bonded products.<sup>20</sup> (scheme 1.5).

Hydroxylation reactions on C-H bonded compounds to give C-OH bond can be carried out by enzyme catalyst<sup>21</sup>. Such reactions proceed with high rate at low temperature. These types of reactions are discussed in details in section 1.2.4.

Other classes of synthetically important hydroxylation reactions include dihydroxylation and aminohydroxylation reactions. Enantioselective dihydroxylation of organic compounds by osmium complexes introduced a new direction in the field of asymmetric synthesis<sup>22</sup>. The asymmetric dihydroxylation of olefins in the presence of cinchona alkaloid derivatives by osmium complexes have proved to be a reliable method in asymmetric synthesis. Few successful ligands<sup>23</sup> for specific enantioselectivities used for almost all olefins are shown in figure 1.1.



Similarly asymmetric aminohydroxylation of olefin using osmium catalyst and dihydroquininyl-phthalazine or dihydroquinidinyl-phthalazine as ligand is highly enantioselective and it produces ee-diastereomer as the major product (equation 1.6 )<sup>24</sup>. In the absence of a ligand such osmium

catalysed reaction major product is dihydroxylation and minor product is aminohydroxylated product. In such case the regioselectivity of the reaction also decreases. Thus, the success of this reaction is sensitive to the design of suitable ligand environment capable of performing aminohydroxylation.

#### **1.2.2 (d) Oxidative coupling reaction**

Oxidative coupling reactions have significant relevance in synthetic chemistry as they can be used to synthesise conjugated diynes, disubstituted ethynes, conjugated polynes etc. Conjugated polynes have received much attention since they are found in many natural products particularly in antifungal agents. Fungal diseases cannot be ignored and the observed infection with mycoses draws more attention towards improvement of the chemistry of antifungal agents<sup>25</sup>. Oxidative C-C and C-O coupling reactions lead to the formation of many important natural products. Many structurally complex molecules such as glycopeptide

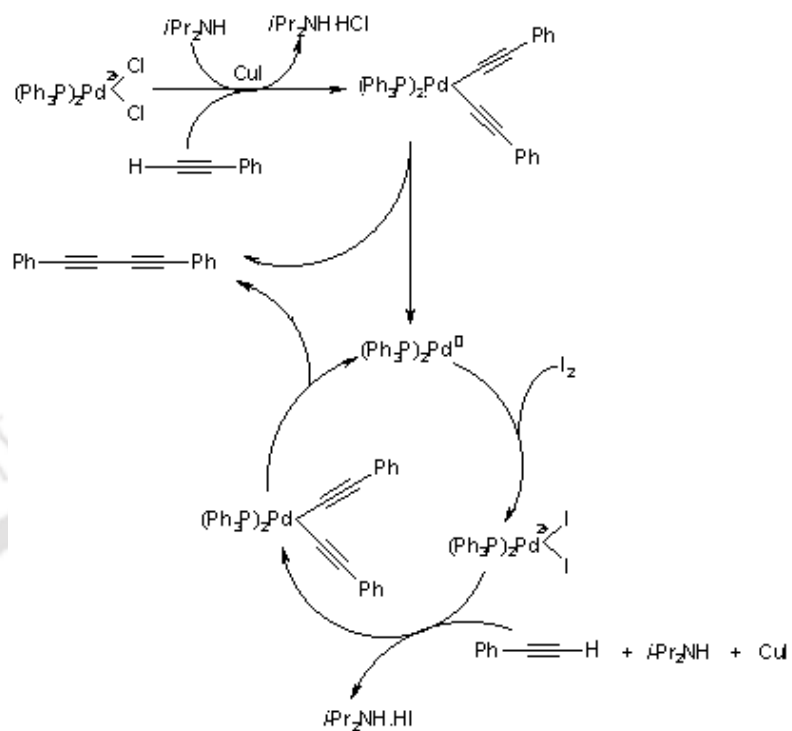
antibiotics, cyclic peptides are biosynthesised by enzyme catalysed C-O and C-C bond formation<sup>26</sup>.

Synthetic transformations of terminal alkynes mostly involve intermolecular and intramolecular homo and hetero coupling reactions between their *sp*-carbon centers, leading to butadiyne or acetylinic derivatives. Oxidative homocoupling (equation 1.7) and heterocoupling reactions of a terminal alkyne with a haloalkyne (equation 1.8 and equation 1.9) are the two most widely used systems. Other methods for the synthesis of butadiynes and polyalkynes using organometallic alkynide derivatives are also available<sup>27</sup>. A good number of natural products have been known to synthesise by oxidative coupling reactions of terminal alkynes, followed by stereo and regioselective addition of hydrogen or organometallic

reagents<sup>28</sup>. The coupling reaction between alkyne Grignard derivatives and 1-haloalkynes using copper(I) and cobalt(I) salts are well established. As catalyst organocopper reagents are found to be most effective for alkynides formation. In these reactions the generation of alkynylcopper species by transmetalation of an alkynyl group to copper is considered to be a key step. Subsequent oxidative dimerisation gives the corresponding 1,3-butadiynes<sup>29</sup>.

The transition-metal catalysed cross-coupling reactions of organometallics with organic halides provide important methods for selective carbon-carbon bond formation<sup>30</sup>. Such processes may involve multiple redox cycles. The redox cycles can only be metal centered or metal centered coupled to an organic redox process. The oxidative coupling reaction of Grignard reagents by palladium catalyst in the presence of N-substituted isocyanide dichloride<sup>27</sup> (equation 1.10) is an example where multiple redox cycles are involved.

In this reaction the isocyanide dichloride serves as a reoxidant of the palladium catalyst via a catalytic cycle<sup>31</sup>. The oxidative coupling of phenylacetylene by a palladium–copper catalyst in the presence of 4-iodo-(3H)-phenothiazin-3-one<sup>32</sup> gives diynes. This is also another example of a reaction that involves multiple redox cycles. The synthesis of symmetrical conjugated diynes can also be performed by the reaction of 1-alkynes with iodine in diisopropylamine in the presence of catalytic amount of *bis*-triphenylphosphine palladium(II) chloride and cuprous iodide<sup>33</sup>. The reaction pathway involved in this case can be represented as shown in the scheme 1.6. The reaction of arylalkynes with triethylamine and chloroacetone



Scheme 1.6

using a mixture of *tetrakis*-triphenylphosphinepalladium(0) and cuprous iodide as catalyst in benzene gives 1,4-diarylbutadiynes<sup>34</sup> (equation 1.11)

Organosilicon compounds such as vinyl, ethynyl and allylsilanes

react via oxidative coupling reaction with organic halides like aryl, vinyl and allylhalides in the presence of tris(diethylamino)sulfonium difluoro trimethylsilicate and allylpalladium chloride dimer as a catalyst to give the corresponding coupled products. These compounds are formed in high yields in stereospecific and chemoselective manner<sup>35</sup> (equation 1.12). In this

reaction

the side products from homocoupling are also less.

The oxidative homocoupling reactions of alkynylsilanes with cuprous chloride in a polar solvent such as dimethylformamide under

aerobic condition leads to conjugated diynes and disubstituted ethynes in good yield equation 1.13

The unsymmetrical diarylethyne are synthesised from the cross coupling reaction of (arylethynyl)trimethylsilanes with aryltriflates or chlorides by the use of palladium(0) catalyst with copper(I) from such reactions. The reaction proceeds via transmetallation of the alkynyl group from silicon to copper followed by oxidative dimerisation leading to the diyne<sup>36</sup>.

Oxidative coupling reactions phenolic compounds could lead to carbon-oxygen or carbon-carbon bond formation. Different peroxidase enzymes can act as catalyst in these transformations. Peroxidase catalyses coupling reactions of various tyrosine and hydroxyphenyl glycine derivatives. Such synthetic methodology is extended to the synthesis of antibiotic such as vancomycin (equation 1.14)<sup>37</sup>. The research work included in this thesis embodies the results on oxidative coupling reactions of phenolic and anilinic compounds by copper(II) and cobalt(II) complexes.

The potential of oxidative coupling reactions are highlighted in a separate section as well as in the introductory part of other chapters. The copper,

cobalt and vanadium catalysts are important in oxidative coupling reaction of activated aromatic compounds and also have interesting material properties. Vanadium pentoxide is one important reagent that is capable of effecting these transformations<sup>38</sup>.

#### **1.2.2(e) Oxidative addition reaction**

Oxidative addition reaction implies the oxidation of a metal center associated with an increase in its coordination number via addition of the substrate. Conventionally, irrespective of the reaction mechanism a two equivalent of change in the oxidation state of the metal center is attributed

to an oxidative addition reaction. In cases where oxidative addition implies one equivalent change of the oxidation state then a radical is supposed to be involved. Both the cases are depicted by the equation 1.15 and equation 1.16.

The oxidative addition forms a larger portion of organometallic chemistry and metal mediated organic synthesis. The scope of such reactions is vast and large number of literature is available in the form of text or reviews<sup>39</sup> so the illustrations are minimized under these category of reactions.

#### **1.2.2(f) Oxygenation reaction**

This category of the reactions concerns with insertion of an oxygen atom from an oxidant to a substrates. One such reaction leading to selective product is the ring expansion of cyclopentanone with an oxidant<sup>40</sup> (equation 1.17).

### **1.2.3 Classification based on stoichiometry**

The classification of oxidation reaction can also be made on the basis of the stoichiometry of the oxidant used in an oxidation reaction. Stoichiometric as well as catalytic oxidation reactions with oxidants like peroxyacids, ozone, molecular oxygen, metal ion etc. are well documented and many examples are included in earlier sections and no further discussion is made.

### **1.2.4 Bio-chemical oxidation**

Oxidation is a principal process involved in biological systems<sup>41</sup>. In a broad sense bio-oxidations can be enzymatic or nonenzymatic. The oxygen carrier proteins such as hemoglobin and myoglobin are built around iron(II) and constitutes a most important aspect in biochemical process. Hemoglobin binds to oxygen through its iron atom and transport oxygen from lungs to the muscles where it is delivered to myoglobin. Myoglobin

stores the oxygen unless it is required for metabolic action. Both the protein contains the heme group through co-ordinated histidine nitrogen. The iron porphyrin complex gets oxidised reversibly by molecular oxygen to give a stable product that cannot function as an oxygen carrier. However, the presence of polypeptide alters the situation and it can function as a carrier of oxygen. The position *trans* to the histidine N-atom is occupied by O<sub>2</sub> in the oxygenated species. The introduction of oxygen causes a change in the oxidation state of the iron present in the heme. This in turn causes important change in the structure of the heme. All oxygen carriers containing iron are found inside the cells; whereas those containing copper are found in the extracellular fluid. This is probably due to favourable reducing environment for iron(II) inside the cell environment. Furthermore cells provide porphyrin rings as ligand which can form non-labile iron(II) complexes.

The biological function of cobalt ion can be exemplified by considering the vitamin B<sub>12</sub> molecule<sup>42</sup>. The macrocyclic ligand present in vitamin-B<sub>12</sub> is called the corrin ring. Vitamin B<sub>12</sub> is also known as cyanocobalamin and it has the cobalt in the (+3) oxidation state. The B<sub>12</sub> coenzyme is associated with a number of enzymes. Diol dehydrase is one such example which catalyses the reactions as shown in scheme 1.7.

More discussion on the role of vitamin B<sub>12</sub> is exemplified in the chapter 2 of the thesis.

The cyanide ligand is not present in any of the active form of the vitamin. In the biological system active form contains the ligand which is likely to be H<sub>2</sub>O. Model compounds of vitamin B<sub>12</sub> the cobalamin can be reduced in neutral or alkaline solution to give Co(II) and Co(I) species known as B<sub>12r</sub> and B<sub>12s</sub> respectively<sup>43</sup>. Vitamin B<sub>12</sub> can also

participate in nonenzymatic oxidations. The cobalt centres in vitamin B<sub>12</sub> effects C-C bond formation and many oxidation reactions.

Horseradish peroxidase is an enzyme that catalyzes the enzymatic synthesis of polyphenols by oxidative polymerization of various phenol derivatives<sup>44</sup>. Horseradish peroxidase is also able to catalyze the oxidation of a wide range of compounds including aromatic amines and phenols in the presence of hydrogenperoxide to generate the corresponding free radical. Similarly the oxidative polymerization of *o*-phenylenediamine is catalyzed by the enzyme horseradish peroxidase. It produces a soluble polymer having an iminophenyl unit (equation 1.18) which is difficult to obtain by conventional oxidative polymerization.

Galactose oxidase is a fungal enzyme that contains a monocopper active site (scheme 1.8)<sup>45</sup>. This enzyme causes two-electron oxidation of primary alcohols to aldehyde<sup>46</sup>. Organic free radicals proximate to a copper(II) is responsible for these oxidation. The scheme shows the one

electron oxidation process that occurs via an initial hydrogen abstraction by the tyrosil radical. The authors do not rule out the two electrons oxidation by molecular oxygen along with one electron oxidation.

Lignin is a biological component of wood tissue having a macromolecular framework formed. Laccase is another enzyme that

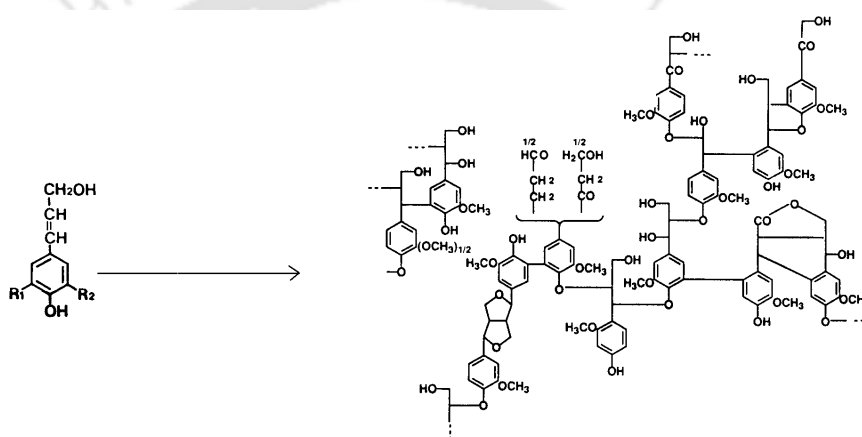


contains copper converts coniferyl alcohol to lignin<sup>47</sup> (equation 1.19)

Lignin formation takes place in a relatively uncontrolled manner through radical formation, which is formed from coniferyl alcohol. The oxidative

polymerization of sinapilalcohol and cumarol are catalysed by metalloenzymes such as laccase, peroxidase.

Many biological systems are able to hydroxylate non activated carbon hydrogen bonds. Thus monooxygenases containing the cytochrome P-450 can cause selective hydroxylation of aromatics. The hydroxylation



where  $R_1 = H$ ,  $R_2 = -OCH_3$

Equation 1.19

reactions of unactivated C-H bonds are catalysed by  $\alpha$ -ketoglutarate-dioxygenases. In biological systems hydroxylation reactions occurs in tissues, liver, kidney, lung etc. Such reactions convert the foreign compounds by hydroxylation followed by oxidative means into products.

In the oxidation of alkanes and fatty acids in the presence of mammalian liver microsome the hydroxylation of a terminal carbon atom occurs. Besides this the neighbouring C-H bond to the terminal carbon atom also undergoes hydroxylation. In the hydroxylation reaction of decanoic acid in the microsomes of rat's liver the major product is 10-hydroxydecanoic acid<sup>48</sup>, however, a minor amount of the 9-hydroxydecanoic acid is also formed in this reaction (equation 1.20)

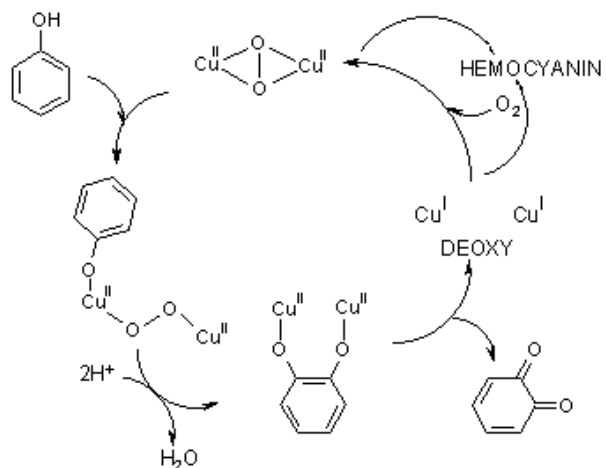
Among these transformations the hydroxylation of saturated hydrocarbons by nicotinamide adenine dinucleotide phosphate dihydride (NADPH) follows the route shown in scheme 1.9<sup>21</sup>.

Enzymes participating in these oxidation processes generally involve a metal ion. The fact of metal ion participation in most enzyme systems, which hydroxylate organic compounds, persuaded chemists to look for analogous chemical systems. The crystallographic data for a P450 enzyme that hydroxylates camphor show that the camphore is bound to protein in close proximity to the metal center<sup>49</sup>. In protein free biomimetic model studies catalytic systems have been devised using both metalloporphyrin and nonporphyrin complexes. The complication arises in these O<sub>2</sub> –oxidations in the presence of competing, direct redox reactions between the O<sub>2</sub> and /or the oxo species, with the co-reductant. Biomimetic studies using ruthenium complexes with O<sub>2</sub> provide new catalytic, selective oxidation systems that operate via nonradical- initiated pathways and

requires direct reaction between the complex and O<sub>2</sub>. Some ruthenium (III) ethylenediaminetetraacetic acid<sup>50</sup> complexes have been used to catalyse the O<sub>2</sub>-oxidation reactions such as cyclohexene to epoxides, cyclohexane to cyclohexanol, cyclohexanol to cyclohexanone and ascorbic acid.

The enzyme tyrosinase has a coupled dinuclear active site of copper(II) and this site is similar to the one found in hemocyanins<sup>51</sup>. The interaction of the metal site of tyrosinase with molecular oxygen forms a new species known as oxy-tyrosinase. A phenol molecule could bind to oxy-tyrosinase in an axial fashion and rearrangement of the substrate complex formed through a trigonal bipyramidal form results in hydroxylation at the ortho position of the phenol followed by loss of water. Further to this the hydroxylated diphenol co-ordinates to the metal center as shown in scheme 1.10. Such a catecholate dicopper(II) complex is known in model systems also<sup>52</sup>.

Cytochrome-C-oxidase is an enzyme which contains copper(II) and causes oxidation reactions. The structural and functional characteristic of copper centre present in most cytochrome-C-oxidase, plays a key role in



Scheme 1.10

respiratory bioenergetics<sup>53</sup>. Another copper containing enzyme tyrosinase has coupled binuclear copper(II) active site<sup>54</sup>. Tyrosinase catalyses *ortho*-hydroxylation of phenol. It also causes two electrons oxidation of *o*-diphenols to *o*-quinones (equation 1.21 and equation 1.22).

Bromoperoxidase is an important enzyme capable of converting aromatic and nonaromatic substrate to bromo derivatives. Vanadium bromoperoxidase (V-BrPO) is one such enzyme that catalyzes the bromination of numerous organic substrates including phenol in presence of hydrogen peroxide<sup>55</sup>. Efficiency of the catalytic process of bromination with V-BrPO is enhanced by the presence of a halide particularly chloride or bromide. Spectroscopic studies indicated that in the process presumably hydrogen peroxide coordinates first to vanadium(V) as a ligand followed by bromide oxidation( scheme 1.11 ). It has also been asserted that vanadium functions here as a lewis acid catalyst by coordinating to hydrogen peroxide without changing its oxidation state which could then oxidise bromide ion.

Scheme 1.11

Manganese peroxidases are somewhat larger heme proteins and can compete the conventional peroxidase cycle but preferentially use Mn(II) as the substrate<sup>56</sup>. Manganese peroxidases oxidise  $\text{Mn}^{2+}$  to  $\text{Mn}^{3+}$  that is stabilized by organic acids such as oxalate, malate, lactate and malonate by chelating the oxidised manganese ion. The chelated  $\text{Mn}^{3+}$  can oxidise phenolic substrates to phenoxyl radicals and also some other organic substrates. A schematic representation of such oxidation is given in scheme 1.12.

### 1.3 Metal catalysed oxidation reactions

The role of metal in oxidation reaction is a subject that cannot separately discussed without overlapping with the earlier discussion. However, a few reactions to illustrate the importance of such reaction is discussed in this portion. The organic oxidation reactions can be effected by metal ions of which the transition metal ions are frequently encountered. This is due to the fact that the reactions are catalyzed by the transition metal complexes and have the special features like regio- and stereo- selectivity. It has been observed that highly regioselective oxidation of C-H bond can be achieved by anchoring the substrate with a metal through complexation. Such selectivities are demonstrated in the case of compounds such as

tetrahydro-2-naphthol and 4-aminomethyl cyclohexylmethanol<sup>57</sup>. A few important industrial processes are also developed for partial oxidation as well as for selective oxidation of hydrocarbons<sup>58</sup>. The importance of metal catalyzed reactions can be understood from the transformations of olefins and



acetylene with *t*-butyl hydroperoxide<sup>59</sup> as shown in scheme 1.13. This scheme demonstrates how a reaction path changes on changing the metal center present in the oxidant. For the sake of simplicity only the metal core and its oxidation state is shown in the scheme 1.13.

The combination of hydrogen peroxide and ferrous salts an effective oxidant. It is capable of oxidizing a large variety of organic substrates. This combination is known as Fenton's reagent<sup>19</sup>. Similar homogeneous oxidative catalysis using hydrogenperoxide and hydroperoxides as oxidants are well developed<sup>60</sup>. Generally substrates that could yield radicals followed by relatively stable carbonium ions are effectively oxidized by ferric ion. In the case of aromatic system it has been observed that hydroxy radical adds up rapidly to aromatic and the resulting hydroxycyclohexadienyl radicals can be observed directly by UV or ESR spectroscopy<sup>61</sup>. Benzene gives biphenyl and phenol in such reactions but when the substituted benzene derivatives are used the overall reactions are much more complicated. Generally the reaction that passes through electrophilic or free radical process gives hydroxylation of aromatic compounds<sup>62</sup> by hydrogen peroxide and the reactions are not selective. However, in the case of intramolecular process leading to stable chelates selectivity can be obtained<sup>63</sup>. Oxidation of phenol with potassium permanganate results in the cleavage of the ring. Homologues of phenol can be oxidized to the corresponding phenolic acid by potassium permanganate provided the hydroxy group is not protected with alkylation or acylation. Hydrogen of the hydroxyl group of phenol can readily be removed by

oxidizing agents that are capable of transferring one electron. For example, alkaline potassium ferricyanide is one such reagent<sup>64</sup>.

The use of molecular oxygen as an oxidant with metal ion is preferred from economic point of view. But selective partial oxidation is easier to control when hydrogen peroxide or organic hydroperoxides are used as oxygen donors. The oxidation of n-alkanes at the terminal carbon atom with high selectivity using molecular oxygen and a pure inorganic catalyst prepared by them, in a liquid phase reaction have diverse possibility to explore<sup>65,66</sup>.

The direct oxidation of paraffin hydrocarbons in natural gas under mild conditions is an intellectually challenging and industrially important objective for the research scientist. It has been observed that nature uses the enzymatic systems like iron-porphyrin based cytochrome P-450<sup>67</sup> or the nonheme protein  $\omega$ -hydroxylase<sup>68</sup> for selective hydroxylation of an unactivated carbon-hydrogen bond. A few systems that are developed for selective oxidation of saturated hydrocarbons are commonly based on the idea of the use of an iron catalyst. The catalyst is reduced by electron transfer and oxidized by molecular oxygen simultaneously in the presence of source of protons. The best known system run with the above principle is

commonly known as Giff's system. The Giff's system has been subjected to increase the efficiency of oxidation of hydrocarbons<sup>69</sup>.

Oxidation of adamantane by biomimetic reactions are important from synthetic and mechanistic point of view<sup>69</sup>. Several transition metal complexes are effective catalysts, which are more or less biomimetic<sup>70,71</sup>(equation 1.24). However these model systems gave poor

yield of the oxidized products<sup>72</sup>. Here it is assumed that the terminal

carbon atom of the reactant approaches the active site and respective alcohols, ketones, and carboxylic acids are formed.

Autooxidation is another important reaction can accompany an oxidation reaction. It refers to oxidation of an organic substrate by molecular oxygen via a free radical chain process<sup>73</sup>. Large number of cobalt and manganese containing compounds are highly efficient catalyst for liquid phase autooxidation reaction. Such reactions pass through free radical pathway with oxygen as the oxidizing agent. The aforesaid liquid phase autooxidation process is schematically represented in scheme 1.14. Alkoxy and alkylperoxy radicals are the intermediates involved in these reactions. When such reactions are carried out in confined medium such as zeolite they are found to be selective<sup>74</sup>. The selectivities in these reactions are governed by shape selectivity of the confined medium. For example it is the restricted space in the zeolite channels that forbids the formation of certain products or intermediates, minimising overall side product formation.

The stability of a reactive intermediate taking part in an oxidation reaction plays a crucial role in achieving better performance in terms of selectivity as well as overall yield. If the reactive intermediate is unstable under ordinary condition it may be possible to provide confinement by incorporating hydrophobic or hydrophilic groups so as to increase its stability as well as to reduce possible side reactions. Two such examples in which reactive intermediates are made stable by such confinement are shown in figure 1.2(a) & (b) and in the case of an oxybridged  $\text{Cu}_2\text{O}_2$  core<sup>75</sup> is stabilised and in figure peroxy bridged  $\text{Cu}_2\text{O}_2$  is stabilised<sup>76</sup>. The

reaction

of the peroxy species shown in fig. 1.2(a) & (b) is tested with different amides and it is found to hydrolytically cleave amide to acid. It is also

important to note that the binding with oxygen in this case is reversible and formic acid can be formed from such hydrolytic reactions within a second.

There are numerous organometallic reactions in which oxygen directly or indirectly participates. Wacker process of oxidation of olefin to aldehyde<sup>77</sup> is promoted by  $\text{PdCl}_2/\text{CuCl}_2$ . This reaction affords methyl ketones selectively from terminal olefins. The Rhodium catalyzed oxidation of a variety of olefin constitute another important example of selective reactions by transition metal catalyst<sup>78,79</sup>. In these reactions the oxidation of linear terminal olefins to corresponding methyl ketone is inhibited by the presence of free water but accelerated by the presence of dehydrating agent such as 2,2-dimethoxypropanol. This reaction is not suitable for internal acyclic olefins. However, cyclic olefins rapidly get oxidized. For example cyclopentene gives mainly 3-alkoxy and 4-alkoxycyclopentene. Table I lists some of the representative results on selectivity obtained from oxidation of 1-hexene in ethanol with molecular oxygen at 40°C using several rhodium complex catalysed reactions with copper or iron as cocatalyst<sup>78</sup>. Simple alkanes can be selectively oxidised by molecular oxygen in the presence of cobalt(III)acetate in acetic acid<sup>80</sup>. For example n-butane reacts with oxygen

in the presence of cobalt(II) acetate in acetic acid gives acetic acid (selectively 83%) at 100<sup>0</sup>-125<sup>0</sup>C with 80% conversion of n-butane(equation 1.26). Cyclohexane is also selectively oxidised by the same to afford cyclohexyl acetate and 2-acetoxy cyclohexanone as the major product. The chemo, regio, and stereoselective oxidation of alcohols to carbonyl compounds are synthetically important

Table I: oxidation of 1-hexene catalysed by Rhodium – Copper or Iron system.

Expt.	Complex, 0.02M	Cocatalyst M	Total O <sub>2</sub>	1-hexene	2-hexanones	Selectivity %	
			uptake, M	consumed M	produced M		
1	RhCl <sub>3</sub> .3H <sub>2</sub> O	none	0.08	0.58	0.034	6	
2	RhCl <sub>3</sub> .3H <sub>2</sub> O	Cu(NO <sub>3</sub> ) (HMPA) <sub>4</sub>	1.16	2.35	2.32	≥98	
3	RhCl <sub>3</sub> .3H <sub>2</sub> O	Cu(ClO <sub>4</sub> ) (HMPA) <sub>4</sub>	1.05	2.13	2.09	≥98	
4 ≥97	RhCl <sub>3</sub> .3H <sub>2</sub> O	CuCl <sub>2</sub>		0.11	0.22	0.21	
5	RhCl <sub>3</sub> .3H <sub>2</sub> O	Fe(NO <sub>3</sub> ) <sub>3</sub> (HMPA) <sub>4</sub>	0.7	1.37	1.35	≥98	
6	Rh(ClO <sub>4</sub> ) <sub>3</sub> .6H <sub>2</sub> O	CuCl <sub>2</sub>	0.7	1.4	1.38	≥98	
7	Rh(ClO <sub>4</sub> ) <sub>3</sub> .6H <sub>2</sub> O	Cu(ClO <sub>4</sub> ) <sub>2</sub> (HMPA) <sub>4</sub>	0.02		0.03		
8	[RhCl(C <sub>8</sub> H <sub>14</sub> ) <sub>2</sub> ] <sub>2</sub>	Cu (ClO <sub>4</sub> )		0.16	0.35	0.33	≥94

HMPA  $\Rightarrow$  Hexamethyl phosphorotriamide



organic reactions. Chromium compounds are found to be most powerful and effective oxidant for this purpose. The Jones reagent<sup>81</sup> (chromiumtrioxide/H<sub>2</sub>SO<sub>4</sub>), the Collins reagent<sup>82</sup> (chromium trioxide/

pyridine complex), pyridinium chlorochromate<sup>83</sup> etc. are some of the reagents used for this purpose. The chromium catalyzed oxidation of allylic alcohols by butylhydroperoxide to carbonyl compound has been reported<sup>84</sup> Chromium(III)(salen) compounds can catalyze the selective oxidation of primary and secondary alcohols at benzylic and allylic C-H

bonds to the corresponding carbonyl compounds<sup>85</sup> (equation 1.26).

Iodosobenzene is used as the source of oxygen in such reactions and allylic alcohols shows exception as they get chemoselectively oxidized to enones. In these reactions no epoxidations are observed. Various oxidative processes by transition metal peroxocomplexes for selective oxidation of both primary and secondary alcohols and of diols to the corresponding carbonyl compounds has been studied with particular interest from synthetic as well as mechanistic point of view<sup>86</sup>. The anionic oxo-peroxo-molybdenum complex  $\text{MoO}_5\text{PICO}$  (PICO = Picolinate-N-oxide anion) causes selective oxidation of both primary and secondary alcohols and of diols to the corresponding carbonyl compounds<sup>47</sup>. The oxidation of glycol is complicated in comparison to that of a monohydric alcohol. Depending on the nature of the oxidant,  $\alpha$ -diketones or carbonyl compounds are obtained by the subsequent cleavage of the carbon-carbon bond. In fact in all these cases the anionic nature of PICO and the nature of the ligand are supposed to play a relevant role<sup>87</sup>. Two of such examples of oxidation carried out by PICO are shown in equation 1.27 and equation 1.28. The Lewis acidity of an oxidant used as catalyst provides selectivity in oxidation reactions. Generally metals with low oxidation potential and high Lewis acidity are superior catalysts for epoxidation. The Lewis acidity of the catalyst also influences the electronic properties of the coordinating ligands. The catalyst having

strongly bound ligands are less reactive due to difficulty in the complex formation between the catalyst and the oxidant. On the otherhand catalyst with loosely bound ligands are active, but less active compared with those with ligands of intermediate stability. Recently, a set of bis( $\mu$ -oxo)dicopper complexes with ligands those are *p*-substituted

N-ethyl-N-[2-(2-pyridyl)ethyl]-2-phenylethylamine and its derivatives have been developed for activation of aliphatic C-H bond<sup>88</sup>. In these cases respective copper complexes decompose to products in which the ligand gets hydroxylated at benzylic position.

The oxidative addition reaction of catechol and triruthenium dodecacarbonyl produces either tetranuclear or hexanuclear complexes which contain  $\pi$ -bound *o*-benzoquinone ligand<sup>89</sup>. Lewis bases readily add

up to these complexes. The use of mild oxidant such as iodine results in the formation of dinuclear complexes where the ruthenium atoms are bridged by both iodine and quinone ligands.

Cobalt complexes with salen ligand/s are efficiently converted to the corresponding organocobalt(III) derivatives such as  $\text{RCo}^{\text{III}}(\text{salen})$  (R= Me) by various hydrazines under oxidative conditions with either dioxygen or tert-butylhydroperoxide<sup>90</sup>. Oxidative alkylation of various cobalt complexes can also be carried out with structurally diverse hydrazines. Extensive studies carried out on the reactive intermediates like superoxo and tert butylperoxo complexes of cobalt(III) derived by oxidation, ligand exchange, ligand induced homolysis of different cobalt(II) and cobalt(III) precursors indicates that such cobalt(III) oxidants are responsible for the two electron conversion of alkyl hydrazines to their diazene derivatives (scheme 1.15). The subsequent extrusion of dinitrogen

gives the organic radical ( $R\cdot$ ) as the key intermediate causing alkylation at the Co(II) center.

The reaction of olefins and cycloalkanes with  $Fe(CO)^+$  results in rearrangement of the olefins in the resulting complexes with  $Fe^+$  to a structure with two or more ligands except in the case of ethylene, propene and isobutene<sup>91</sup>. These rearrangements are consistent with the addition of an allylic C-C bond to the metal ion followed by abstraction of a  $\beta$ -hydrogen atom to form a hydrido  $\pi$ -allyl intermediate. Transfer of the hydrogen atom to the allylic fragment produced a bis-olefin complex. The oxidative addition of aryl halides to nickel(I) complex like  $Ni(PPh_3)_3Br$  results in replacement of a triphenylphosphine group by the aryl group<sup>92</sup>. Aryl iodides are found to be more active than aryl bromide and aryl chloride does not react.

Metal catalyzed oxidation reactions are also classified as homolytic and heterolytic<sup>3</sup>. The homolytic types of catalysis make use of metal salts (homogeneous) such as acetates of cobalt, manganese, iron, copper. This necessitates the recycling of the metal species between several oxidation states by one equivalent change. Free radicals are formed as intermediate in

these reactions from the organic substrates. For example the cobalt(III) catalysed reaction of toluene (equation 1.29). In this reaction toluene gives

benzyl radical as intermediate. The radical formed may either react by electron transfer or by ligand transfer. The nature of the ligand determines the possibility. In the case of copper(II) catalysed oxidation reactions of alkyl radicals hard ligands such as acetate favours electron transfer. While the soft ligands such as bromide ligand prefers ligand transfer<sup>93</sup> (equation 1.30). The reaction of benzyl bromide with

$\text{Co}^{\text{III}}(\text{OAc})_2\text{Br}$  in the presence of bromide ions reduces  $\text{Co}(\text{III})$ .

Furthermore, relative to cobalt(III)acetate the cobalt(II)acetate is stable (equation 1.31). Heterolytic catalysis involves reactions of organic

substrate/s coordinated to transition metals. It occurs with metal complexes having Lewis acidity or complexes that can formally undergo two equivalent changes. In these reactions free radicals are not intermediate. For

example, the oxidative substitution of benzene by lead tetratrifluoroacetate complex (equation 1.32) is accompanied with decrease in oxidation number

of lead(IV) to lead(II)<sup>94</sup>.

The homolytic type of catalysis has been known for a long time while the heterolytic types are developed more recently. Accessibility of

several oxidation states and the capability of having various coordination numbers are two properties of transition metal complexes. These two features are also important in metal catalyzed oxidation reactions. Metal complexes derived from cobalt, manganese, iron and copper catalyses homolytic reactions. The conversion of *p*-xylene to terphthalic acid by cobalt acetate is one commercially important homolytic process<sup>95</sup>. Similarly industrial epoxidation of olefins with alkyl hydroperoxide using molybdenum, vanadium, tungsten etc as catalyst constitutes the example of heterolytic process.

The phosphorus-vandium oxides are used as catalysts for the selective oxidation of butane to maleic anhydride. In these reactions the active catalysts are pyrophosphates  $(VO)_2P_2O_7$  which is obtained from orthophosphate such as  $(VO)_2H_4P_2O_9$  through a topotactic transformation<sup>96</sup>. Selective catalyst resembling zeolite catalyst containing small amounts of cobalt or manganese ions can be designed. In these reactions tuning of the pore diameter of zeolite framework controls the approach of the terminal carbon atom of the n-alkane to the catalytically active sites<sup>97</sup>.

Studies carried out on synthetic model complexes copper(I) to make an understanding of the dioxygen binding and activation by metal

ions in biological and other catalytic system reveals the intermediate formation of peroxometal species in oxidative chemical processes.<sup>98</sup> It has been observed that the interaction of copper(I) with hydrogen peroxide produces  $[\text{Cu}_2\text{O}_2]^{2+}$  core which can exist in either

( $\mu\text{-}\eta^2 : \eta^2$  peroxo) dicopper form or  $[\text{Cu}_2(\mu\text{-O}_2)]^{2+}$  form and

both the forms are interconvertible. Recently it has been observed that the copper(I) complex of a new binucleating ligand on interaction with molecular oxygen gives a peroxodicopper (II) ( $\text{Cu}_2\text{-O}_2$ ) intermediate which leads to oxo-transfer reaction to effect amine to N-oxide formation and also biomimetic regioselective oxidative dealkylation chemistry.<sup>99</sup>

#### **1.4 Classification based on the method of oxidation**

Further to the classification depicted above the oxidation reactions further can be classified on the basis of the reaction conditions such as photochemical, electrochemical etc. However, for the sake of brevity and overlapping nature of the topic brief description is being made in the following sections.

##### **1.4.1 Electrochemical oxidation**

The fundamental process in electrochemical reactions involves redox processes. They can be either used for stoichiometric and catalytic

reactions. There are numerous examples of oxidation reactions of organic and inorganic compounds.

Nickel catalysed cross coupling reactions of aromatic halides<sup>100</sup> by electrochemical means involves regeneration of redox cycle by electrochemical means (scheme 1.16). The chemoselective electrochemical



Cleavage of alkyl, aryl ethers have been found to catalyse by  $[\text{Ni}(\text{bipy})_3](\text{BF}_4)_2$ . The reaction proceeds through in situ generated nickel(0) complexes. These nickel complexes can oxidatively add to the C-O bond of the aryl-alkyl ether to form a  $\pi$ -allyl-nickel(II) complex which on hydrolysis gives phenol and propene (equation 1.33). Similar reactions can be performed by sacrificial electrolysis in the presence of electrodes which take part in the catalytic cycle by either one or two electron transfer

process<sup>100</sup>.

#### 1.4.2 Photochemical oxidation

Among the various photochemical oxidation reactions the singlet oxygen oxidation are important and are well studied. For example alkenes are oxidized by singlet oxygen<sup>101</sup>. One example showing allylic hydroxylation of cyclo-octene to give 1-cyclooctene-3-ol<sup>102</sup> is shown in equation 1.34.

The photochemical oxidation by singlet oxygen gives useful optically active natural product which has advantage over conventional thermal oxidation giving racemic mixture (equation 1.35)<sup>103</sup>. The ring opening reactions are

also useful oxidation reactions that are well studied. One of such ring opening reaction<sup>104</sup> is shown in equation 1.36.

### 1.5 Scope of the study

The classification of oxidation reactions clearly indicates the importance and emergence of new and selective reagents for oxidative transformations. The understanding of many naturally occurring oxidation processes have necessitated to design model studies of biologically important molecules and synthesis of model compounds. The oxidation reactions by metal stabilized radical species that are present in biological systems such as in galactose oxidase, hydrophobic confinement in stabilizing the reactive intermediates have emerged as two important topics that have drawn the attention of chemists. The growth of supramolecular chemistry has made it relatively easier to stabilize reactive intermediates by providing correct environment which in turn can be used for selective transformations. The other aspects of oxidation reactions that require clear attention is the need of development of bio-friendly non hazardous reagents. Any reagent that would lead to non-hazardous degradable product will always be preferred for an oxidation reaction. Nevertheless the use of catalytic oxidant will continue to attract attention. Other important point of a metal catalyzed oxidation reaction is the relevance to biological reactions to synthesis of lignin. Lignin is wood tissue comprises major portions of natural plant biopolymer. It plays the crucial role of protection against degradation, water transport in plants. Lignin id believed to be formed by

oxidative transformations of coniferyl alcohol by various enzymes through oxidation reactions. Since our interest is to understand oxidative reactions of phenolic compounds by copper and cobalt complexes we choose to make study under neutral condition with a non-hazardous oxidant hydrogen peroxide. There are several facets of such reactions. Use of a dioneoxime cobalt complex to carry out oxidation reactions will have implication in mimicing biological reactions of vitamin B<sub>12</sub>. Use of amino acid complex of copper(II) catalyst will show correlation of such reactions with biological reactions of enzyme like tyrosinase, galactose oxidase etc.



## CHAPTER-2

### Cobalt-catalysed oxidative reactions

#### 2.1 Background

Cobalt ion plays key role in organic transformations<sup>105</sup> and it is also an important constituent of biologically important compound such as vitamin B<sub>12</sub><sup>106</sup> (fig 2.1). The cobalt ion binds to the cofactor of vitamin B<sub>12</sub> through nitrogen atoms of the corrin ring<sup>107</sup>. The cobalt center

## Vitamin B<sub>12</sub>

Fig. 2.1

of Vitamin B<sub>12</sub> has a major role in C-C bond formation and oxidation of organic substrates<sup>108</sup>. Out of several Vitamin B<sub>12</sub> promoted / catalysed oxidative reactions, few reactions are illustrated in scheme 2.1. Vitamin B<sub>12</sub> is also used as catalyst in electro-organic synthesis<sup>109</sup>. It promotes electron transfer from cathode to electrophilic organic substrate by acting as mediator.



Study of model compounds for mimicking reactivity of vitamin B<sub>12</sub> has relevance in understanding its role in organic transformations. The

dimethylglyoximato cobalt(II) complex<sup>110</sup> (2.1) is one such complex that shows close analogy of reactivity with vitamin B<sub>12</sub> on modification. Several cobalt (II)-salophen complex and their derivatives (Salophen is the condensation product of salicylaldehyde with ethylenediamine) also mimic reactivity of Vitamin B<sub>12</sub>. It is important to note that when Vitamin B<sub>12</sub> is chemically or electrochemically reduced, it acts as a powerful nucleophile. The reduced species on oxidative addition reaction<sup>111</sup> with alkyl halide get converted to alkyl derivative. The homolysis of the Co-C bond are relatively easy as Co-C bond strengths are 70-100 KJ mol<sup>-1</sup>. As a consequence of the low value of Co-C bond energy, these compounds can generate alkyl/aryl radicals under photochemical condition. The principle is extended for synthesis of biologically important molecules.

Dimethylglyoxime can act as chelating ligand and it reacts with Co(III) complexes to give a complex called cobaloxime (equation 2.1)<sup>112</sup>.

In cobaloxime the oxime units form a planer cyclic structure. This



Compound on reduction with sodium amalgam gives cobalt(I) dimethylglyoxime complex which is a potent nucleophile and leads to facile reaction with alkyl halides. The cobalt complex in low oxidation state oxidatively adds to form alkyl cobaloxime. The alkyl cobaloxime are key intermediates in several carbon-carbon bond formation reactions. Analogous compounds of various nitrogen bases capable of maintaining planer geometry around metal are also studied. The selective role in organic

transformation<sup>113</sup> of complexes like (2.II), (2.III), (2.IV) is an attractive feature of their complexes.

The above discussion illustrates that the cobalt complexes having N, N; N, O bond with planar geometry are capable of performing radical induced organic reactions. When cobalt catalysts are used, such oxidation reactions are usually carried out by different oxidant such as alkyl/aryl

peroxides, hydroperoxides, hydrogen peroxide, oxygen. The oxygen being a gas, it can be either generated in situ through a reagent in the system or it is to be supplied from external source. Moreover, alkyl/aryl peroxides, hydroperoxides, gives biproduct/s that requires extra separation of the

undesired products. Among all these reagents hydrogen peroxide is environmentally friendly and lead to water and oxygen as side product. Environmentally benign oxidising substrate is always demanding for such studies.

## **2.2 Synthesis and characterization of cobalt-dionemonoxime complexes**

The section 2.1 highlights that the cobalt complexes having chelating ligand attached to the metal through N, N; N, O atoms are capable of mimicking the reaction of vitamin B<sub>12</sub>. The dimethylglyoxime(DMG) is one such ligands whose cobalt complexes have been successfully used for mimicking reactivity of vitamin B<sub>12</sub>. Due to the charge neutralization by anionic form of oximes they form soluble complexes. In contrast to the study of reactivity of Co-DMG complex there is very limited study on the diacetylmonoxime or analogous monoxime of cobalt complexes. The reasons for this is that the diacetyl monoxime itself can disproportionate between dione and dioxime(equation 2.2) leading to dioxime complex instead of a monoxime complex <sup>114</sup>. There is another problem that is

being faced is that the diionemoxime complexes can be dimeric and has lesser reactivity<sup>115</sup>. Further complicacies may arise as monoximes can form metal complexes in neutral form as well as in anionic form.

In order to study oxidative reaction of cobalt diionemoxime complex a diacetyl monoxime complex (**2.V**) was prepared from a solid state reaction between cobalt(II)chloride hexahydrate and diacetylmonoxime at 110<sup>0</sup>C (equation 2.3). The synthesis was performed

in solid state to avoid the possible disproportionation depicted in equation 2.1. Elemental analysis of the product support it to have the

molecular composition as  $\text{Co}_2(\text{DAM})_7\text{Cl}_4$  (where DAM= diacetylmonoxime). The IR spectra of the complex and diacetylmonoxime are shown in figure 2.2. The IR spectra of the complex absorption at  $3201\text{cm}^{-1}$  due to hydroxyl groups, the absorption at  $1648\text{ cm}^{-1}$  is due to carbonyl groups, the C=N stretching appears at  $1573\text{ cm}^{-1}$ . The antisymmetric stretching of the methyl groups appears at  $3047\text{cm}^{-1}$  and  $2919\text{ cm}^{-1}$ . The asymmetric deformation of methyl group is observed at  $1455\text{ cm}^{-1}$  and the symmetric deformation band is observed at  $1367\text{ cm}^{-1}$ . The absorption peak of the complex at  $988\text{cm}^{-1}$  is assigned to the metal oxygen bond stretching. The absorption peak for the carbonyl group for the complex has been found to shift by  $27\text{cm}^{-1}$  to the lower side from the one observed for diacetylmonoxime, the ligand has the carbonyl

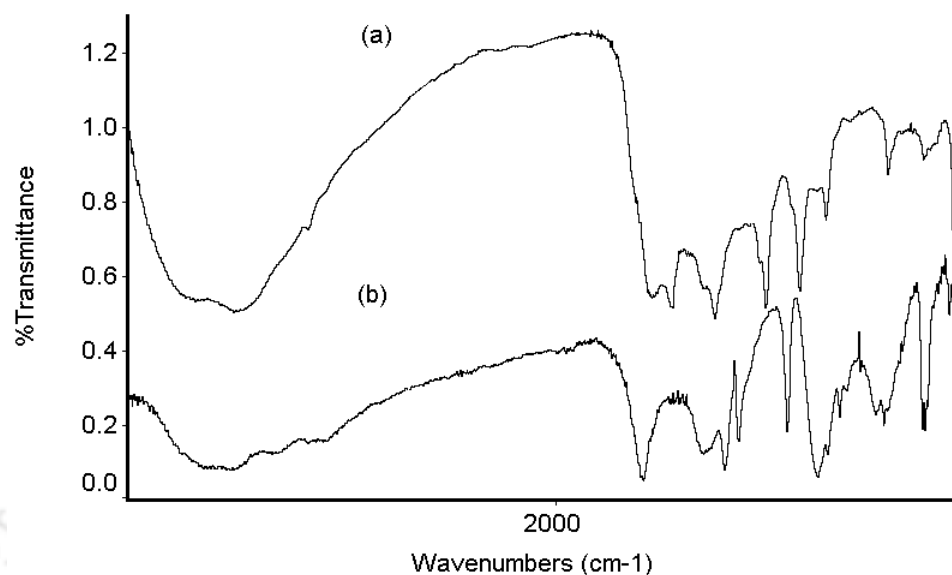
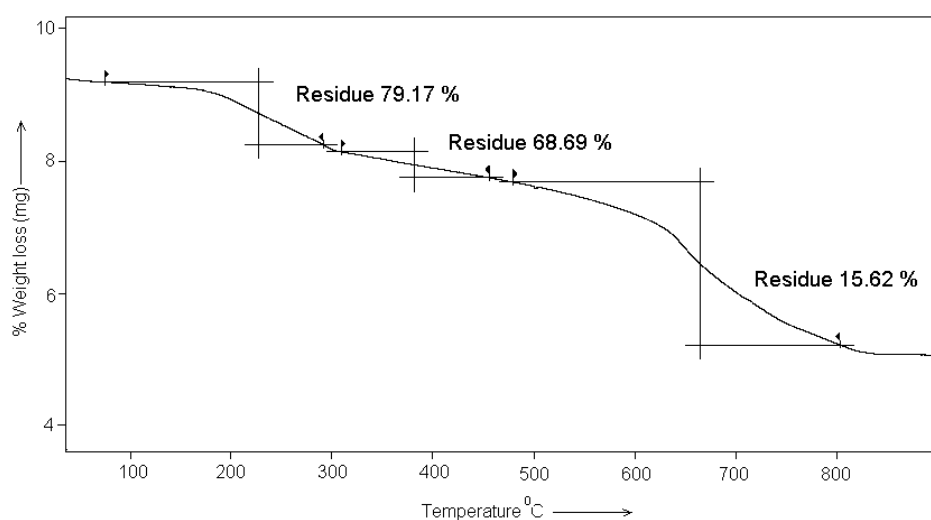


Fig. 2.2 : IR spectra of (a) cobalt diacetyl monoxime complex (2.V)  
(b) diacetyl monoxime

absorption peak at  $1675\text{cm}^{-1}$ . The lowering of absorption frequency can be attributed to the coordination of the oxygen atoms to the metal that weakens the carbon – oxygen double bond of the carbonyl group. The complex 2.V has two prominent absorption maxima at  $587\text{ nm}$  ( $\epsilon = 298.2\text{ mol}^{-1}\text{cm}^{-1}$ ) and  $683\text{ nm}$  ( $\epsilon = 338.26\text{ mol}^{-1}\text{cm}^{-1}$ ) and these corresponds to the d-d transition of the complex and are assigned to the transition from  ${}^4\text{T}_{1g} \rightarrow {}^4\text{A}_{2g}$  and  ${}^4\text{T}_{1g} \rightarrow {}^4\text{T}_{2g}$ . This supports the geometry around cobalt in the complex is octahedral. There is also another

absorption at 657 nm ( $\epsilon = 54.7 \text{ mol}^{-1}\text{cm}^{-1}$ ) which is assigned to the d-d transition  ${}^4 T_{1g} \rightarrow {}^4 T_{1g} (P)$ . The molar conductivity of the complex is  $485 \text{ ohm}^{-1} \text{ cm}^2 \text{ mole}^{-1}$ . This value suggests it to be an ionic complex having eight charges. Based on these observations the structure is assigned as shown in equation 2.3.

The thermogravimetry of the cobalt diacetyl monoxime



complex (figure 2.3) shows a loss of weight (18%) of the compound in

Fig. 2.3: Thermogram of (2.V) (heating rate  $5 \text{ }^{\circ}\text{C}/\text{min}$ )

between the temperature range 190-320<sup>0</sup>C. This weight loss corresponds to degradation of the compound by losing the axial ligands. The compound shows a second weight loss in the range of 320-600<sup>0</sup>C (14%), this loss corresponds to the loss of another diacetylmonoxime group that bridges the two cobalt units. Beyond this temperature the thermogram is associated with another loss of weight that is estimated to be 84.38% from its original weight. This weight loss is attributed to the loss of the remaining diacetylmonoximes as well as the chlorides as HCl to give CoO. The weight loss in thermogravimetry of the complex is represented in scheme 2.2.

The magnetic moment value after diamagnetic correction is found to be 3.48 BM per cobalt atom at 25<sup>0</sup>C. This value corresponds to a cobalt (II) in an octahedral environment. (spin only magnetic moment for cobalt(II) in weak field is 3.87 BM and  $\mu$ -effective observed are in the range of 4.2 to 4.4 BM.).

The lowering of the value of magnetic moment than the expected one probably occurs due to the antiferromagnetic coupling between the two cobalt centres. Because in the case of binuclear or polynuclear complexes where the two paramagnetic centers are joined by suitable bridging group

interaction between the two can occur. In the case of the cobalt diacetylmonoxime complex the two paramagnetic cobalt centers are joined





by a bridging diacetyl monoxime ligand and therefore interaction between the cobalt centers takes place which lowers the value of magnetic moment than the expected one.

Similar reaction of cobalt chloride with benzil monoxime compound in neutral condition failed to give an isolable complex, in pure form in solution as well as in solid state. However, the reaction of benzilmonoxime with cobalt(II)acetate in methanol forms a neutral complex(2.VI) where the benzilmonoxime act as a chelating ligand (equation 2.4) Elemental analysis suggests it to have the composition  $\text{Co}_2(\text{BMO})_4(\text{BMOH})$

( where BMO= benzilmonoxime anion and BMOH is benzilmonoxime itself).

The IR spectrum of the compound shows one absorption peak at 3436  $\text{cm}^{-1}$  due to hydroxy group. This absorption appears at 3390 $\text{cm}^{-1}$  in benzilmonoxime. The carbonyl frequency of the chelating benzilmonoximato part appears at 1608  $\text{cm}^{-1}$  whereas the benzilmonoxime is at 1654 $\text{cm}^{-1}$ . Thus there is a shift of 46  $\text{cm}^{-1}$  in the carbonyl frequency from the ligand due to the co-ordination of the carbonyl group to the ligand. The absorption peak due to the C=N group observed at 1521 $\text{cm}^{-1}$ . The IR of the benzilmonoxime and the complex is shown in figure 2.5 . As the elemental analysis suggests that there is a distribution of one unit of the benzilmonoxime per two units of cobalt centers; the compound may have a polymeric structure. The GPC of the samples (Fig. 2.5) was recorded to determine the molecular weight distribution and observed

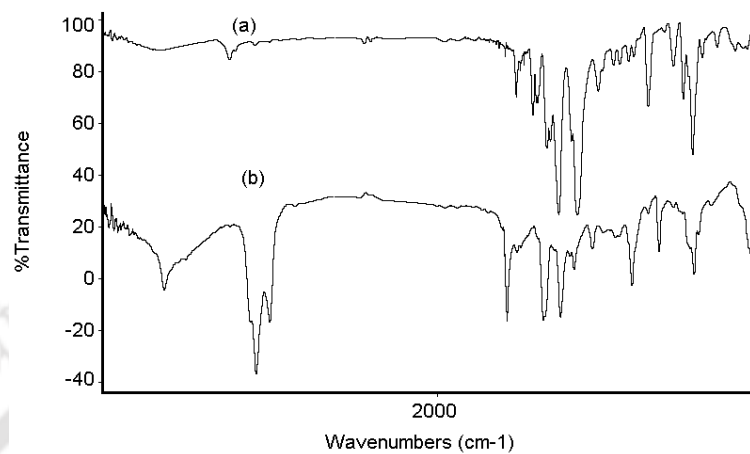


Fig. 2.4 : IR spectra of (a) cobalt benzilmonoxime complex(2.VI)  
(b) benzilmonoxime

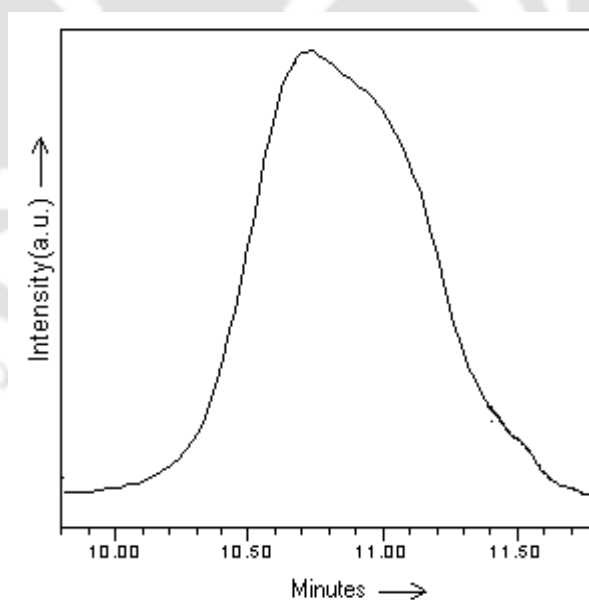


Fig. 2.5 GPC of 2.VI

that there was a well defined peak having Mn value 2453. The Mn/Mw value of the substrate was observed to be 1.003 this showed it to have uniform structure and it comprises of units having four Co centers in the complex.

The molar conductance of the complex is found to be  $11.6 \text{ ohm}^{-1}\text{cm}^2\text{mole}^{-1}$ . The thermogram of the cobalt benzilmonoxime complex (fig 2.6).showed a loss of 52 % weight in between  $180^{\circ}\text{C}$  to  $300^{\circ}\text{C}$ . This

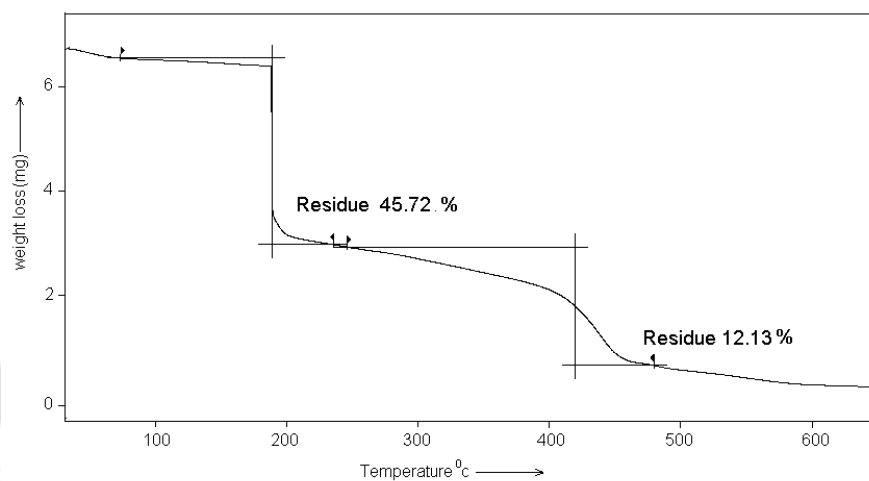


Fig. 2.6 Thermogram of cobaltbenzilmonoxime complex  
( Heating rate  $5^{\circ}\text{C} / \text{min}$  )

shows that complex loses three units of benzilmonoxime yielding dimeric compound with Co-O-Co bridge (theoretical weight loss corresponds to

53%). Another weight loss was also observed in the temperature range 250-490<sup>0</sup>C. The total weight loss recorded in this region was 74%. This loss of weight accounts for the loss of the remaining benzilmonoximate units with concomitant formation of CoO. The thermogravimetry is shown in scheme 2.3.

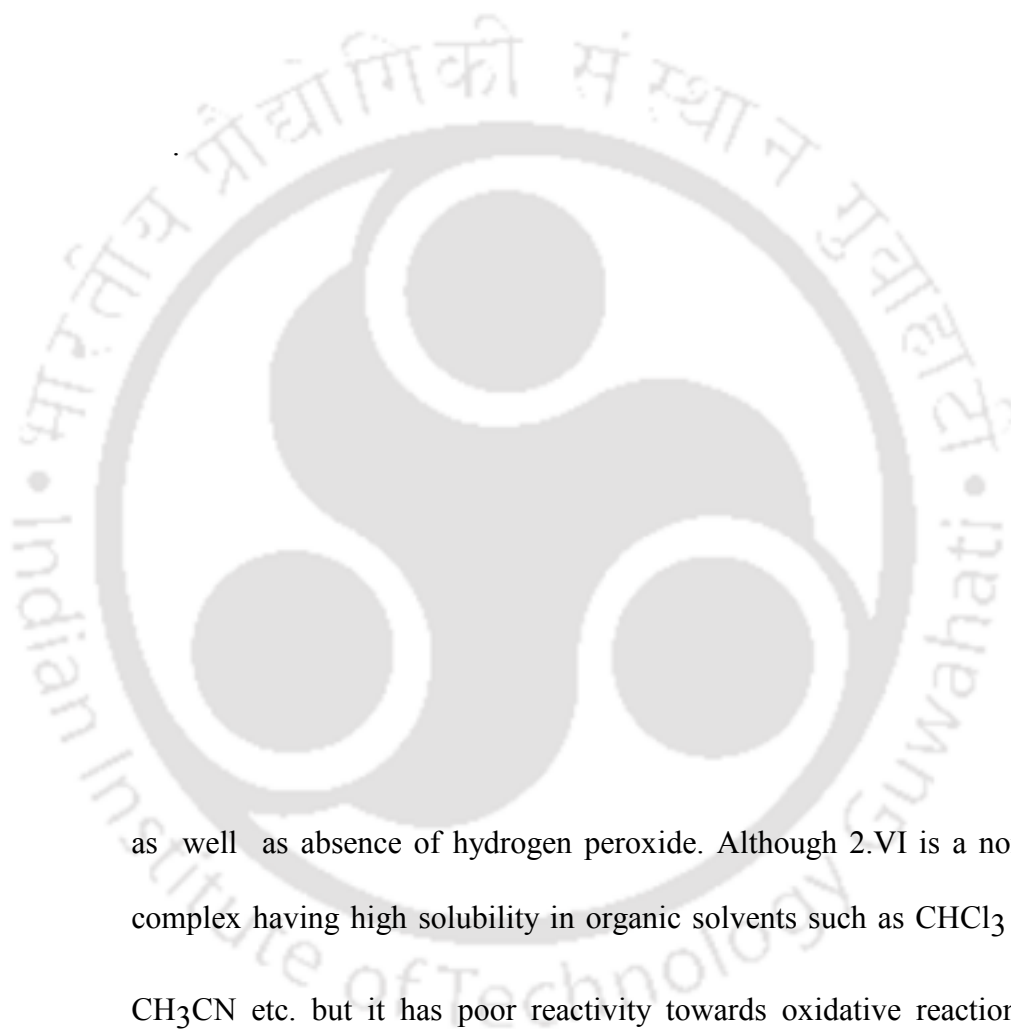


Its magnetic moment per cobalt atom is 1.58 BM. The theoretical value expected for low spin complexes of cobalt (II) is 1.78 BM. In this case similar explanation as drawn for the cobalt diacetyl monoxime complex holds good to explain the lowering of magnetic moment than the

expected value. Because in this case also two cobalt centers are joined by a bridging benzilmonoxime complex and therefore antiferromagnetic coupling between the two cobalt centers causes lowering of the value of magnetic moment.

### 1.3 Oxidative reactions of 2.V and 2.VI with aromatic compounds:

The aromatic compounds are attractive substrate for understanding of oxidative reactions. An aromatic compound can get oxidized or hydroxylated at the side chain or at the aromatic nucleus. For example the side chain oxidation of toluene can give benzylalcohol, benzaldehyde or benzoic acid depending on reaction condition. The aromatic nucleus can be hydroxylated to give *ortho* or *para* cresol (scheme 2.4). Various oxidative reactions of aromatic compounds were tested with the catalytic and stoichiometric amount of the complex 2.V and 2.VI in the presence



as well as absence of hydrogen peroxide. Although 2.VI is a non polar complex having high solubility in organic solvents such as  $\text{CHCl}_3$  , THF,  $\text{CH}_3\text{CN}$  etc. but it has poor reactivity towards oxidative reactions. The ionic complex 2.V is found to catalytically active and its reactivity as

catalyst is described in the subsequent subsections.

### 2.3.1 Oxidation of toluene

Toluene reacted with hydrogen peroxide in presence of catalytic amount of cobalt dionemoxime complex (2.V) at boiling temperature of acetonitrile under atmospheric pressure. This reaction gave benzyl alcohol as the major product. In addition to benzylalcohol, benzaldehyde and traces of *p*-cresol and *o*-cresol were formed. The gas chromatogram of the reaction mixture after 6hrs of the reaction at 80<sup>0</sup>C is shown in figure 2.7.

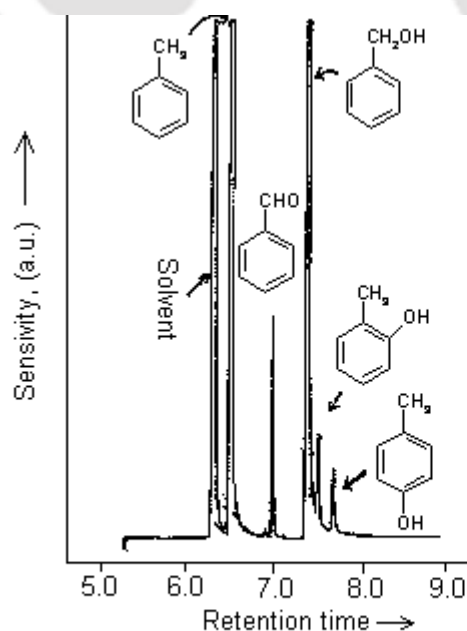


Fig. 2.7 Gas chromatogram(FID) of the reaction mixture of toluene 2.IV in presence of hydrogen peroxide after 6hrs at 80<sup>0</sup>C.

The retention time of the product shows that benzyl alcohol, benzaldehyde, *o*-cresol and *p*-cresol were formed in this reaction. The identity of each product was established either by comparing retention time of individual component with authentic samples or with comparing the gas chromatograph with the intensity of peak enhancement by adding a particular substrate. In order to ascertain whether similar reaction of benzyl alcohol with catalytic amount of cobalt diacetylmonoxime complex (**2.V**) in H<sub>2</sub>O<sub>2</sub> gives benzaldehyde, an independent experiment was carried out with benzylalcohol with catalytic amount of **2.V** in the presence of hydrogenperoxide. In this reaction benzyl alcohol was converted to benzaldehyde along with benzoic acid. Benzaldehyde in turn gets slowly oxidised to benzoic acid by **2.V** in the presence of hydrogen peroxide. The stepwise conversion of benzyl alcohol to benzaldehyde suggests that oxidation of toluene to benzaldehyde pass through benzyl alcohol. The maximum overall conversion of the toluene during this oxidation reaction observed was 12 percent. No significant yield enhancement could be achieved further by extending the time of reaction as well as by performing the reaction at slightly elevated temperature. The reaction was also carried

out with cobalt benzilmonoxime complex (**2.VI**) and the complex was not found to be effective for these transformations.

### 2.3.2 Reactions of phenols

The cobalt complexes are useful in selective oxidation of phenolic compounds to quinone<sup>116</sup> and are also capable of mimicking lactase like reactivity in polyphenol synthesis<sup>117</sup>. Thus a phenolic compound can undergo following kind of reactions (scheme 2.5).



Phenols react with hydrogen peroxide in the presence of diacetylmonoxime cobalt(II) catalyst in acetonitrile at 60<sup>0</sup>C to give

oxidative oligomerisation (equation 2.5 ). The  $M_n$  and  $M_w$  values of the oligomers prepared from different phenols are listed in table 2.1.

The IR spectra of all the oligomers have broad signal around  $3400\text{cm}^{-1}$ . This occurs due to the O-H end group present in the oligomers.

Thus O-H deformation band in the oligomers are observed at  $1200\text{ cm}^{-1}$ .



Table 2.1

Molecular weight of different polyphenylene ethers

Type of oligomer	$M_n$	$M_w$	Polydispersity
Poly phenylene ether	3500	8400	2.4

Poly( <i>o</i> -methyl phenylene ether)	3348	3542	1.058
Poly( <i>m</i> -methyl phenylene ether)	3580	3736	1.044
Poly( <i>p</i> -methyl phenylene ether)	3494	3678	1.053

The C-O bond stretching at  $1490\text{ cm}^{-1}$  is also observed. The IR absorption band at  $1610\text{ cm}^{-1}$  and  $1590\text{ cm}^{-1}$  are observed due to the C=C bond stretching of the aromatic nucleus. The O-H stretching frequency for the oligomers from *o*-cresol, *m*-cresol and *p*-cresol were obtained respectively at  $3395\text{ cm}^{-1}$ ,  $3381\text{ cm}^{-1}$  and  $3370\text{ cm}^{-1}$ . For the oligomer obtained from *o*-cresol the other peaks observed at  $2919\text{ cm}^{-1}$  due to the alkyl group,  $1702\text{ cm}^{-1}$  due to overtone of OH absorption,  $1600\text{ cm}^{-1}$  and  $1480\text{ cm}^{-1}$  due to the aromatic C=C stretching, at  $1191\text{ cm}^{-1}$  due to C-O stretching and another one at  $757\text{ cm}^{-1}$  due to the alkyl group. The respective peaks for the oligomer obtained from *m*-cresol are observed at  $2929\text{ cm}^{-1}$ ,  $1702\text{ cm}^{-1}$ ,  $1616\text{ cm}^{-1}$  and  $1492\text{ cm}^{-1}$ ,  $1282\text{ cm}^{-1}$  and  $750\text{ cm}^{-1}$ . In this case the O-H deformation band is also observed at  $1196\text{ cm}^{-1}$ . Similarly for the

oligomer obtained from *p*-cresol the IR absorption bands at  $1727\text{ cm}^{-1}$  ,  $1620\text{ cm}^{-1}$   $1520\text{ cm}^{-1}$  ,  $1217\text{ cm}^{-1}$  and  $825\text{ cm}^{-1}$  in analogy with the products from *o*-cresol and *m*-cresol. We have made a comparison on the nature of products formed from different isomer of cresols, on the basis of the available IR spectra of the oligomers. The IR spectra obtained from *o*-, *m*-, and *p*-Cresols with the ones obtained from SBP catalysed ones are shown in figure 2.8 (a) and (b). There are few salient features that can be distinguished in the two cases. The vibration due to phenolic O-H bond is observed at a longer wavelength region in the case of SBP (Soyabean peroxidase) catalysed polymers compared to those prepared by our method. In the case of SBP catalysed oligomers there is sharp O-H peaks showing presence of intramolecular hydrogen bonding which probably occurs through the hydroxylated or the O-H group that are left free on the main chain during the C-C bond formation. Second point is the clear observation



of quinonic type of absorption in SBP catalysed reactions, in our case we do not observe quinonic type of absorptions, but we observe the overtone of the OH frequency of the end groups and the water of crystallisation in this region.

The importance of these oxidative oligomerisations will be enhanced if organised oligomers are formed without too many side reactions. The choice of appropriate reagent for selective C-O bonded oligomers is one of the points to focus. Success has been also made in copper catalysed oligomerisation reaction by blocking the *p*-position of the phenol by a phenyl group in preparing di, trimer of C-O bonded phenolic compounds<sup>118</sup>.

The proton nmr spectrum of the oligomer of phenol prepared by cobalt dione monoxime complex (**2.V**) catalysed reaction shows that it has broad signal in the aromatic region. The unsubstituted phenol has different possibilities for C-O bond formation leading to unspecific amount of crosslinked products. Such observation is very common in oligomerisation of phenols.

We have investigated the <sup>1</sup>H and <sup>13</sup>C nmr as a tool to probe the uniformity of the backbone during the oligomerisation of three isomers of cresols by **2.V** as catalyst. The reason for choosing the three isomer is that phenolic groups have *ortho* and *para* directing effects and these effects would be controlled by the available sites on a ring as well as by steric factors of the groups. For example *para*-cresol will lead to oligomerisation through linkage at *ortho* positions. The *ortho*-cresol would give rise to two sets of

oligomers, of which one will have C-O bond formation at *ortho* position with respect to the OH group and the other at *para* position with respect to the OH group. The *meta*-cresol will give two sets of isomers through C-O bond formation at *ortho* and *para* position of the ring with respect to the original OH group (Scheme 2.6). The  $^1\text{H}$  nmr (400 MHz) of the three cresols showed multiplets (Fig 2.9) due to aromatic protons in the aromatic region and the methyl groups at about 2  $\delta$  value in addition to the OH end group as a minor peak at 8-9  $\delta$  value. The integration ratio of the protons at aromatic and aliphatic region of poly (*p*-methyl phenylene ether) is 1:1. Which suggests that these oligomers are formed through monosubstitution of the aromatic ring. It cannot explain precisely the position of the ring where the C-O bonds are formed.

The chemical shift in  $^{13}\text{C}$  nmr spectroscopy is a strong tool that can describe the electronic environment around a carbon center. We have used the carbon  $^{13}\text{C}$  signals of the oligomers to distinguish between the structures of the oligomers. The  $^{13}\text{C}\{^1\text{H}\}$  signals of the oligomers are relatively simple and can be used for ascertaining the oligomers structure. The three isomers of cresols having hydroxyl group at *ortho*, *meta*, *para* positions with respect to methyl group can get oligomerised to give C-O bonded oligomers that are shown in figure 2.10. The  $^{13}\text{C}\{^1\text{H}\}$  signals







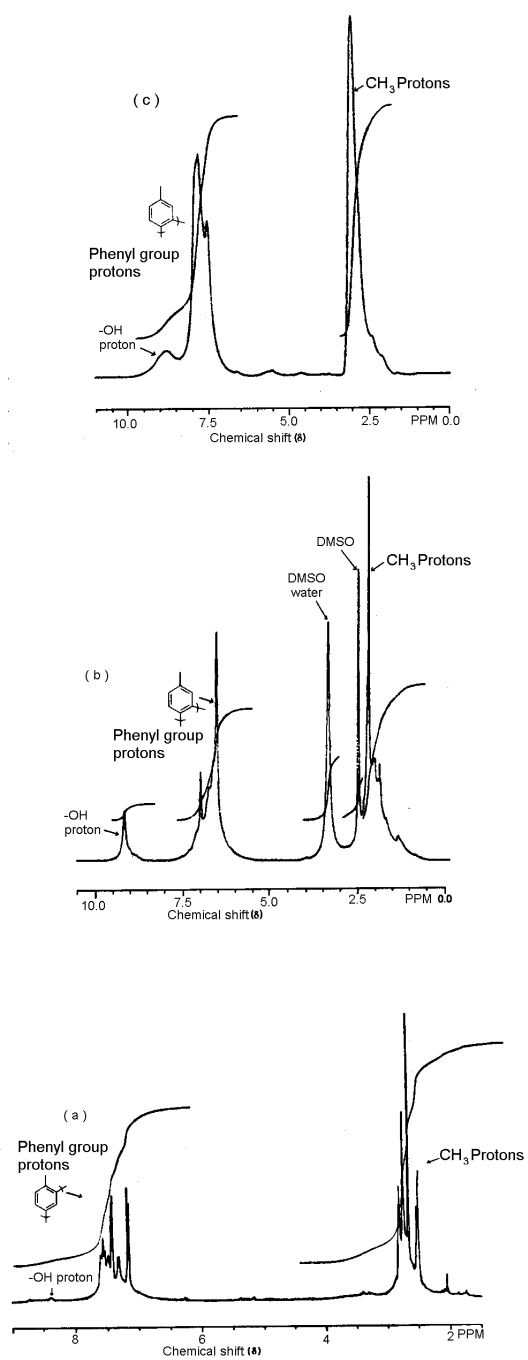


Fig. 2.9 <sup>1</sup>H nmr spectra of (a) poly (*o*-methyl phenylene ether) (b) poly (*m*-methyl

phenylene ether) (c) poly (*p*-methyl phenylene ether)



of the oligomers are shown in fig. 2.10. The methyl signals in each set of



Fig. 2.10

oligomers are observed at 16, 21 and 20 $\delta$  respectively in case of oligomers of *o*-, *m*- and *p*-cresols. In *o*-cresol, *m*-cresol, *p*-cresol they appear at 16, 22 and 21  $\delta$  values. It is interesting to note that the skeletons from mono substitution in the *o*, *p*, *m* isomer of cresol led to A, B or C ; three forms only (scheme 2.6)

The  $^{13}\text{C}$  signals obtained from the aromatic carbons of the respective oligomers can be used to ascertain the position of C-O bond. Due to the only three possible skeletal structure for the product, the polymer formed in each case can be ascertained. The proposed structures are for the three different cases can be represented as shown in fig 2.10. The assignments of the signals is made for each carbon in the skeletal structure proposed and the assignments are depicted by putting numerals against the signal as well as to the respective carbons of the oligomers as depicted in fig 2.11. In the case of poly (*p*-methyl phenylene ether) we expect seven different  $^{13}\text{C}$  signals from the proposed structure and in practice we get seven different  $^{13}\text{C}$  signals as expected. So is the case with poly (*m*-methyl phenylene ether) and poly(*o*-methyl phenylene ether). The results indicates that the proposed structure of the oligomers can explain the observed  $^{13}\text{C}$  signals for the respective oligomers and the reactions are

specific for one isomer. However in the case of fig. 2.11(b) we have three unassigned small signals which may arise from the side products.



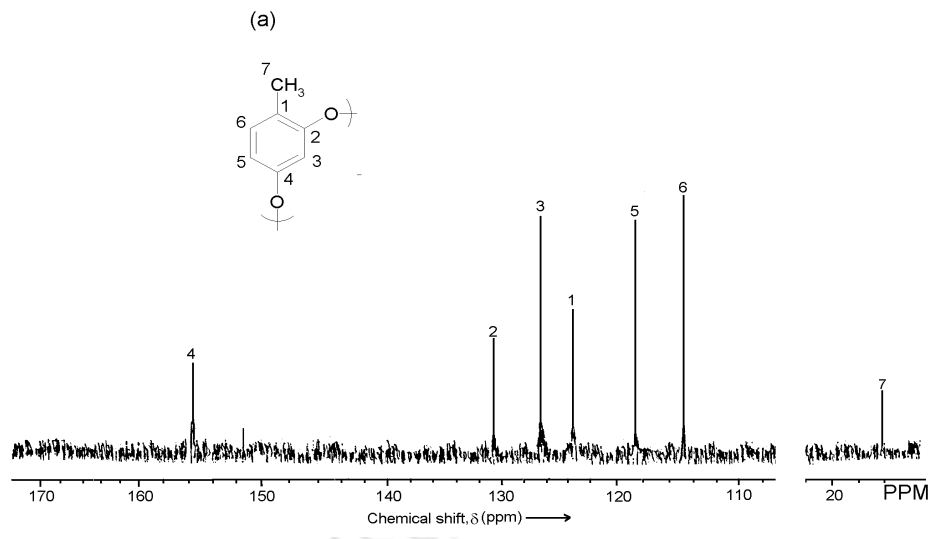
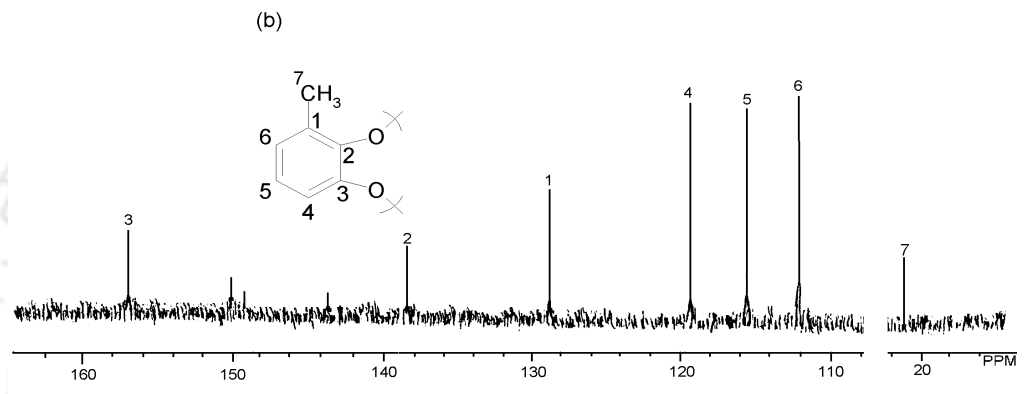
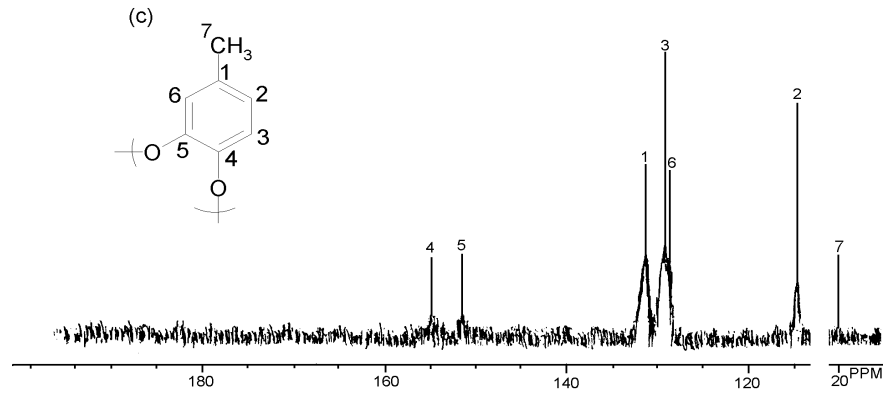




Fig. 2.11:  $^{13}\text{C}$   $\{^1\text{H}\}$  nmr spectra of (a) poly (*o*-methyl phenylene ether) (b) poly (*m*-methyl phenylene ether) (c) poly (*p*-methyl phenylene ether)

The GPC of these oligomers are relatively simple. They have low molecular weight having  $M_n$  values in the range of 1000-3500 with

respect to the polystyrene standard. The dispersity of the oligomer ( poly *p*-methylphenylene ether )was found to be highest among the four and shows a wide spread of the molecular weight. The GPC of the oligomer of polyphenylene ether is shown in figure 2.12.

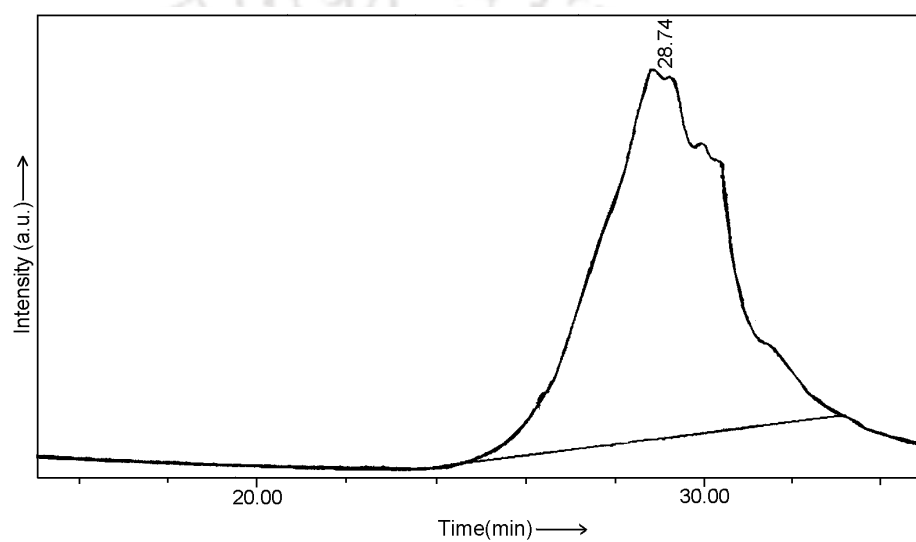


Fig.2.12 : GPC profile of poly phenylene ether

The phenolic compounds having 2 and 6 positions blocked by a methyl group should result in a linear oligomers. This type of oligomer have found wide application as engineering plastic. However , in our case we observed that the linear oligomers can be prepared by oxidative

coupling reaction of 2,6-dimethylphenol with hydrogen peroxide using cobalt diacetylmonoxime complex as the catalyst ( Equation 2.6 ) The product obtained in this case is also characterised by spectroscopic techniques.

The assignment of the proton nmr spectra of the oligomer is shown in fig 2.13. The spectrum has three sets of signals from the methyl group, the aromatic protons and hydroxy proton. The aromatic proton appears as sharp singlet at 7.1 $\delta$  suggests that they are magnetically equivalent. However, this result can not distinguish the C-O and C-C bonded oligomers. To distinguish between C-C and C-O bonded oligomer the  $^{13}\text{C}$  nmr was recorded. The  $^{13}\text{C}\{^1\text{H}\}$  nmr spectra of the compound suggests the linear and uniform nature of the oligomer (fig 2.14). The monomer has

$^{13}\text{C}$  signals at 15.80, 120.16, 122.94, 128.53 and 152.04  $\delta$  but on oligomerisation same number of prominent signals at 16.70, 124.40, 125.85, 131.53 and 152.03  $\delta$  are observed. In addition to these there is a minor signal at 128.13  $\delta$  from the end group. However, in this case to our surprise we have observed that there is a C-C as well as C-O bond rather than uniform C-O bond as depicted in figure 2.14.

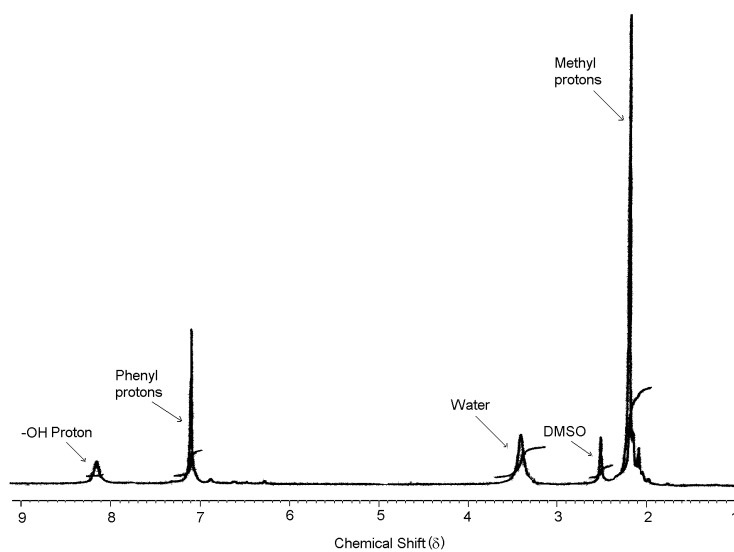


Fig. 2.13 :  $^1\text{H}$  nmr spectra ( DMSO- $d_6$  ) of oligomer of 2,6-dimethyl phenol

IR spectra of the compound gives a sharp broad peak at  $3438\text{ cm}^{-1}$  due to the hydroxyl group. The O-H deformation band is observed at  $1200\text{ cm}^{-1}$ . The C-O bond stretching for the molecule is observed as a sharp signal at  $1489\text{ cm}^{-1}$ . The characteristic stretching frequency for the methyl groups is observed at  $2919\text{ cm}^{-1}$  as a sharp signal. The absorption due to the aromatic C=C bond stretching is observed at  $1591\text{ cm}^{-1}$ . The oligomer has  $M_n$ ,  $M_w$  values as 1017 and 1101 with the polydispersity value 1.08.

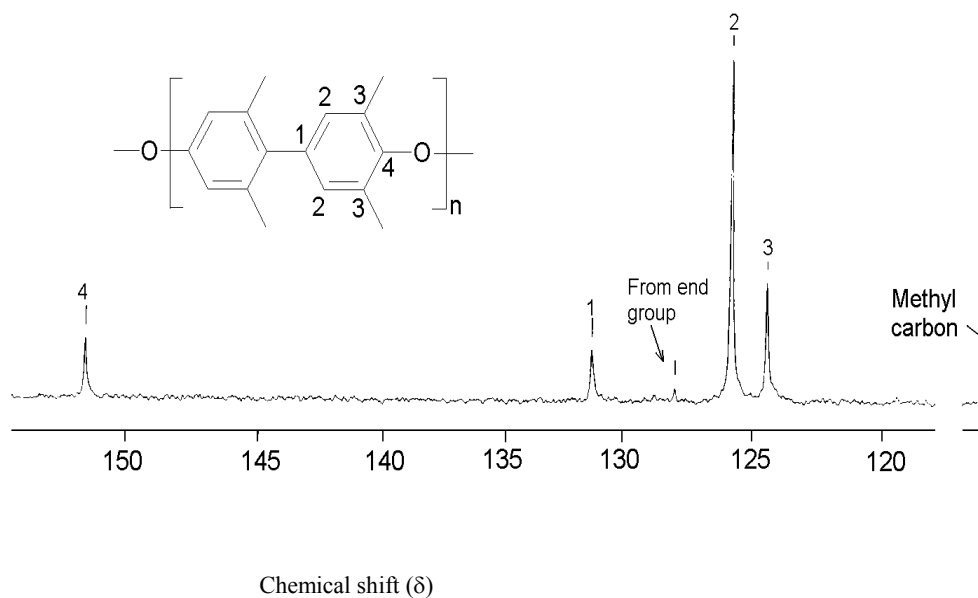


Fig. 2.14 :  $^{13}\text{C}$   $\{^1\text{H}\}$  nmr spectra the oligomer of 2,6-dimethyl phenol

The GPC of the oligomer is shown in fig. 2.15.

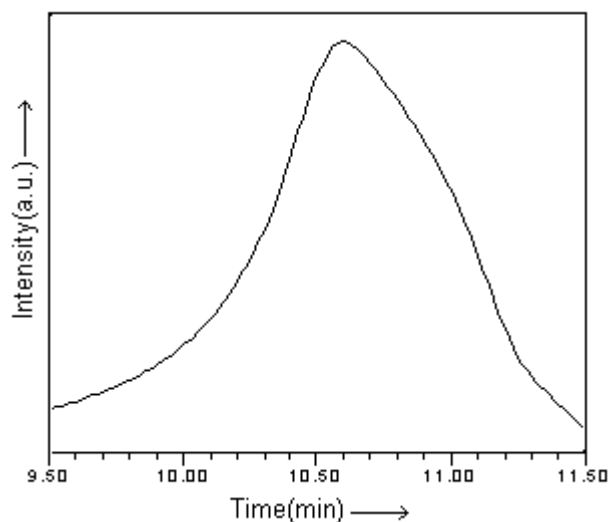


Fig. 2.15: GPC of the oligomer of 2,6-dimethyl phenol

These results indicate that the reaction of phenols with cobalt catalyst is substrate dependent. Depending on the substrate the C-C as well as C-O bonded compounds are formed. Possibly C-O and C-C bond formation are dependent on the stability of a radical generated *in situ* that can either undergo C-C or C-O bond formation<sup>120</sup>. Frontier molecular orbital calculation also supports preferential coupling of delocalised radical at the site of high spin density<sup>119</sup>. From esr studies of alkyl substituted phenoxy radicals the spin density at the para position was found to be

almost twice as that of the ortho position<sup>120</sup>. But the presence of two methyl groups adjacent to the oxygen atom make the C-O attack less prominent and thus C-C bonded compounds are formed which in turn oligomerises to the product. However in the case of *o*, *p*, *m*-cresol they prefer to have C-O bond formation owing to the relatively less steric effect and the reaction proceeds through path A (scheme 2.7). These kinds of C-C and C-O bond formation are common in oxidative coupling reactions<sup>121</sup>.

In order to obtain information on the actual mass of the oligomer the mass spectra of poly (*m*-methyl phenylene ether) is recorded and is shown in figure 2.16. The mass spectrum shows a distribution of *m/e* values in the range of 1630-2636. The oligomers thus have comparatively narrow molecular weight distribution ranging from 13 to 21 units. The different mass fractions obtained in this case are at 2626.34, 2560.08, 2528.15, 2125.39, 2048.06, 1706.16, 1667.31 and 1630.37.



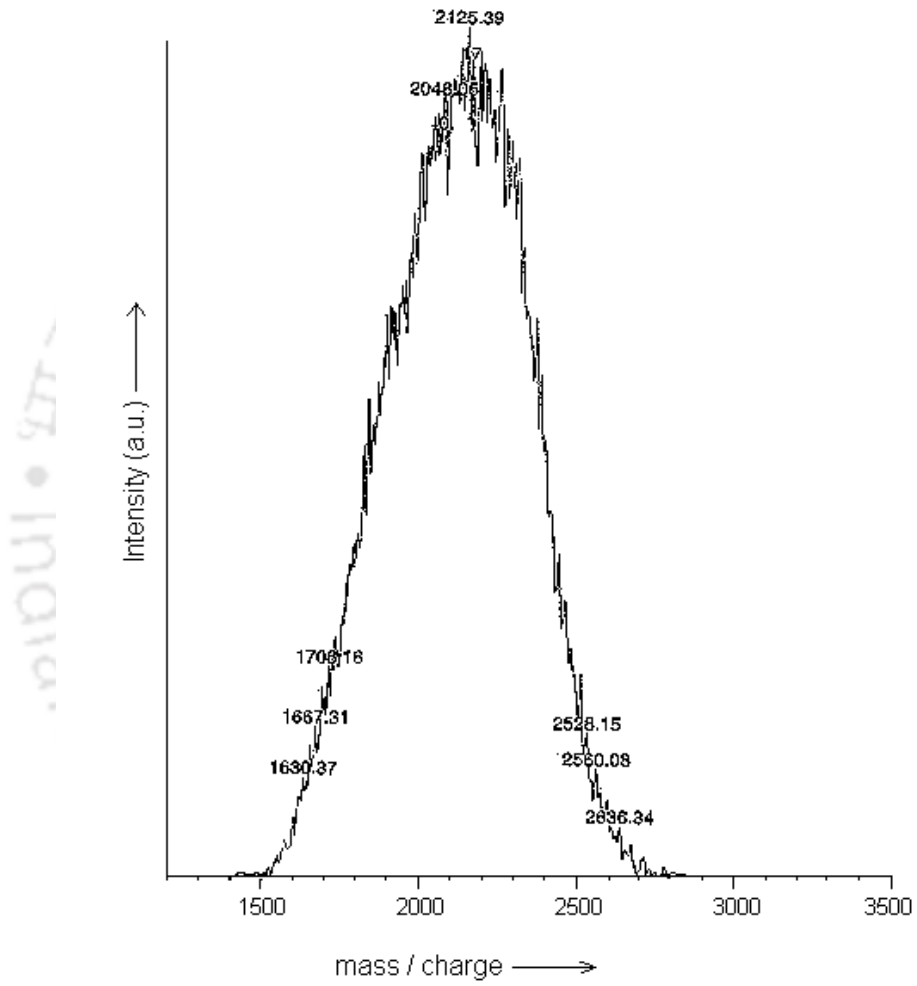
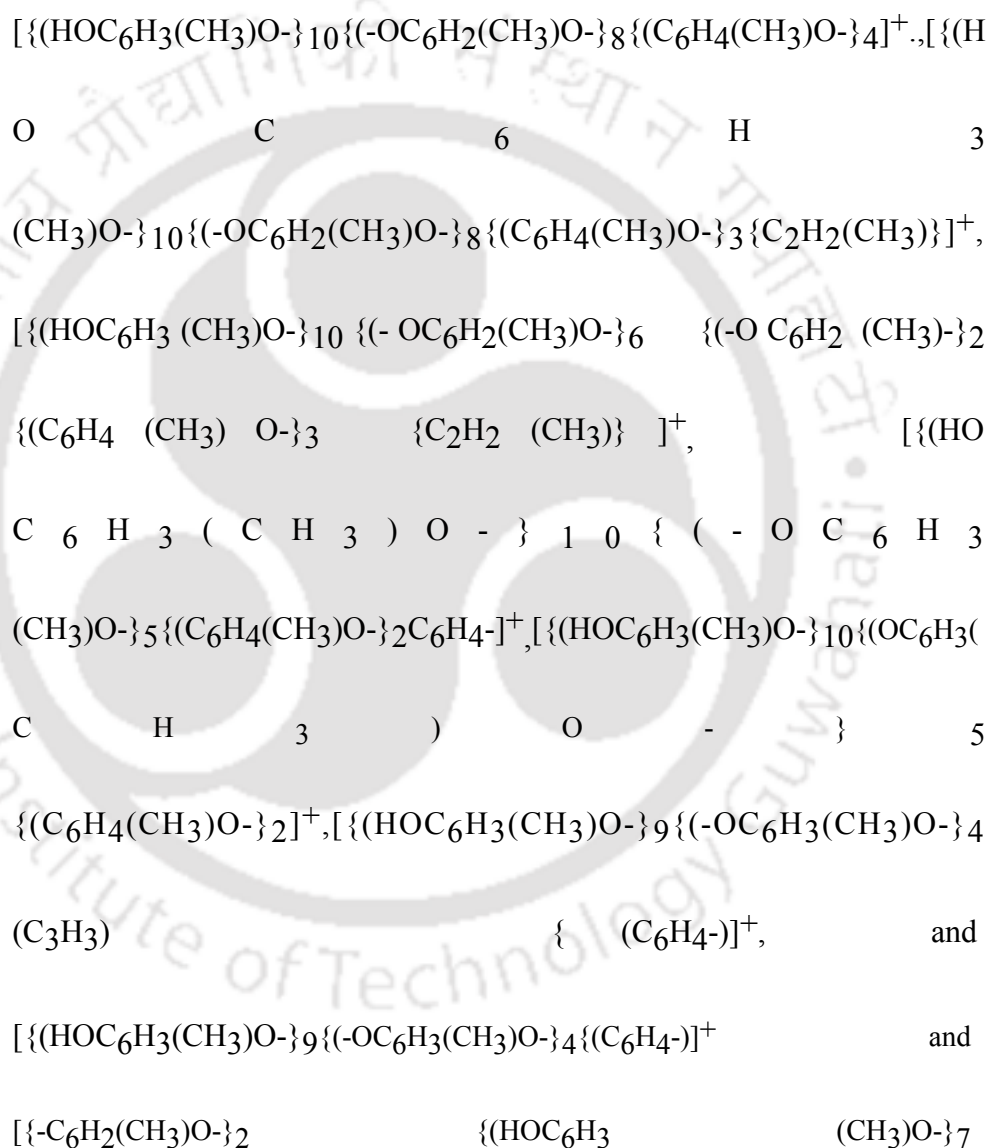


Fig. 2.16 : MALDI mass spectra of poly ( m-methyl phenylene ether )

These can respectively be assigned as due to the compositions



$\{(-OC_6H_3(CH_3)O-)_4(C_6H_4-)\}^+$ . The highest intensity peak (base peak) is observed at 2125.39.

The thermal studies would not only provide understanding of their thermal stability but also the extent of water being adsorbed on the oligomers and it will also provide information regarding possible phase transitions. The polyphenols are referred to as high thermal resistant material<sup>122</sup> and have found application in industry. We have found that these oligomers are hygroscopic and contain water of crystallisation. The DSC trace of polyphenylene ether is shown in figure 2.17. The DSC profile indicates that the oligomer exhibit endothermic process at 30-80<sup>0</sup>C. Above 140<sup>0</sup> C it shows continuous exothermic process. This is indicative of a internal structural change of the product molecule at that temperature range.

The DSC traces for the other three oligomers namely poly (*o*-methyl phenylene ether), poly (*m*-methyl phenylene ether) and poly (*p*-methyl phenylene ether) are shown in the figure 2.18. In this case also

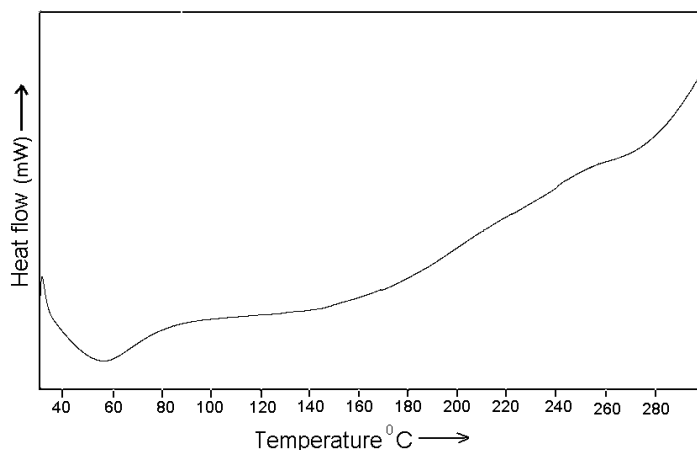


Fig. 2.17 : DSC trace of polyphenylene ether (heating rate of 5<sup>0</sup>C / min.)

also it has been observed that the oligomers exhibit endothermic behavior to a definite temperature characteristic of every compound and beyond that temperature the compounds exhibit exothermic behavior. The compound does not melt within this temperature range. The characteristic temperature to which the initial endothermic process occurred are 60<sup>0</sup>C for poly (*p*-methyl phenylene ether), 58<sup>0</sup>C for poly (*o*-methyl phenylene ether), and 70<sup>0</sup>C for poly (*m*-methyl phenylene ether). DSC trace of the product from *m*-isomer shows a sudden increase of heat desorption at around 280<sup>0</sup>C

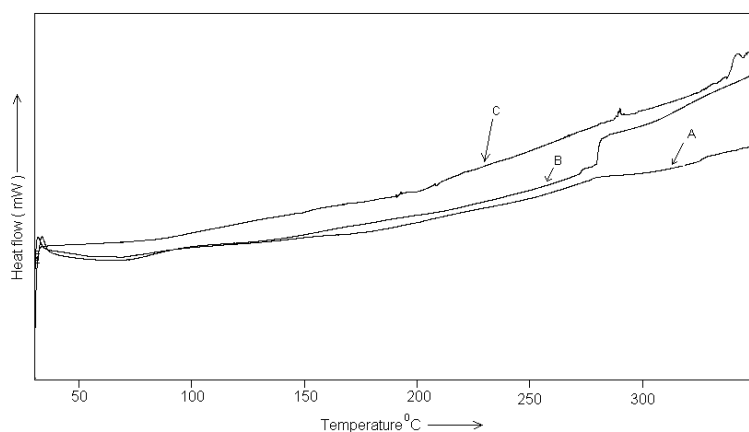
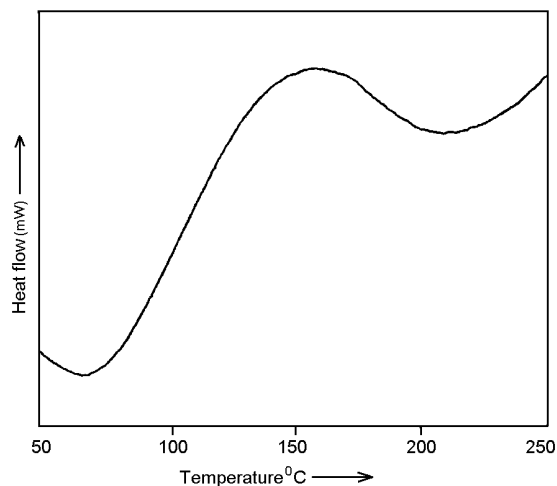


Fig 2.18 : DSC traces of (A) poly (*o*-methyl phenylenether), (B) poly (*m*-methylphenylene ether) and (C) poly (*p*-methylphenylenether) (heating rate of 5<sup>0</sup>C / min.)

which is indicative of some internal structural change of the compound at that temperature range. This may be attributed to a possible glass transition taking place at this temperature. In thermogravimetric analysis (TG) there is no sudden weight loss at this temperature which also supports our view (fig 2.21). The continuous nature of the DSC traces of the other two compounds from *o*-cresol and *p*-cresol follows a slightly different path from 200<sup>0</sup>C onwards with a relatively higher rate of heat desorption.

The DSC of the oligomers derived from *para* cresol is compared with the corresponding oligomer prepared by enzyme catalysed reaction. This is shown in figure 2.19. The comparison indicates that the an



exothermic peak is observed in case of the poly(*p*-methyl phenylene ether) prepared by SBP catalysed reaction at 150<sup>0</sup> C while the same is absent in

Fig. 2.19 : DSC trace of poly (*p*-methyl phenylene ether) obtained by SBP catalysed reaction

case of the polymer obtained by our method. The appearance of the exothermic peak may correspond to cleavage of the branching and / or crosslinking of the polymer. Similar DSC traces were also obtained in case

of the polymers prepared by horseraddish peroxidase catalysed polymerisation of phenol. This indicates that the possibility of branching in the case of the polymers obtained by other methods with hydrogen peroxide using cobalt diacetylmonoxime (2.V) as the catalyst. The

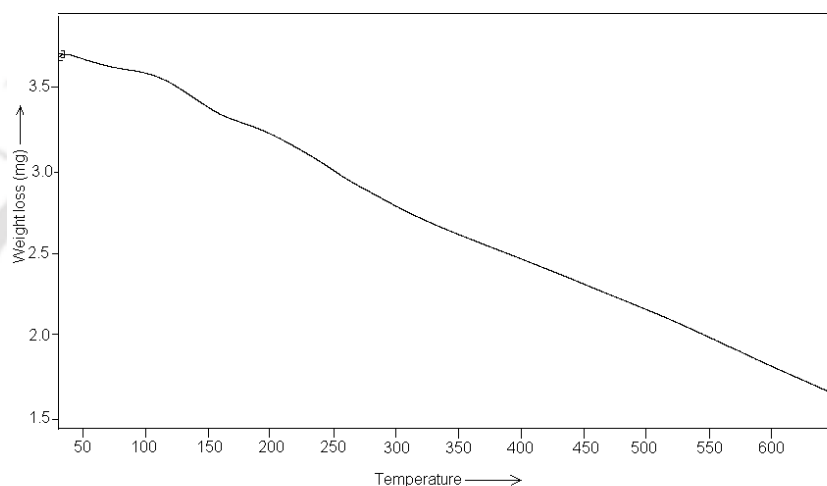


Fig. 2.20 : Thermogram of polyphenylene ether ( heating rate of 50°C / min under nitrogen atmosphere.)

thermogram of polyphenylene ether (fig. 2.20) in between the temperature range 30-650°C shows that the polymer gradually loses weight leading to a continuum. There is 46 % residue remained on heating the sample to

650<sup>0</sup> C under nitrogen. The residue may be carbonised product such as polyacene and graphite like polymer<sup>123</sup>. It is apparent from the thermogram that the polymer is unstable beyond 200<sup>0</sup> C. Similar thermogram obtained for the products obtained from three different cresols are shown in figure 2.21. The TG traces of the products from *o*-cresol, *p*-cresol and *m*-cresol follows continuous loss of weight in a similar way as that obtained for polyphenol. In all the cases in an average 30-40 % weight of the products are remained as residue at 650<sup>0</sup>C under nitrogen.

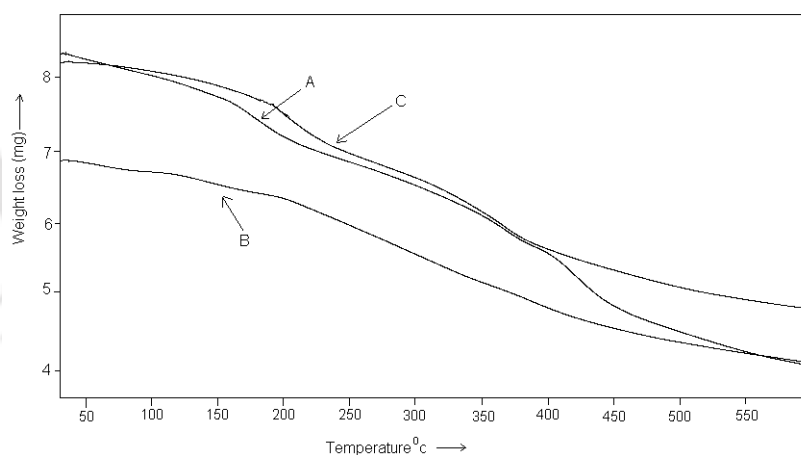


Fig. 2.21 : Thermogram of (A) poly (*o*-methyl phenylene ether), (B) poly (*m*-methylphenylene ether) and (C) poly (*p*-methylphenylene ether) ( heating rate of 50C / min under nitrogen atmosphere)

### 2.3.3 Oxidative polymerization of aniline

Polyaniline comprise of a class of polymers obtained from aniline through C-N bond. These class of polymers have wide applications in the field of electrical, electrochemical and optical display<sup>124</sup>. They are usually prepared by oxidative polymerisation reactions. The oxidative polymerisation includes enzymatic as well as use of common oxidants<sup>125</sup>.

Polyaniline can have different forms depending on the extent of oxidation. They are of three types namely, Leucomeraldine, Emeraldine and Pernigraniline(fig 2.22). Depending on the methodology applied during the synthesis; synthesis of specific form is possible. The form A can be distinguished from the B and C as the benzenoid rings are not present in A. B and C has both the benzenoid and benzene structures but the benzenoid structures are relatively less in the case B.

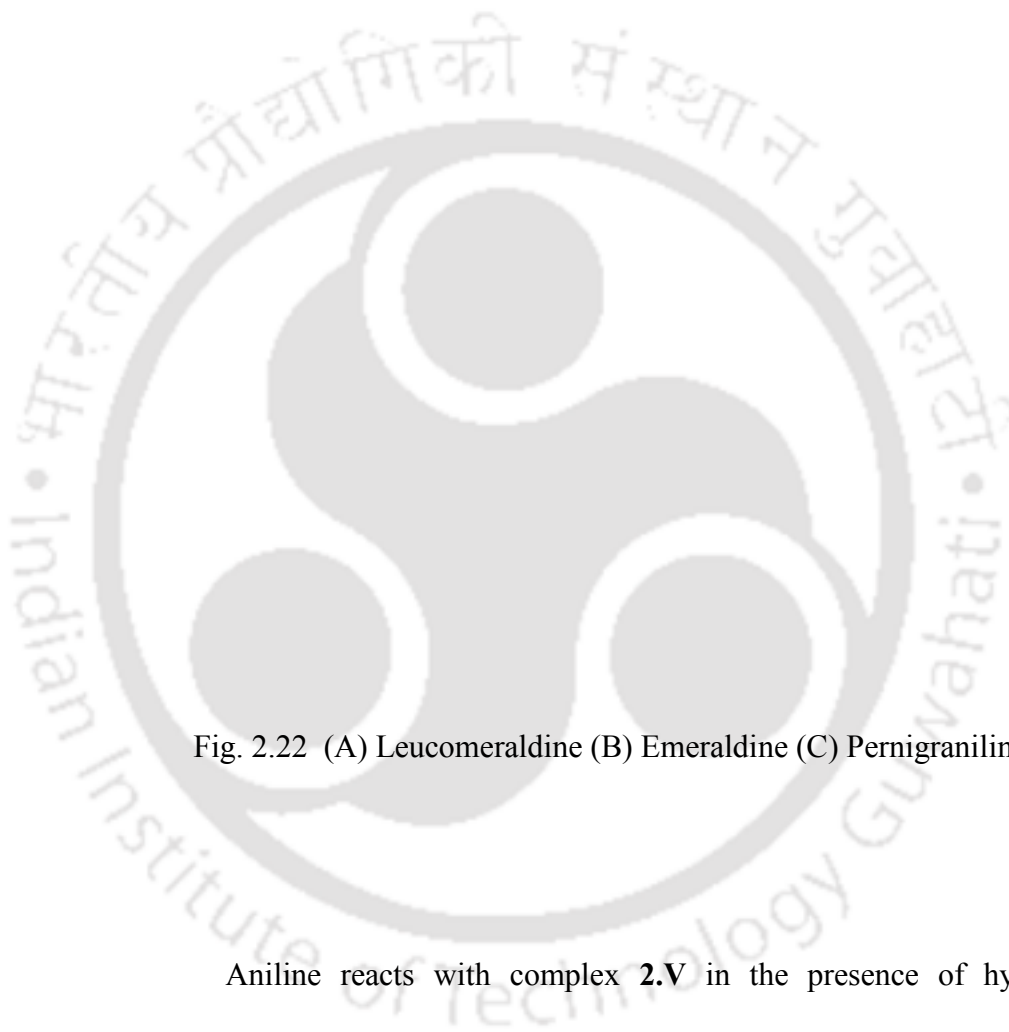


Fig. 2.22 (A) Leucomeraldine (B) Emeraldine (C) Pernigraniline

Aniline reacts with complex **2.V** in the presence of hydrogen peroxide at  $60^{\circ}\text{C}$  gave polyaniline. This reaction is represented by equation 2.7.

The IR spectrum of polyaniline has broad absorption at  $3300\text{cm}^{-1}$  corresponding to the N-H antisymmetric stretching frequency. The weak absorption at  $2925\text{ cm}^{-1}$  corresponds to N-H symmetric stretching frequency. The N-H deformation band is observed at  $1670\text{cm}^{-1}$ . The characteristic *p*-substituted derivatives of aniline are observed at  $1642\text{ cm}^{-1}$

The  $M_n$  and  $M_w$  values for the polyaniline prepared by cobalt diacetylmonoxime complex catalysed reaction are 1256, 1892 respectively. The GPC of the oligomer is shown in (fig.2.23). The narrow polydispersity of the polyaniline suggests a narrow distribution of chain length and also suggests the termination of the oligomerisation at

comparable chain length. The proton nmr of the oligomers has multiplets in the region of 8-6.6 ppm (fig 2.24). for a simple pernigraniline type of oligomer the proton nmr are simple in the aromatic region. But we have observed a relatively complex nmr spectra in this region. This suggests

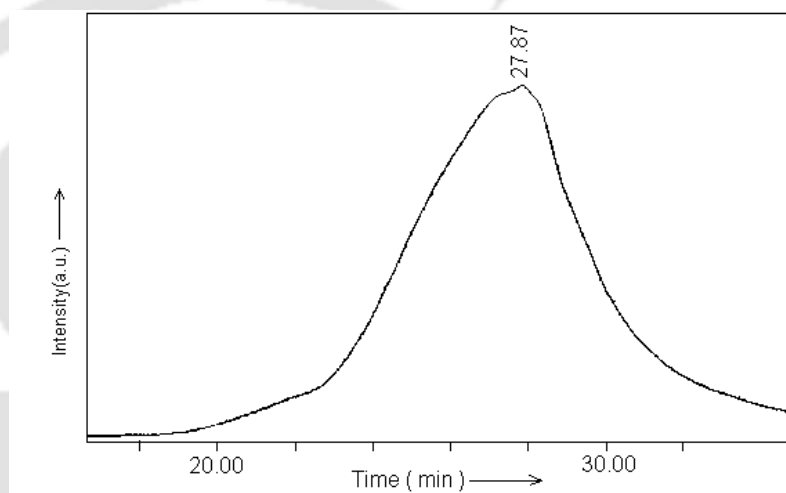
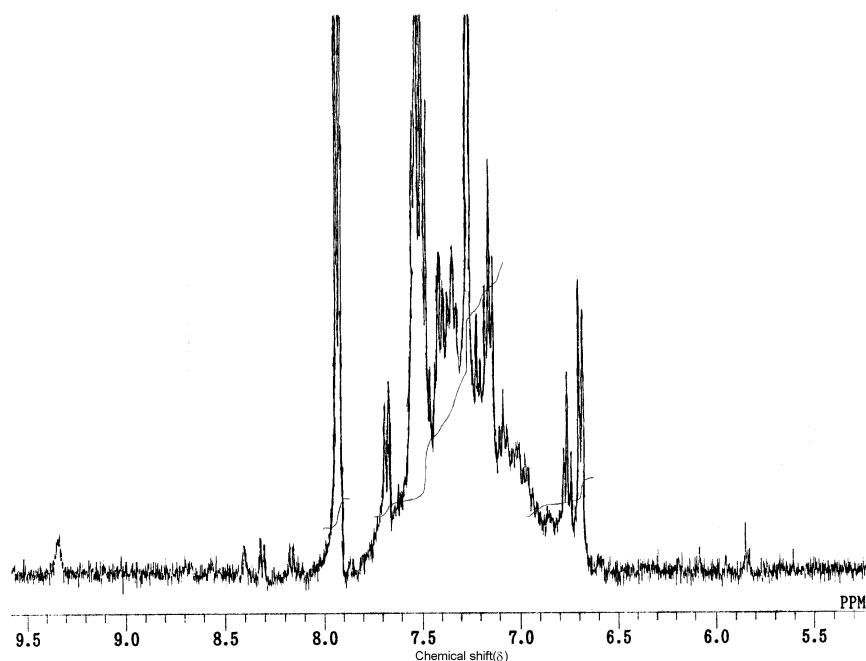


Fig 2.23 : GPC of polyaniline

Fig. 2.24  $^1\text{H}$  nmr spectra of polyaniline

that it may be possible that C-C bond formation during the oligomerisation has taken place.

The existing literature has also reports on the alternate C-C and C-N bonded oligomer(form B of figure 2.25). Such oligomers have characteristic nmr signals. But in proton nmr the aromatic region of our



oligomer is complicated to clearly assign the peaks. But the  $^{13}\text{C}$  nmr is relatively simple and has six signals. Literature suggests that the form A of

polyaniline has four signals, two due to the quinonic type and two due to reduced type of aromatic nuclei. It is important to note that we have not isolated diphenylamine nor diphenyl amine can be oligomerised by the same catalytic system under analogous condition to give the oligomer. Thus we prefer to assign the oligomer as short chain C-N bonded partially oxidised oligomer having structure B.

The  $^{13}\text{C}$  nmr signals can be a tool to ascertain the skeletal structure for the polyaniline. The  $^{13}\text{C}$  nmr signals for quinonic and benzene type of rings are simple to understand. In addition to each of these units being symmetric, they would have only two sets of carbon signals. It is to be noted that polyaniline oligomers may be end-capped with a variety of groups such as phenyl amine etc<sup>126</sup>. Since the GPC is relatively simple and having dispersity close to unity therefore there is little possibility of *ortho*-,

*para*- branching in the product. In fact in the  $^{13}\text{C}$  nmr spectra of the oligomer gives six  $^{13}\text{C}$  signals. Thus we can draw different possibilities for the structure of the polyaniline as shown in fig 2.25. This includes the emeraldine form of the oligomer along with the one accompanying with carbon carbon bond formation. The another possibility that accompanying with carbon carbon bond formation (B) can be ruled out on the basis of the number of signals obtained. This possible form should give a total of ten signals in the  $^{13}\text{C}$   $\{^1\text{H}\}$  nmr spectrum. Therefore the probable structure is (A) and the observed  $^{13}\text{C}$  signals are assigned assuming this as the skeletal structure. Thus the oligomer have a short chain structure in which there is oxidised and reduced form of aromatic ring.

The  $^{13}\text{C}\{^1\text{H}\}$  nmr spectra of the oligomer is shown in fig. 2.26. with the assignment of the individual carbon atoms for each  $^{13}\text{C}$  signal.

Polyaniline prepared by cobalt catalysed reactions has IR absorbance which has resemblance with reported IR of polyaniline prepared by nickel catalysed dehalogenative coupling reactions<sup>127</sup>. However, elemental analysis deviates from the calculated elemental analysis of polyaniline. This suggests that the polyaniline has metal ion bound to the oligomer. To know about the exact mass of the oligomer MALDI mass spectra of the

sample is recorded and the spectra is shown in (figure2.27 ). The highest m/e obtained at 1405.9 is due to a composition of  $[C_6H_5(NHC_6H_4)_{13}NH_2 CoCl_2]^+$  unit, few of the other mass fragments obtained are at 1310.6, 1219.1, 1190.7, 1126.9, 1050.2, 1034.9, 973.7, 957.8, 941.9, 774.3, 757.6,

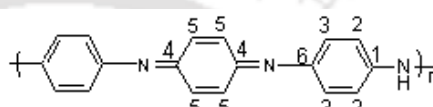
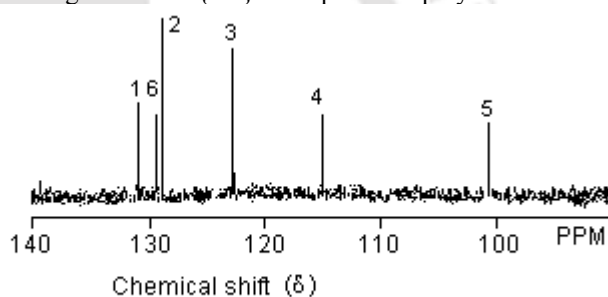
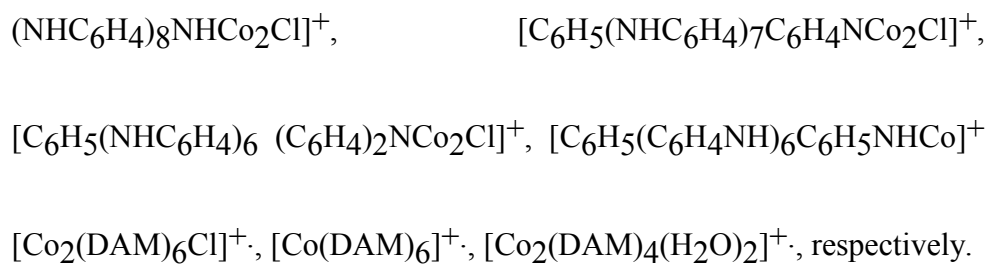


Fig. 2.26  $^{13}C\{^1H\}$  nmr spectra of polyaniline



664.1 and 558.8 can be assigned as due to the compositions  $[C_6H_5(NHC_6H_4)_{13}NHCl]^+$ ,  $[C_6H_5(NHC_6H_4)_{12}NHCl]^+$ ,  $[C_6H_5(NHC_6H_4)_{11}NHCl]^+$ ,  $[C_6H_5(NHC_6H_4)_{10}NHCl]^+$ ,  $[C_6H_5(NHC_6H_4)_{9}NHCl]^+$ ,  $[C_6H_5(NHC_6H_4)_{8}NHCl]^+$ ,  $[C_6H_5(NHC_6H_4)_{7}NHCl]^+$ ,  $[C_6H_5(NHC_6H_4)_{6}NHCl]^+$ ,  $[C_6H_5(NHC_6H_4)_{5}NHCl]^+$ ,  $[C_6H_5(NHC_6H_4)_{4}NHCl]^+$ ,  $[C_6H_5(NHC_6H_4)_{3}NHCl]^+$ ,  $[C_6H_5(NHC_6H_4)_{2}NHCl]^+$ ,  $[C_6H_5NH(NHC_6H_4)_{13}N_2Cl]^+$ ,  $[C_6H_5NH(NHC_6H_4)_{12}N_2Cl]^+$ ,  $[C_6H_5NH(NHC_6H_4)_{11}N_2Cl]^+$ ,  $[C_6H_5NH(NHC_6H_4)_{10}N_2Cl]^+$ ,  $[C_6H_5NH(NHC_6H_4)_{9}N_2Cl]^+$ ,  $[C_6H_5NH(NHC_6H_4)_{8}N_2Cl]^+$ ,  $[C_6H_5NH(NHC_6H_4)_{7}N_2Cl]^+$ ,  $[C_6H_5NH(NHC_6H_4)_{6}N_2Cl]^+$ ,  $[C_6H_5NH(NHC_6H_4)_{5}N_2Cl]^+$ ,  $[C_6H_5NH(NHC_6H_4)_{4}N_2Cl]^+$ ,  $[C_6H_5NH(NHC_6H_4)_{3}N_2Cl]^+$ ,  $[C_6H_5NH(NHC_6H_4)_{2}N_2Cl]^+$ ,  $[C_6H_5NH(NHC_6H_4)N_2Cl]^+$ ,  $[C_6H_5N_2Cl]^+$ ,  $[C_6H_5NH_2]^+$ ,  $[C_6H_5NH]^+$ ,  $[C_6H_5N]^+$ ,  $[C_6H_5]^+$



UV-vis. spectra of the compound has a  $\pi - \pi^*$  absorption peak at 404 nm. The Leucomeraldine type polyaniline gives the absorption peak at 325nm.<sup>128,129</sup> The bathochromic shift observed in our case may be due to the  $\pi$ -conjugation system giving pernigraniline type of oligomer. Our system has also clear distinction from C-C, C-N bonded polyaniline

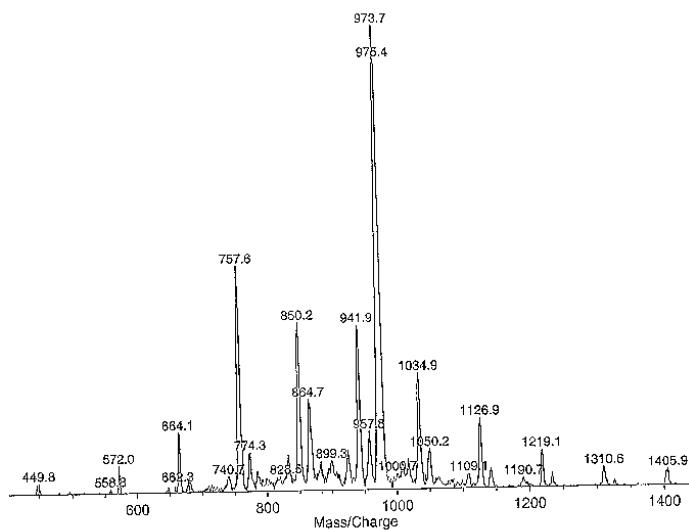


Fig. 2.27 : MALDI mass spectra of polyaniline

having the backbone A in fig. 2.11. Poly(diphenylamine-4,4'-diyl), has the  $\pi - \pi^*$  absorption peak at 380 nm.<sup>128</sup> The UV-vis. spectra of the compound is shown in fig. 2.28.

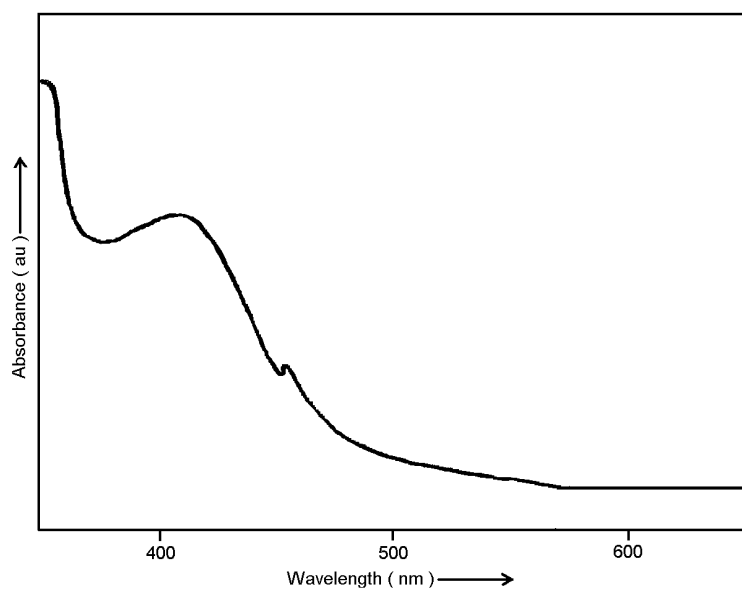
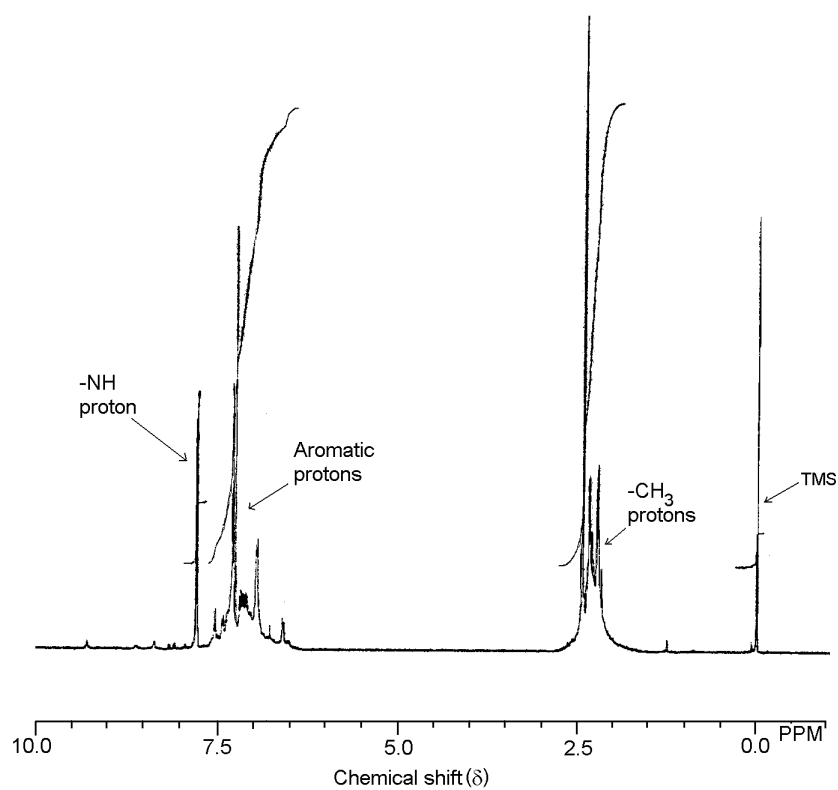


Fig.2.28. UV-visible spectra of the polyaniline

In analogous manner it is possible to oligomerise the *p*-methylaniline, *p*-methoxyaniline to give polyaniline. The proton nmr spectra of the oligomer obtained from *p*-methylaniline shows two sets of multiplets arising from the aromatic protons and the methyl protons together with a singlet due to the NH protons (fig.2.29). The integration ratio of the two sets of multiplets is 1:1 which indicates that the oligomerisation reaction has given a uniform backbone with linear cross link. IR spectra of the oligomer possess the characteristic vibrational frequencies for –NH protons. The –NH antisymmetric stretching is

observed as a sharp broad signal at  $3306\text{cm}^{-1}$  and the  $\text{-NH}$  symmetric vibration is observed as a weak signal at  $3029\text{cm}^{-1}$ . The  $\text{-NH}$  deformation band is observed as a weak signal at  $1680\text{cm}^{-1}$ . The



characteristic absorption for the methyl group is observed at  $2922\text{cm}^{-1}$ .

Fig. 2.29 :  $^1\text{H}$  nmr spectra of oligomer of p-methyl phenol

The absorption due to C=C stretching of the aromatic nucleus is observed at  $1605\text{cm}^{-1}$  and  $1514\text{cm}^{-1}$ . Molecular weight determination of the oligomer shows it to have the ( $M_n$ ,  $M_w$ ) values as (985, 1035) and the polydispersity is 1.05.

Similarly the product from oxidative oligomerisation of *p*-methoxy aniline has the proton nmr spectra having two sets of multiplet at 6.0-7.5  $\delta$  and 3.0-3.5  $\delta$  due to the aromatic protons and the methyl protons respectively. They have equal integration ratio and this suggests that the linear chain oligomers are formed. The IR spectra of the compound possess the characteristic -NH stretching at  $3306\text{cm}^{-1}$  as broad and sharp absorption. The characteristic absorption for the methyl group attached as ether is observed at  $2832\text{cm}^{-1}$ . The absorption due to the vibration of the C=C bond is observed as strong signal at  $1610\text{cm}^{-1}$ . The number average and weight average molecular weight ( $M_n$ ,  $M_w$ ) of the product, were found to be 959 and 967 respectively with the polydispersity value as 1.01.

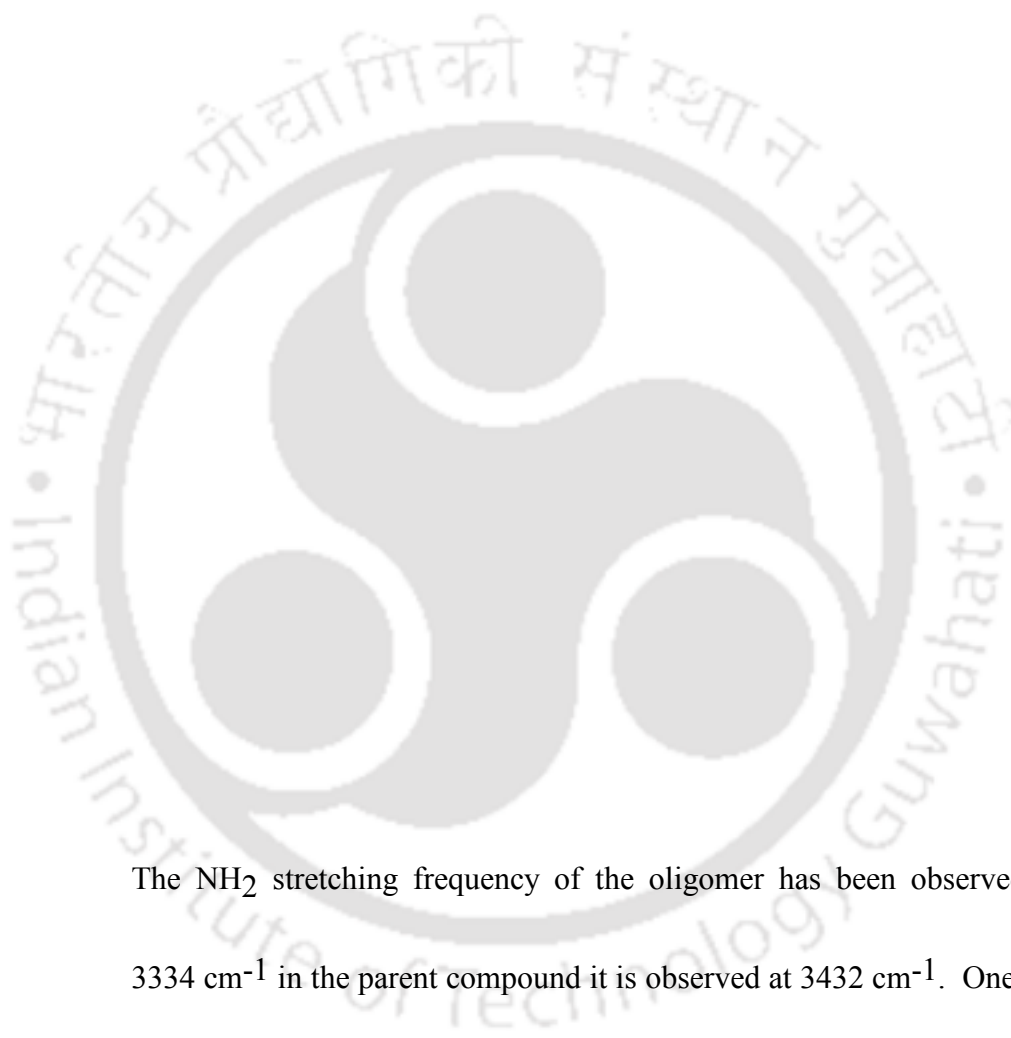
The narrow distribution suggests it to comprise of 8-10 units of the monomer in the oligomeric product.

### 2.3.4 Reactions of diaminobenzenes

Diaminobenzene compounds are important class of building block for construction of C-N as well as N-N bonded oligomers. There are reports in which it suggests that these oligomers either form cyclic compounds through di, trimerisation or gives C-N or N-N bonded oligomer depending on reaction condition such as the reagent or controll of  $p^H$  during the oxidation reaction<sup>130</sup>. There are reports in which N=N bonded oligomers are prepared from oxidative reactions of phenylene diamine derivatives. In a N=N bonded oligomer there are different possibilities<sup>131</sup> of orientation about the N=N bond which are depicted in figure 2.30. The orientation may be in a *cis-cis* or *cis-trans* or *trans-trans* depending on the orientation of the N=N bond with respect to the phenyl groups. 1,4

- Diaminobenzene oligomerises to give low molecular weight oligomer when reacted with hydrogen peroxide in presence of diacetylmonoxime cobalt(II) catalyst. The reaction of 1,4-diaminobenzene can be depicted as shown in (equation 2.7).

The reaction leads to N-N bonded oligomers. The IR spectra of the oligomer has infrared absorptions at  $3334\text{cm}^{-1}$  due to antisymmetric N-H stretching, at  $2665\text{ cm}^{-1}$ , and at  $1603\text{ cm}^{-1}$  due to NH stretching ,  $1544\text{ cm}^{-1}$  due to aromatic nucleus,  $1272\text{ cm}^{-1}$  and  $1235\text{ cm}^{-1}$  due to C-N stretching.



The NH<sub>2</sub> stretching frequency of the oligomer has been observed at 3334 cm<sup>-1</sup> in the parent compound it is observed at 3432 cm<sup>-1</sup>. One strong absorption observed at 2665 cm<sup>-1</sup> can be attributed to strong intermolecular hydrogen bonding among the free NH<sub>2</sub> group with the NH-NH or N=N

group. Another absorption was observed at  $1545\text{ cm}^{-1}$  which is assigned to the trans N=N bond stretching.

The  $^1\text{H}$  NMR spectra of the oligomer shows signals at 6.7(s), 6.0(s), 5.75(s) and 5.0(broad s)  $\delta$  due to the aromatic nuclei and NH protons (fig.2.31).  $^{13}\text{C}\{^1\text{H}\}$  NMR spectra of the compound is shown in fig. 2.32.

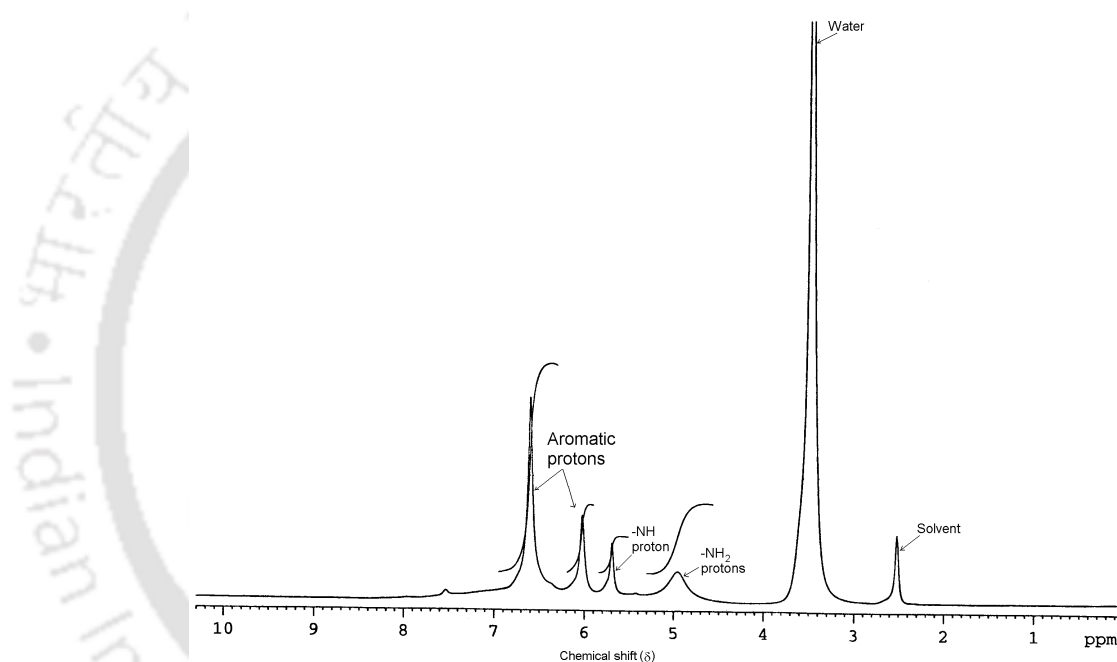


Fig. 2.31  $^1\text{H}$  nmr (DMSO- $d_6$ ) spectra of the oligomer of 1,4-phenylenediamine

The observed six different  $^{13}\text{C}$  signals can be assigned as shown in the fig. 2.32. Assuming the skeleton of the backbone of the product as shown

along with the nmr spectra in fig. 2.32 the oligomer can be explained to be linear one without undergoing any branching as well as C-N bond formation. Thus the  $^{13}\text{C}$  spectra of the oligomer contains signals from both quinonic and benzenoid type of nuclei in the oligomer.

This indicates the presence of both  $-\text{N}=\text{N}$  and  $-\text{NH}-\text{NH}-$  type of bonding in the product. It is to be noted that the parent compound contains

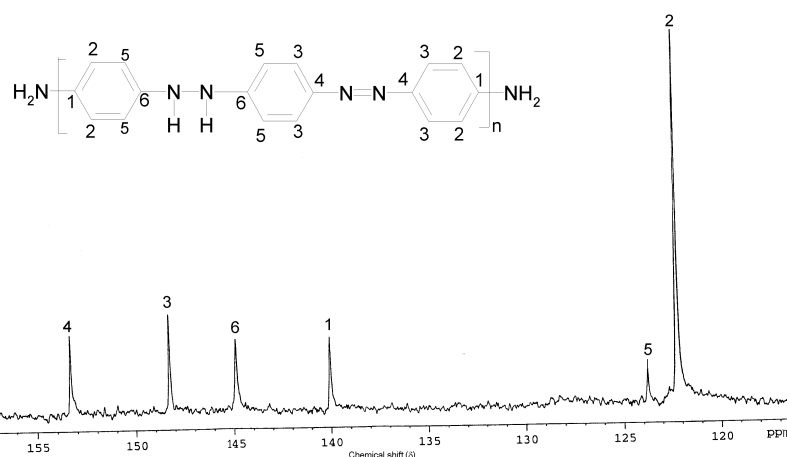


Fig. 2.32 :  $^{13}\text{C}\{^1\text{H}\}$  nmr (  $\text{CDCl}_3$  ) spectra of oligomer of 1,4- phenylenediamine

two  $^{13}\text{C}$  signal at 115.29 and 138.69  $\delta$ .

In the UV-visible spectra of the oligomer it possess strong absorption at 473nm ( $\epsilon = 9.965 \text{ lit. g}^{-1}\text{cm}^{-1}$ ) and 332nm( $\epsilon = 13.02 \text{ lit. g}^{-1}\text{cm}^{-1}$ ) ( Fig. 2.33). (Poly diphenylamine-1,4-diyl) also shows  $\pi - \pi^*$

transition and strong absorption at 325nm<sup>128</sup>. Which suggests that there is extensive delocalisation in the system through C-N=N-C back bone.

Similar reaction with 1,3-diaminobenzene and 1,2-diaminobenzene yielded mixture of low molecular weight compounds and since it did not give any major isolable product, it was not possible to characterise them by



conventional techniques.

The thermal stability of the oligomer of 1,4-diaminobenzene is

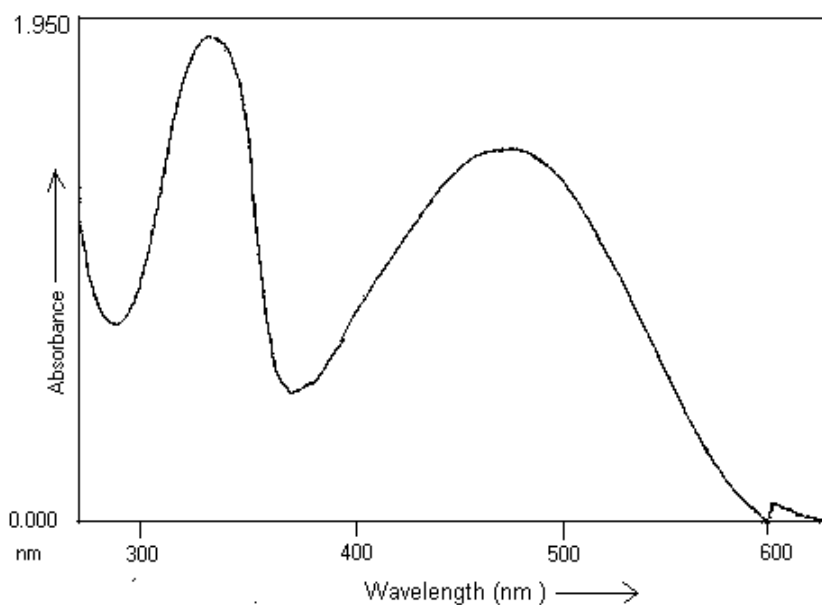


Fig. 2.33

determined from the TG traces in the temperature range of 30-650<sup>0</sup>C ( fig. 2.34). The thermograms here shows a continuous loss of weight with increasing temperature. The weight loss observed for the oligomer at 650<sup>0</sup>C is 57 %. The continuous weight loss probably occurs due to the cleavage of

N=N bond whereby it loses dinitrogen molecule and also loses smaller unit as anilinic part.

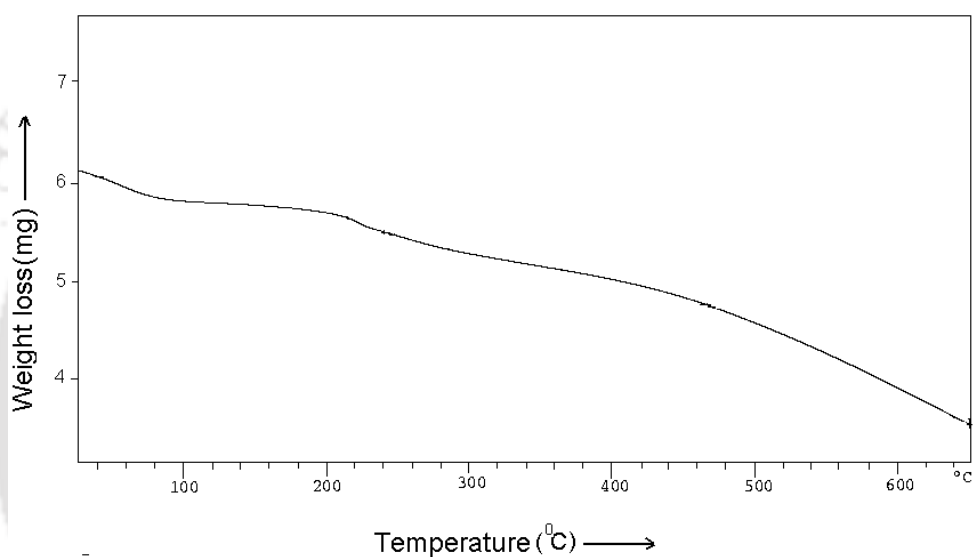


Fig. 2.34 : Thermogram of oligomer of 1,4-phenylenediamine

#### 1.4 Mechanistic study of the reactions

##### 2.4.1 Recycling of oxygen from hydrogen peroxide during cobalt catalysed oxidative reactions

It is an established fact that hydrogenperoxide can be decomposed to oxygen by various metal salts<sup>132</sup>. Cobalt salts are not exception to this. It is important to know whether oxygen liberated during cobalt catalysed oxidation reactions can be recycled during oxidation reactions. Depending on the nature of the cobalt complexes it may have primary interaction with O<sub>2</sub> leading to reversible binding with cobalt(II) during oxidation reactions<sup>133</sup>. This may follow oxidation of the metal center to a higher oxidation state. The oxidized metal center thus may contribute to the catalytic process of oxidation or it may activate the oxidant and participate in the oxidation.

With these points in mind the possibility of recycling of oxygen during oxidation of organic substrate was studied. The oxidation of benzylalcohol to benzaldehyde (equation 2.8 ) by hydrogen peroxide is catalysed by cobalt(II) acetate, however in this reaction the yields are

increased when the reactions are performed under closed condition when the evolved oxygen gas is arrested in the reaction vessel. The results on the reactions carried out at different reaction conditions are mentioned in the table 2.2.

The results tabulated in table 2.2 indicate that the yield of the reaction is dependent on the control of oxygen escaping the reaction flask and also on the surrounding environment. The result also indicates that the decomposition of hydrogen peroxide to oxygen is an independent process and this competes with the oxidation process. The recycling of oxygen to the reaction shows that oxygen can be activated by cobalt(II) to give a catalytic precursor as shown in the scheme 2.8.

To ascertain whether the molecular oxygen alone can directly interact with cobalt(II) acetate to give the catalytic precursor reaction under identical condition in absence of  $N_2$ ,  $O_2$  but with  $O_2$  was performed. Such reactions were performed by replacing hydrogen

Table 2.2 Cobalt(II) catalysed oxidation of benzyl alcohol by  $H_2O_2^a$

Entry No.	Reaction condition	Moles of benzyl alcohol reacted per mole of cobalt(II) acetate

1	In O <sub>2</sub>	31
2	In N <sub>2</sub>	29
3	In Air	17 <sup>b</sup>
4	In H <sub>2</sub>	32
5	Without cobalt(II) acetate in air	Nil <sup>b</sup>

a,b → refer to experimental section

peroxide with molecular oxygen in a closed schlenk tube and under analogous condition gave no conversion of benzyl alcohol to benzaldehyde. This result further strengthens the proposition that the recycled oxygen is obtained from the decomposition of hydrogen peroxide. The reaction carried out under hydrogen atmosphere does not make any significant difference than the one carried out under nitrogen atmosphere but improves slightly the overall yield of the reaction. To know whether these reactions are caused by cobalt(III) species generated *in situ* or it is due to a peroxy-species generated in situ, two approaches were adopted. In the first approach we compared the reaction with existing results on catalytic reaction of cobalt-peroxy complexes. It is already known that cobalt-peroxy compounds can cause oxidation of organic substrates. There are also reports that describe the cobalt (III) ions to play crucial role in these oxidations<sup>134</sup>. Few cobalt(III) complexes that were tested for this purpose in the absence of oxygen were  $[\text{Co}(\text{NH}_3)_6]\text{Cl}_3$ ,  $[\text{Co}(\text{NH}_3)_5\text{Cl}]\text{Cl}_2$ ,  $\text{Co}(\text{AcAc})_3$  and they were found to be inefficient for the purpose. So, it is believed that cobalt peroxy complexes to be involved in the reactions rather than a cobalt(III) center without a peroxy group alone.

Oxidation of organic substrates by cobalt(II) acetate along with dioxygen is a well documented reaction.<sup>3</sup> The generation of radicals by an oxidation process carried out by cobalt complexes are well known and the activation of alkyl aromatics by cobalt(III) complexes is also an well known process.<sup>135</sup> Complexes are generally prepared by adding hydrogen peroxide or bubbling oxygen to hot solution of cobalt(II). All these supports towards involvement of a peroxy cobalt(III) species taking part in the reaction.

#### **2.4.2 Kinetics of the oxidative reactions by visible spectroscopy**

To ascertain whether the dione monoxime complex itself is causing the reactions or gets converted to some other species in solution the UV-visible absorption of the cobalt dione monoxime complex in acetonitrile is recorded in presence of hydrogen peroxide. The complex has its absorption at 681nm and 581nm. The two absorption of the complex on interaction with hydrogen peroxide losses slowly indicating that the absorption decreases proportionately with time ( fig. 2.35).

Based on these observation an initial interaction of hydrogen peroxide to oxidise cobalt(II) to cobalt(III)<sup>136</sup> can be suggested<sup>137</sup>.

Cobalt(III) alkyl peroxy complexes of strong field ligands affords ROO·

and RO· radicals upon mild heating in solution which facilitate the oxidation of hydrocarbon by these complexes under mild conditions<sup>138</sup>.

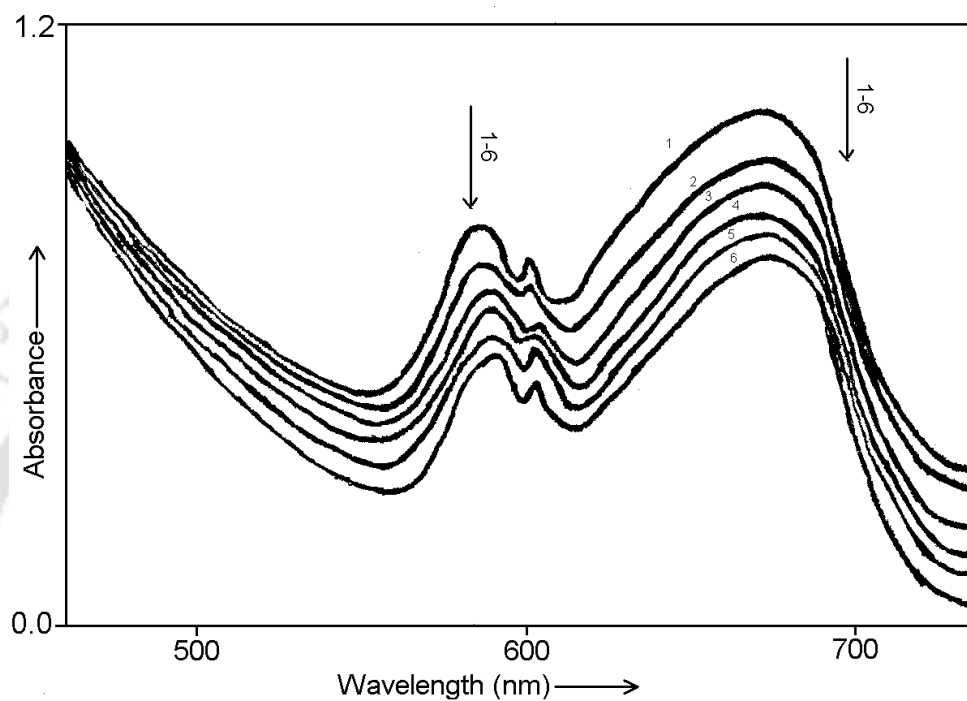


Fig. 2.35 : UV-visible spectra of the solution containing cobalt diacetylmonoxime complex ( 3mg, 0.003mmol), hydrogen peroxide ( 3 $\mu$ l , 30%, 100V) in acetonitrile (3ml). 1-6 represents the respective scan obtained after every two minute interval.

The alkyl peroxocomplexes such as  $[\text{Co}(\text{dmgH})_2(\text{Py})(\text{OOR})]$  (R = -CMe<sub>2</sub>Ph, -CHMe-*p* Tol ; dmgH<sup>-</sup> = monoanion of dimethyl glyoxime)<sup>139,140</sup>  $[\text{Co}(\text{BPI})(\text{OCOPh})(\text{Oo}^t\text{Bu})]$  ( BPI = 1,3-bis

(2-pyridylimino)isoindoline)<sup>141</sup> [ Fig. 2.36 (a) & (b)]are example of such complexes which were well

characterised. Thus, there can be two probable paths for the oxidation reactions involved. The reaction may be a metal centered one in which case the first case is the oxidation of the metal center to a higher oxidation state. The metal center with higher oxidation state thus formed then reacts with the substrate for example phenol to produce the phenoxy radical. Alternatively it may also be likely that the metal ion first interacts with hydrogen peroxide and thereby leading to homolytic or heterolytic cleavage

of peroxide to initiate the radical reaction. Both the aspects are depicted in Scheme 2.9.

It is noteworthy that hydroxylated products such as hydroquinone and catechol were not obtained from cobalt diacetylmonoxime catalysed reactions of phenols in presence of hydrogen peroxide. The involvement of high oxidation species such as  $M=O$  ( $M$ =metal) in similar reactions by first row transition metal catalysts were documented to explain formation of quinones from phenols by cobalt catalysed reactions.<sup>142</sup>

The reaction between phenol and hydrogen peroxide in presence of cobalt diacetylmonoxime compound (2.V) was monitored against time by titrating the remaining of hydrogen peroxide by standard hypo solution during the course of the reaction. The results obtained indicated that the peroxide concentration did not follow any sequential order, rather the concentration was found to follow random changes. There was increase in concentration and also decrease and then increase in the peroxide concentration showing an oscillation in the peroxide concentration. The oscillation of the concentration change of hydrogen peroxide was not effected by environment, for example when carried out in the presence or absence of oxygen. This implies that the inherent nature of the reaction leads to regeneration of peroxospecies that are involved in the reaction and there is also regeneration of peroxy species in the reaction. The observations also support the formation of peroxocomplexes during the oligomerisation reaction.

Since it was not possible to isolate and characterise inorganic complexes participating in the catalytic reaction the mass spectra of the residual mass that is soluble in water was recorded. The highest mass ion peak at 971.4 was observed. This is probably due to a composition  $[\{C_6H_4(OH)_2\}Co_2(HO_2)_2Cl_2(DAM)_6]$  that might have formed through hydroxylation of phenol. Thus some of the other peaks obtained at m/e

values such as 828.1, 757.3, 737.7, 691.8, 664.7, 649.8, 602.5, and 558.4 can similarly be assigned as due to the composition

$$[\{C_6H_4(OH)_2\}Co_2(HO_2)_2Cl_2(DAM)_4CH_3CHNOH]^+, Co_2(DAM)_6Cl]^+$$

$$[\{C_6H_4(OH)_2\}Co_2H_2O_2Cl_2(DAM)_4]^+,$$

$$[\{C_6H_4(OH)_2\}Co_2O_2Cl_2(DAM)_3CH_3CNOH]^+, [Co(DAM)_5][\{C_6H_4(OH)_2\}Co_2O_2Cl_2(DAM)_3CH_3]^+,$$

$$\{C_6H_4(OH)_2\}Co_2Cl_2(DAM)_3]^+, \text{ and } [Co_2(DAM)_4(H_2O)_2]^+.$$

Based on these observations and also to explain product distribution in the catalytic reaction of **(2.V)** with hydrogen peroxide the following reaction mechanism is proposed (scheme 2.10). This mechanism can



explain the product formed from oxidative reaction and similar reaction mechanism was earlier used for explaining cobalt(II) bipyridyl complex catalysed epoxidation, oxidative reactions of olefinic and aromatic

compounds<sup>143</sup>. The involvement of Co(III)-O· is further supported from the esr signal that can be observed from the residual metal in the oligomer. About the presence of such radical in the oligomer is described in the next section.

### 2.4.3 Study on metal content and ESR studies of the oligomers

With the advent of nano materials it has become important to understand the traces or the residual metal content present in a polymeric systems. Presence of a minute quantity of metallic species either in the form of ion or metal can alter the properties of an oligomers<sup>144</sup>. Since we had carried out our reactions with the help of metal catalysed oxidative transformation it is expected that there can be residual metal attached to the oligomeric framework as well as there may be radical that are being stabilised due to the possible confinement the oligomers. With these view in mind the metal content in the oligomers were determined with the aid of atomic absorption spectroscopy. The metal(cobalt) content was found in each oligomers, they are shown in table 2.3.

The electron spin resonance spectra of the product oligomers were also recorded. The electron spin resonance spectra of poly (*m*-methyl phenylene-ether) gives an esr signal at 3220G having resemblance to a

Table 2.3

Type of oligomer	Metal content ( % )
Polyphenylene ether	1.56
Poly ( <i>o</i> -methyl phenylene ether)	0.85
Poly ( <i>m</i> -methyl phenylene ether)	2.1
Poly ( <i>p</i> -methyl phenylene ether)	0.56

radical ( Fig. 2.37 ). Owing to the absence of hyperfine it is believed to

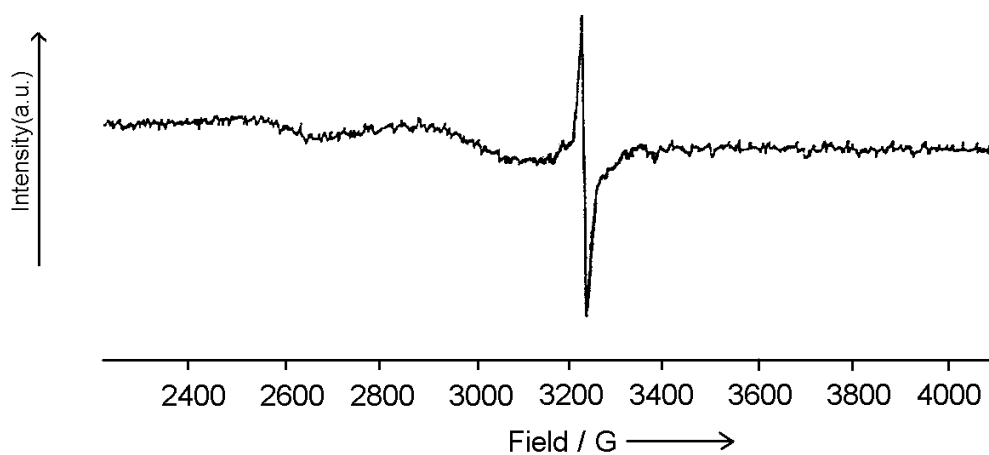


Fig. 2.37 : Esr spectra of poly m-methyl phenylene ether ( central field applied 3200G with sweep width 1500G )

originate from a  $\text{Co}^{\text{III}}\text{-O}\cdot$  species that could be generated from degradation of oxy/peroxy bridged cobalt complexes that participated in the oxidative

polymerisation reaction or from degradation of a cobalt-peroxy intermediate(refer section 2.10). Upon heating the sample to  $90^{\circ}$  causes an increase of intensity of the signal at 3220 G. The increase was ten times in the case of polyphenylene ether. The observation suggested that traces of  $\text{Co(III)-O-O-Co(III)}$  species are anchored to the oligomer can degrade on heating to give rise to  $\text{Co(III)-O}\cdot$ .

Similar observation was also recorded in case of polyaniline prepared by cobalt diacetylmonoxime complex catalysed reaction. The ESR spectra of this oligomer possess only one signal at 3200G due to a radical (fig.2.38).

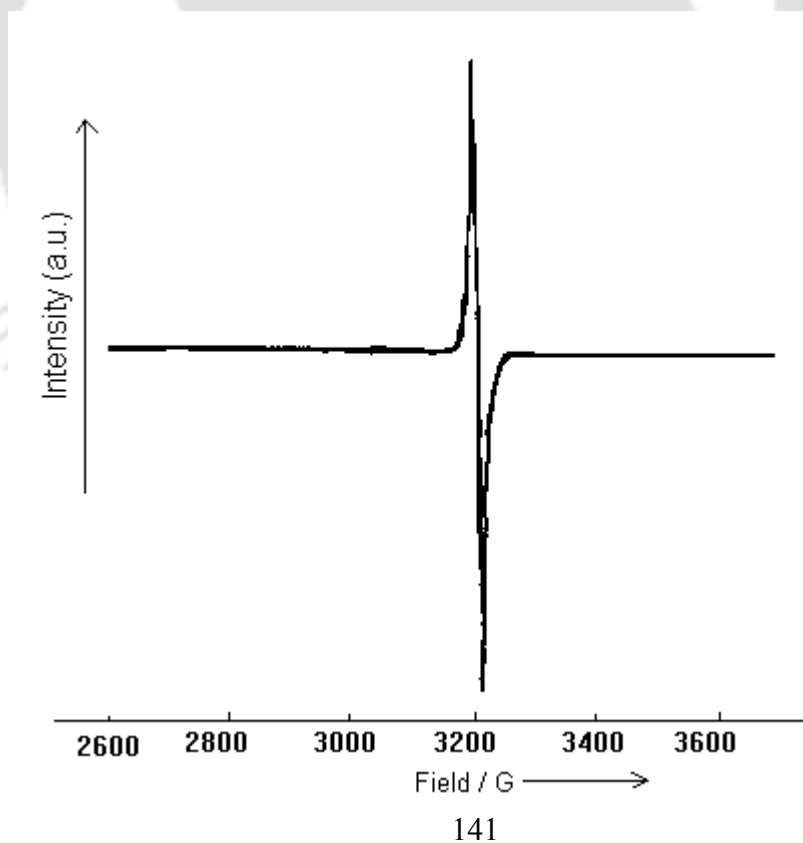


Fig. 2.38 : ESR spectra of polyaniline ( Central field applied 3200G with 1500G sweep width.)

In this case also the enhancement of signal intensity was observed. This supports the the explanation offered for the intensity enhancement of signal in the case of polyphenylene ethers prepared by catalytic reaction of **2.V**. The oligomer prepared from 1,4-phenylenediamine also showed an esr signal at 3180G from the residual  $\text{Co(III)-O}\cdot$  type species in the oligomer. The radicals are probably stabilised by metal centers embedded in the interstices of the possible  $\pi$ -stacks of the oligomer. The metal stabilised radicals are well documented in the literature<sup>145</sup>, but without a

crystal structure it is difficult to draw a three dimensional structure of such metal stabilised radical additionally the available results can not rule out the possibility of dimeric oxo-bridged species too<sup>146</sup>

It is probable that during the process of oxidation [LCo<sup>III</sup>-OOH] type of species is generated which can remain in the polymer matrix. Such species can decompose to Co(II)-O· type of radical. The radical thus formed is entrapped in the matrix of the oligomer show an esr signal in each case at approximately at the place where a dpph radical is observed.

### **2.5 Electrical properties of the Oligomers**

Functionalised organic conducting polymers and oligomers are studied with greater scientific interest due to the possibility of their involvement in macroscopic devices such as sensors, memories , logic circuits etc.<sup>147</sup> Molecular chain of these polymer and oligomer shows regular alteration of single and double bond as exemplified by the conducting polymers such as polyacetylene, polyaniline, polypyrrole etc. These low dimensional materials can be described by a fully occupied valence band and an empty conduction band formed by the conjugated  $\pi$  and  $\pi^*$  orbitals respectively. In these states these polymer shows conducting properties associated with a band gap of about 2 eV. The projection of holes or electrons into these chains by p-type or n-type doping

respectively leads to electrical conductivity due to creation of soliton or polaron states in the gap<sup>148</sup>.

We have studied the change of resistance profile for each of the polymers with temperature. Although they are found to be insulator their resistance profiles are of importance because thermal effect on the electrical properties can unearth their utility in practical field. The variation of resistance normalised to resistance at room temperature with temperature are shown in fig. 2.39. In all these cases we have not plotted the absolute values of the resistance because we had measured the resistance offered by the films made on glass plate, where non uniformity on the thickness may occur . Secondly the normalisation makes an uniform arbitrary scale suitable for drawing and representation.

The oligomer obtained from cobalt diacetyl monoxime catalysed reactions of phenol had resistance such that it increased to 50<sup>0</sup>C and then fell continuously in the region of 50<sup>0</sup>C to 170<sup>0</sup>C.[fig2.39(c)] The resistance profile for the products obtained from *p*-cresol, *o*-cresol and *m*-cresol are



also similar to semiconductor in the range of 30-180<sup>0</sup>C. The oligomer obtained from *o*-cresol using cobalt diacetyl monoxime of 140-180<sup>0</sup>C [Fig 2.39(a)]. The polyaniline has a profile [Fig. 2.39(f)] which shows continuous decrease of normalised resistivity from room temperature to 90<sup>0</sup>C and then increases slightly. Beyond 120<sup>0</sup>C it decreases again and then increases from 140<sup>0</sup>C onwards. The oligomer of 1,4-phenylenediamine has a resistivity profile such that it decreases from room temperature to 88<sup>0</sup>C and then increases up to 150<sup>0</sup>C and then decreases again. When the DSC of the oligomers were compared it is observed that there is an endothermic process taking place below 200<sup>0</sup>C. The minimum of the endothermic process corresponds to the temperature at which the highest hike in the resistance occurs. TG study suggests that there is weight loss in the region 30-200<sup>0</sup>C. Secondly esr studies have shown the increase in the intensity of the esr signal in each case on heating. All these results taken together the overall effect on the resistance change is controlled by the proton conductivity due to the water molecule present as well as NH, OH group present in the oligomers and the radical conductivity due to the metal species attached as end group.

## 2.6 Electrochemical studies on the oligomers

A comparative electrochemical studies of the phenylene ether oligomers and with starting phenols were carried out with the objective to differentiate the redox properties and also to check whether electropolymerised species are same as chemically synthesised oligomers. It also would demonstrate the presence of any quinonic unit in the main chain. The quinonic compounds are electroactive and has very well defined redox cycles due to their equilibrium with monoanionic and dianionic radical species. Cyclic voltamogram of a newly synthesised compound may also provide data about all its accessible oxidation process, the formal potential of the corresponding redox couples and the relative stability of the electrogenerated species. The voltamograms obtained for the three different cresols with multiple cycles are shown in the figure 2.40. Similar voltamogram were also recorded for the three corresponding starting material namely *o*-cresol, *m*-cresol and *p*-cresol.

Comparison of the sets of the starting material and products shows that the irreversible oxidation peak of the phenols obtained in all the three cases has been shifted towards the positive direction compared with their corresponding peak obtained for the starting material. The shifting of the oxidation potential towards positive region indicates that the oligomers are relatively less prone towards oxidation compared to the corresponding starting compound.

The cyclic voltamogram for multiple scan of the oligomer of phenol shows an irreversible oxidation peak at 0.888V for the potential scan between the range  $-0.6$  to  $1.2$  (fig. 2.41).

The scans were done in the region  $-1.2$  to  $+1.2$  did not show



additional peak suggesting that no quinonic units being present in the oligomer. Importantly there is only minor change in the current on multiple

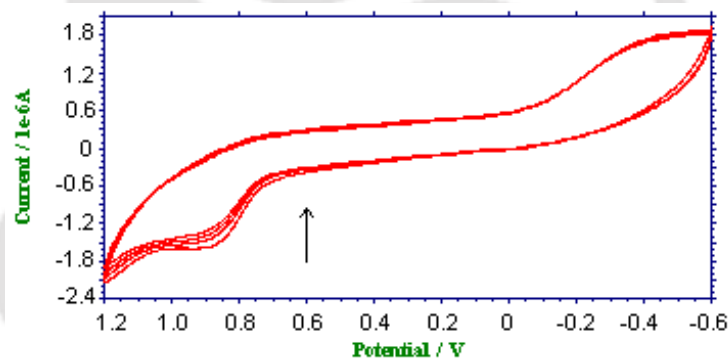


Fig. 2.41: Scan dependency of the cyclic voltammogram of polyphenylene ether ( multiple scan)

scan of the oligomer of phenol suggests that it is electroinactive. This result is explained on the basis of the cross linking of the oligomer making it to be unreactive towards electrochemical oxidation.

## 2.7 Experimental

### 2.7.1 General:

The IR spectra were recorded on a Nicolet DSP-800 FT-IR either in KBr mode or by recording neat spectra by making a thin film made up from a paste of the oligomer on KBr plate.

ESR spectra were obtained from RSIC, Madras. The X-band of a EPR-E-112 esr spectrometer was used for this purpose. A quartz cell was employed for X-band measurements. In all these measurements diphenyl picryl hydrazyl radical (DPPH) was used as the standard. Unless stated central field applied in the measurement was 3200G with 1500G sweep width and frequency applied was 9.70 GHz microwave frequency.

UV and visible spectra were recorded on Hitachi U-2001 spectrophotometer. For this appropriate quantities of the samples were dissolved in measured amount of appropriate solvent. The solution was then taken on a quartz cell, which was then placed onto the sample chamber along with another one containing the solvent alone. Then the sample solution was scanned. For visible range the Xenon lamp was used while for UV region Deuterium lamp was used for irradiation. Prior to the scanning

of the sample solution, a blank scan was performed with the solvent used for dissolution of the sample. Time scan were made by setting the wavelength at appropriate wavelength and monitoring with time.

The  $^1\text{H}$  and  $^{13}\text{C}$  nmr were recorded either on a Bruker 400 MHz nmr spectrometer or on a JEOL EX-400 NMR spectrometer. These were obtained from SIF, Indian Institute of Science, Bangalore. The spectra were recorded in  $\text{CDCl}_3$  or acetone- $\text{d}_6$  or  $\text{DMSO-d}_6$  depending on the solubility of the sample using tetramethyl silane as the standard.

MALDI mass were recorded on Kratos PC-Kompact instrument by dissolving the sample in tetrahydrofuran with dithranol and  $\text{AgTFA}$  and spectra were recorded in positive ion mode. These spectra were recorded in the molecular biophysics department of Indian Institute of Science, Bangalore.

Gas chromatograph were recorded on a Hewlett Packard Gas chromatograph 6890 using SE-30 capillary column and FID as detector and nitrogen as the carrier gas. The oven, detector temperature for the reaction varried but usually used temperature for oven, inlet, detector was 150, 220, 220 $^{\circ}\text{C}$  at 5.6 Bar inlet pressure. The retention time varies with change in inlet pressure and it decreases with increasing inlet pressure. The results were recorded on a HP 3395 Integrator attached to the equipment.

GPC analysis of the oligomers were carried out with Tosoh HLC-8020 instrument and Waters Millennium<sup>32</sup> GPC instrument with a refractive index (RI) detector. The solvent used in case of the former was dimethyl formamide(DMF) containing 0.02 M LiCl eluent and tetrahydrofuran in case of the later. The flow rate in both the cases was 0.5 mL/min. The calibration curve for GPC analysis were obtained using polystyrene standards.

The resistance of the samples were measured of film made on mica plate by using a set up comprising of Hewlett Packard 34401 multimeter, Kiethley 6512 programmable electrometer and Agronics 93-C DC power supply unit. The schematic representation of the instrumental setup for the measurements to carry out is given in figure 2.42 below. The measurements were based on the principle of measuring the resistivity changes as well as resistance with change in temperature. A thin mica sheet is used to make a

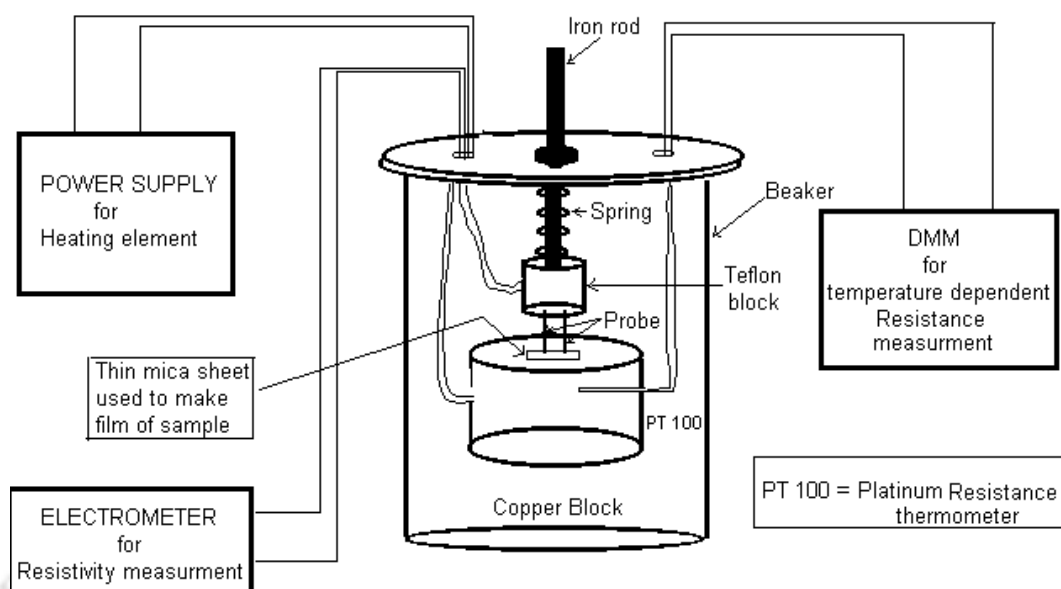


Figure 2.42: Two probe method

film of the sample under investigation. The film is made by spreading a paste of the sample over the mica sheet followed by drying of the sheet by slow evaporation. The film so obtained is now ready for the measurement. The mica sheet is now placed in between the two probes and the copper block as shown in figure 2.42 so that the two probes just touches the film. Switching on the electrometer, DMM and power supply unit will enable one to get the resistance at various temperatures.

Elemental analysis were carried out with Perkin Elmer 2400 series II elemental analyser.

Metal contents of oligomers were determined from atomic absorption spectroscopy. Atomic absorption measurements were done on a

Perkin Elmer atomic absorption spectrophotometer, Model 2380 from dilute aqueous solution of the compound.

The cyclic voltamogram of the compounds were recorded with a CH-Instruments model-680 cyclic voltameter. The following electrodes were used in the instrument to record the cyclic voltamogram of the sample. One platinum working electrode, one Ag / AgCl electrode was used as the reference electrode together with a platinum wire auxillary electrode. For electrochemical measurement 10 mg of the sample was dissolved in acetonitrile (5ml) and tetrabutyl ammonium perchlorate was used as the supporting electrolyte. For polyphenylene ether and poly (*p*-methyl phenylene ether), the scan rate employed was 0.05 volt/sec with sample interval 0.001 and in the case of poly (*o*-methyl phenylene ether) and poly (*m*-methyl phenylene ether), the scan rate was 0.1 volt/sec with 0.001 sample interval. The solution was then scanned in the positive direction and the output was recorded. The instrument is controlled by a IBM PC compatible to windows 95.

The measurement of magnetic moment was carried on a Sherwood Scientific Magnetic Susceptibility Balance. Weighed amount of the finely ground solid sample was taken in a previously weighed sample tube tube. Before this, the empty sample tube into the tube guide of the instrument and magnetic deflection caused by the tube was recorded as  $R_0$ . The sample

tube with the sample was stated above was then inserted into the tube guide and magnetic deflection caused by the tube was then recorded as R. The mass susceptibility,  $X_g$  was then calculated using equation (A).

Then effective magnetic moment ( $\mu_M$ ) is calculated from the equation (B)<sup>149</sup>.

The thermal analysis were carried out with a Mettler Toledo TGA / SDTA 851<sup>e</sup> and Mettler Toledo DSC 821<sup>e</sup> thermal analyser. The thermogravimetric (TG) instrument consists of a furnace connected to a sensitive, reliable and thermally stable microbalance. For thermogravimetry analysis an alumina crucible is placed in an arm of the microbalance inside the furnace and its weight tared. Then the crucible was removed gently and

5-10 mg of finely ground sample was introduced there. The crucible was then again placed on the arm inside the furnace and the furnace was locked. The weight of the sample was noted with time/temperature and the output was recorded with a heating rate of  $5^{\circ} / 10^{\circ}$  per minute under nitrogen atmosphere. Similarly for DSC analysis 5-10 mg of the sample was placed on a platinum crucible with lid. The crucible was then placed in the furnace together with a reference crucible at appropriate places. The heat change of the sample was observed with time/ temperature and the output was recorded. Both the equipment was fully automated and controlled by a PC based software named Solaris.

### **2.7.2 Reagent and starting material**

All the reactions were carried out with Analar grade reagents. The solvents used in the reaction were distilled by literature procedure<sup>150</sup> and were dried over specific reagents wherever necessary. Some of the starting materials like aniline were distilled before use. Wherever required the compounds were recrystallised from appropriate solvent. Diacetyl monoxime was obtained from S. D. Fine chemicals (India) and used without further purification. Benzil monoxime was prepared by literature procedure<sup>151</sup> ( m.p.  $140^{\circ}\text{C}$  ). Different cobalt salts such as cobalt acetate, cobalt chloride hexahydrate were purchased from Mercks India limited and

were used as obtained. Synthesis of  $[\text{Co}(\text{NH}_3)_6]\text{Cl}_3$  ,  $[\text{CoCl}(\text{NH}_3)_5]\text{Cl}_2$  ,  $\text{Co}(\text{AcAc})_3$  [AcAc= acetyl acetonate] were done by standard literature procedure<sup>152</sup>.

### **Preparation of cobalt -diacetylmonoxime complex, 2.V**

A mixture of cobalt(II)chloride hexahydrate (118mg, 0.5mmol) and diacetyl monoxime [Abbreviated as DAM] (303mg, 3mmol) were mixed together and ground to make a homogeneous mixture in a pastel and mortar. This mixture on keeping in oven at 110<sup>0</sup>C for 4 hrs resulted in a crystalline mass. The crystalline mass on washing with petroleum ether (20ml) gave a black compound having molecular composition  $\text{Co}_2(\text{DAM})_7\text{Cl}_4$  (234mg ), Elemental analysis found C, 34.41, H, 4.97, N, 10.02, Cl, 14.93; Calculated for  $\text{C}_{28}\text{H}_{49}\text{Cl}_4\text{N}_7\text{O}_{14}\text{Co}_2$  C, 34.74, H, 4.97, N, 10.01, Cl 14.68. IR (KBr) 3201(b,s), 3047(w), 2919(w), 1648(s), 1573(s), 1455 (bs), 1367(s), 1084(s), 988 (w)  $\text{cm}^{-1}$ . The molar conductivity of the compound in acetonitrile is 485  $\text{Ohm}^{-1}\text{cm}^2\text{mol}^{-1}$ . The magnetic moment is 3.4 B.M.

### **Preparation of cobalt benzilmonoxime complex, 2.VI**

Solution of cobalt(II) acetate (0.480g , 2.45 mmol ) in methanol ( 10ml ) and benzilmonoxime (0.9g 4.0 mmol) in 40ml of methanol were

mixed together in a round bottom flask. The resulting mixture was stirred at room temperature for 45 minute. A reddish pink solution was obtained. The resulting solution was allowed to stand for half an hour. The product obtained was then filtered. Pink coloured solution was obtained which was evaporated to obtain 2.VI. Elemental analysis found C, 68.11, H, 4.23, N, 6.00, Calculated for  $C_{70}H_{51}N_5O_{14}Co_2$  C, 67.79, H, 4.12, N, 5.65. IR (KBr) 3436(b,s), 3067(s), 1608(s), 1521(s), 1444 (s), 1388(s), 1291(s), 1193(s), 932(s). The molar conductivity of the compound was found to be  $11.6 \text{ Ohm}^{-1}\text{cm}^2\text{mol}^{-1}$ . The magnetic moment of the compound was found to be 1.57 B.M.

#### **Reaction of toluene with hydrogen peroxide in the presence of [ 2.V]**

A mixture of hydrogen peroxide (1ml, 30%), cobalt diacetylmonoxime complex (0.050g, 0.679 mmol) and toluene (1ml) was heated at  $80^\circ\text{C}$  for 6 hrs in a schlenk tube under closed condition To the resulting mixture 5 ml water was added and extracted with dichloromethane (2X25ml). The dichloromethane extract was dried over anhydrous sodium sulphate. The products were analysed by gas chromatography with FID detector and  $N_2$  as carrier gas and SE-30 as cappillary column. Column, detector, injector temperature was 150, 220,  $220^\circ\text{C}$  respectively. Flow rate

of nitrogen was fixed at 10ml / minute with a backinlet pressure of 5.6 Bar. The retention values of the products were comparable with that of benzaldehyde, benzyl alcohol, toluene and cresols. The percentage conversion of toluene was found to be 12%, (determined by naphthalene as internal standard). The products were further confirmed by comparing with GC of authentic samples and also further confirmed by peak intensity enhancement by externally adding each substrate to the reaction mixture.

#### **Recycling of oxygen from hydrogen peroxide during cobalt catalysed oxidative reactions**

Cobalt(II) acetate tetrahydrate (24 mg, 0.01mmol) was taken in a schlenk tube. The tube was flushed with the appropriate gas used (nitrogen, oxygen, air and hydrogen ) during the reaction. Degassed water (5ml) and hydrogen peroxide (1ml, 30 %) were added to this followed by benzyl alcohol (500mg, 4.6 mmol). The reaction mixture was closed under positive flow of the appropriate gas in the schlenk tube. A pink coloured solution was obtained. The schlenk tube was immersed in a thermostatic bath at 70<sup>0</sup> C for two hours. The reaction mixture slowly turned orange yellow. After two hour the reaction mixture was extracted with dichloromethane and analysed by using a Hewlett Packard 6890 GC with SE-30 as capillary column and FID as the detector. The column, detector, injector temperature was 150, 220, 220 at 5.6 bar pressure. Further, the organic product was

isolated by purification through column chromatography and confirmed to be benzaldehyde.

#### **Reaction of Benzyl alcohol with hydrogen peroxide in presence of [2.V]**

A solution of benzyl alcohol ( 1 ml, 10 mmol) and cobalt diacetylmonoxime complex ( 50 mg, 0.679mmol) was taken in a schlenk tube. Degassed water ( 5ml ) was added to the mixture followed by the addition of hydrogen peroxide (1ml, 30 %). The schlenk tube was then immersed in a thermostatic bath and the reaction was allowed to proceed at 70<sup>0</sup>C for about three hour. The reaction mixture assumes yellowish colouration and after three hour the product was extracted with dichloromethane and analysed by Hewlett Packard 6890 GC with SE-30 as capillary column and FID as the detector. The oven , detector, injector temperature was 150, 220, 220 at 5.6 bar pressure. The analysis indicates the formation of benzaldehyde from benzyl alcohol.

#### **Reaction of phenol with hydrogenperoxide in presence of [2.V]**

A well a stirred solution of phenol (0.564 g, 6 mmol) and cobalt diacetyl monoxime complex (**2.V**) (0.050g, 0.052mmol) in acetonitrile, hydrogen peroxide (1cm<sup>3</sup>, 30%, 100vol) was added and the reaction was allowed to proceed at 90<sup>0</sup>C for 6hrs. The solvent was removed under

reduced pressure at room temperature to obtain a black paste. The black paste thus formed was washed repeatedly with water ( $2 \times 20 \text{ cm}^3$ ) followed by petroleum ether ( $2 \times 20 \text{ cm}^3$ ). Yield of the reaction was 25%. IR(neat film) spectra gives the following vibrational frequencies : 3400(bw), 1610(s), 1590(s), 1490(s), 1200(s), 1100(w), 830(s), 750(s), 690(m).  $^1\text{H}$  NMR ( DMSO- $d_6$  ) 6.1-7.6 (bm) $\delta$ . Elemental analysis C, 76.92 H, 4.12. Calculated for the composition  $(-\text{C}_6\text{H}_4\text{O}-0.1\text{H}_2\text{O}-)_n$  were C, 76.76, H, 4.48. GPC (THF)  $M_n$ , 3500,  $M_w$  8400.

#### **General reaction of cresols with hydrogenperoxide in presence of [2.V]**

Cresol 0.648g (6 mmol ) was dissolved in acetonitrile(10ml) along with cobalt diacetyl monoxime complex (**2.IV**) (0.050g, 0.052mmol). Hydrogen peroxide ( $1 \text{ cm}^3$  30%, 100vol) was added to the solution and the reaction was allowed to proceed at  $90^\circ\text{C}$  for 6hrs. The solvent was removed under reduced pressure at room temperature. A black paste was obtained. The black paste thus formed was washed repeatedly with water ( $2 \times 20 \text{ cm}^3$ ) followed by petroleum ether ( $2 \times 20 \text{ cm}^3$ ).

Analytical and spectroscopic data obtained for three different oligomers of cresols are as follows:

**Oligomer of *o*-Cresol** : In case of *o*-cresol the yield of the reaction was calculated to be 37%. IR (KBr) 3395(bs), 2919(s), 1702(s), 1600(s), 1480(s), 1191(s) and 757(s).  $^1\text{H}$  NMR (DMSO- $d_6$ ) 2-2.6  $\delta$  (m, 3H) and 7-8.5  $\delta$  (m, 3H).  $^{13}\text{C}\{^1\text{H}\}$  NMR (400 MHz, DMSO- $d_6$ ) 16, 114, 118, 124, 126, 130, 156. GPC ; ( $M_n$ ,  $M_w$ ) 3348 and 3542. Elemental analysis ; C, 70.70 H, 5.4, and the calculated for the composition  $(-\text{C}_7\text{H}_6\text{O}-0.75 \text{H}_2\text{O})_n$  are C, 71.18 H, 5.59.

**Oligomer of *m*-Cresol** : The yield of the reaction in case of the reaction of *m*-Cresol was calculated to be 12 %. The IR (KBr) 3381(b,s), 2929(m), 1702(s), 1616(s), 1492(s), 1282(m), 1196(s), 1000(w), 750(m).  $^1\text{H}$  NMR (DMSO- $d_6$ ) 1.9-2.5  $\delta$  (m, 3H), another one at 6.6-7  $\delta$  (m, 3H) and a singlet at 8.8  $\delta$  (s, 0.3H).  $^{13}\text{C}\{^1\text{H}\}$  NMR (400 MHz, DMSO- $d_6$ ) ; 21, 112, 116, 119, 129, 139, 150, 158 GPC (THF) ; ( $M_n$ ,  $M_w$ ) (3550, 3736). Elemental analysis ; C, 71.49, H, 5.70 and calculated for the composition  $(-\text{C}_7\text{H}_6\text{O}-0.75 \text{H}_2\text{O})_n$  are C, 71.18, H, 5.59.

**Oligomer of *p*-Cresol** : yield 42 %. IR (neat film) 3370(b,s), 1727(s), 1620(s), 1520(s), 1217(s), 825(s).  $^1\text{H}$  NMR (DMSO- $d_6$ ) 7-7.8  $\delta$  (m, 3H),

2.5-2.9  $\delta$  (m, 3H).  $^{13}\text{C}\{^1\text{H}\}$  NMR ( 400 MHz, DMSO- $d_6$ ) 20, 115, 129.5, 130, 131, 152, 155. GPC (THF) ; ( $M_n$ ,  $M_w$ ) (3494, 3678). Elemental analysis, found C, 74.46 H, 6.06 and the calculated for the molecular composition ( $\text{C}_7\text{H}_6\text{O} \cdot 0.33 \text{H}_2\text{O}$ ) $_n$  are C,75.00, H, 5.63.

**Reaction of 2,6 dimethylphenol with hydrogen peroxide in the presence of [2.V]**

2,6-dimethyl phenol (0.7388g 6mmol) and cobalt diacetylmonoxime complex (50 mg, 0.679mmol) was taken in 10ml acetonitrile in a round bottom flask. To this solution hydrogen peroxide was added (1ml, 30%, 100V ) and the reaction mixture was allowed to stir at 70 $^{\circ}\text{C}$  in a thermostatic bath for two hours. Solvent from the reaction mixture was then removed under reduced pressure. The product obtained was then washed with distilled water (2x20ml ) followed by petroleum ether( 3x25ml ). IR(KBr) Finally the product was dried over vacuum to obtain a dark brown solid. Yield of the reaction was 30%. IR(KBr) 3438(b,s), 2919(s), 1591(s), 1484(s), 1200(s), 825(s).  $^1\text{H}$  NMR ( DMSO- $d_6$  ) 8.2-8.1 $\delta$  (1H), 7.2-7.0  $\delta$  (2H), 2.2  $\delta$  (6H).  $^{13}\text{C}\{^1\text{H}\}$  NMR ( 400 MHz, DMSO- $d_6$ ) 16.7, 124.4, 125.8, 128.1, 131.5, 152. GPC (THF) ; ( $M_n$ ,  $M_w$ ) (1017, 1101).

**Reaction of aniline with hydrogen peroxide in the presence of [2.V]**

To a well stirred mixture of aniline ( 1g, 11 mmol) and hydrogen peroxide ( 1ml, 30%, 100V), cobalt diacetylmonoxime complex (0.050g, 0.679mmol) was added. The reaction mixture was kept at 60 °C for 2 hrs. The reaction mixture was then cooled and the solvent was removed under reduced pressure. The residue thus obtained was washed with cold water (3ml) followed by petroleum ether ( 2 X 25 ml) to obtain a black solid. Elemental analysis ; found C, 72.05 H, 5.04 N, 13.75, calculated for  $(-C_6H_6N 0.5H_2O)_n^-$  ; C,72.00; H, 6.00, N 14.00.  $^1H$  nmr ( $CDCl_3$ ) 8-6.6(m).  $^{13}C\{^1H\}(CDCl_3)$  151,139,131, 129.2, 129.0, 121.3, 112.4,100.2. IR(KBr) 3300(b), 2925(w), 1670(m), 1600(s), 1500(s), 1440(m), 1310(m), 750(s), 690(s).

**Reaction of *p*-methyl aniline with hydrogen peroxide in presence of [2.V]**

A mixture of *p*-methylaniline (1.1ml ,10 mmol) and cobaltdiacetylmonoxime complex(50mg, 0.679mmol) was taken in 5ml acetonitrile was taken in a round bottom flask and to this mixture hydrogen peroxide (30%, 100vol, 1cm<sup>3</sup> ) was added. The reaction mixture was placed on a thermostatic bath at 70<sup>0</sup> C under continuous stirring for five hours. The product obtained was then washed with distilled water (2 x

25ml) followed by hexane (3x25ml). Finally the solvent was removed under reduced pressure and the product was dried over vacuum. Yield 15%. IR (KBr) 3306(b,s), 3029(w), 2922(s), 1680(w), 1605(s), 1514(s), 1408(s), 1329(s), 1242(s), 1160(s), 1029(s), 821(s), 522(s). GPC (THF) ; (  $M_n$  ,  $M_w$  ) (985, 1035).  $^1\text{H}$  nmr (400 MHz,  $\text{CDCl}_3$  ), 6.5-7.4  $\delta$  (m, 3H) and 2.0-2.5  $\delta$  (m, 3H), 7.75 $\delta$  (s, 1H).

**Reaction of *p*-methoxy aniline with hydrogen peroxide in presence of [2.V]**

To a mixture of *p*-methoxyaniline (0.741g , 6 mmol) and cobalt diacetyl monoxime complex (50 mg. 0.023mmol) in 5ml acetonitrile hydrogen peroxide ( 30%, 100Vol, 1cm<sup>3</sup>) was added and the reaction mixture was stirred at 70<sup>0</sup>C for three hour. The solvent was removed under reduced pressure from the reaction mixture and the product obtained was then washed with water (3x25ml) followed by petroleum ether (3x 25ml). Yield , 72 %. IR (KBr) 3280(b,s), 2938(w), 2832(s), 1680(w), 1610(s), 1509(s), 1296(s), 1247(s), 1168(s), 1029(s), 826(s), 533(s). GPC record of the product gives two sets of peaks having the values for (  $M_n$  ,  $M_w$  ) as ( 1578, 1599) and ( 959, 967)  $^1\text{H}$  nmr ( 400 MHz,  $\text{CDCl}_3$  ) 3.8  $\delta$  (s, 3H), 6.5-7.5(m, 3H).

**Reaction of 1,4-diaminobenzene with hydrogen peroxide in the presence of [2.V]**

To a well stirred solution of 1,4-diaminobenzene (653mg, 6mmol), cobalt diacetylmonoxime complex (50mg, 0.679mmol) in water (1cm<sup>3</sup>) hydrogen peroxide ( 30%, 100Vol, 1cm<sup>3</sup>) was added in portion and the reaction mixture was stirred continuously for 6 hrs over a water bath at 80<sup>0</sup>C. Water from the resulting solution was removed under reduced pressure to obtain a black paste. The paste obtained was washed with cold water (2X10cm<sup>3</sup>) followed by washing with a mixed solvent of ethylacetate (10%) in petroleum ether (10cm<sup>3</sup>) to obtain a black powder. Yield , 65%. Elemental analysis found C, 61.03, H,5.11, N,21.42. The calculated for the molecular composition ( C<sub>6</sub>H<sub>4</sub>N<sub>2</sub>)<sub>6</sub>(C<sub>6</sub>H<sub>6</sub>N<sub>2</sub>)<sub>3</sub>.CoCl<sub>2</sub> are C,60.17, H, 3.8, N, 23.39. <sup>1</sup>H NMR ( 400 MHz, CDCl<sub>3</sub> ) : 6.7 δ (s), 6.0 δ (s), 5.75 δ (s), 5.0(b, s). <sup>13</sup>C{<sup>1</sup>H} NMR (CDCl<sub>3</sub>) 153.31, 148.26,144.86, 140.03, 122.23, 114.32, 90.63 δ. IR(KBr) 3334(bs), 2665(s), 1603(s), 1544(s), 1500(s), 1272(s), 1235(s), 1165(m), 832(s). Molecular weight ( M<sub>n</sub> , M<sub>w</sub> ) 1017 and 1101 .





## CHAPTER-3

### Copper(II) Catalysed reactions of activated aromatics with hydrogen peroxide

#### 3.1 Background

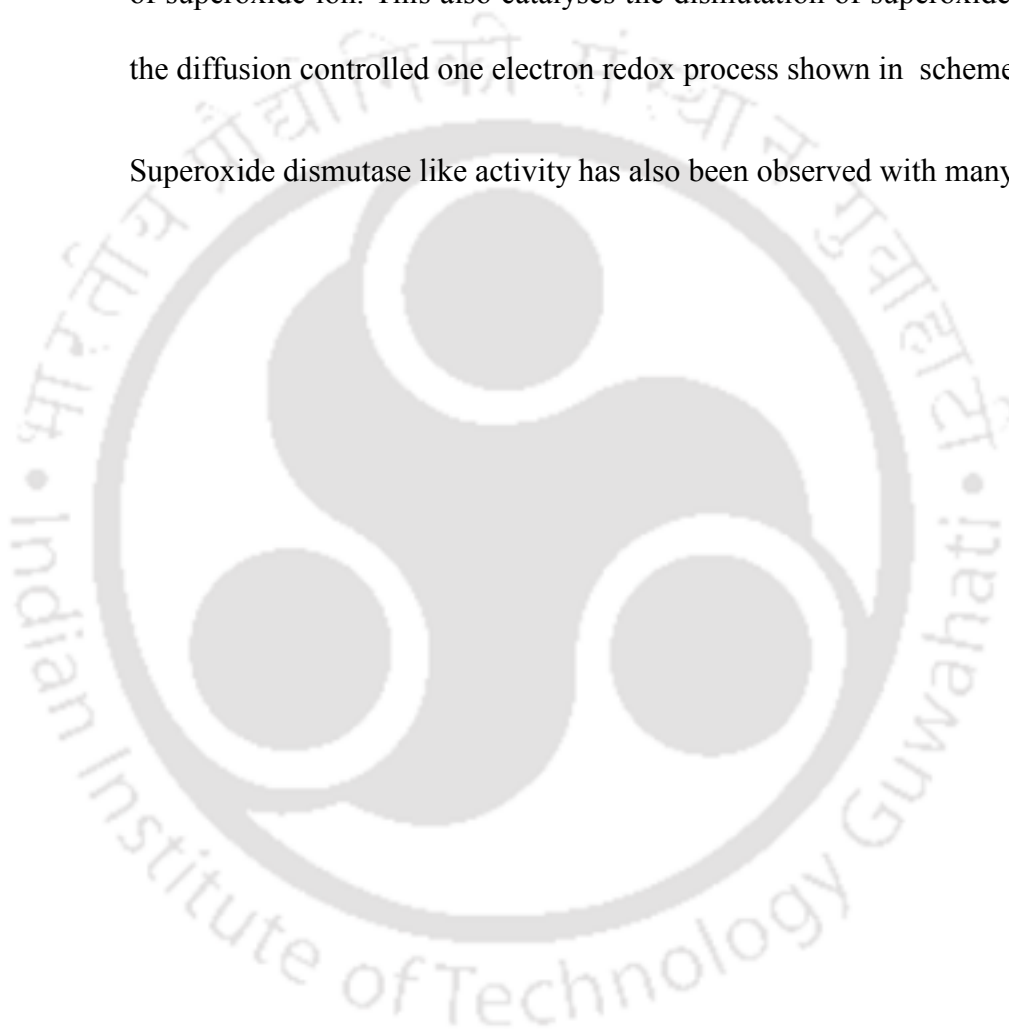
Copper complexes play important role in oxidative reactions of aromatic compounds. Among these aromatic hydroxylation finds important place in biological chemistry<sup>153</sup>. Preparation of model compounds for selective catalytic hydroxylation constitutes the backbone of this research<sup>154</sup>. The biochemical process such as tyrosinase activity<sup>155</sup> and biosynthesis of lignin<sup>153a</sup> involves copper(II) catalysed aromatic hydroxylation. The cleavage of DNA by copper(II) complexes having phenolic groups as a part of the ligand is well established<sup>156</sup>. Success has been made in mimicking of galactose oxidase by radical containing copper(II) phenoxo complexes<sup>157</sup>. Although very few model complexes can mimick stoichiometric and catalytic reactivity of the corresponding enzyme under consideration, the development of biomimetic model complexes for mimicking the structural and catalytic aspects of the active

sites in metalloproteins, like the copper site in galactose oxidase are in progress<sup>158</sup>. Galactoseoxidase does catalytic oxidation of primary alcohols to corresponding aldehydes where dioxygen is reduced to hydrogen peroxide. The active site consists of a mononuclear copper ion assuming a square pyramidal coordination geometry.<sup>159</sup> Copper(I) catalyst together with nitrogen bases in the presence of oxygen gives linear polymer of 2,6-dimethylphenol having ether linkage<sup>160</sup>. Oxidation of copper(I) phenoxides passes through hydroxylation<sup>161</sup>. In stoichiometric reactions copper(II) complexes can effectively cause selective hydroxylation on aromatic rings <sup>162</sup>. In contrast to these the anilinic compounds easily oligomerises under oxidative condition by transition metal catalysts to give polyanilines<sup>163</sup>. These oxidative oligomerisations are usually performed with the anilinium salts.

One electron transfer reaction is one of the simplest reactions that do not require cleavage of any bond<sup>164</sup>. In such reactions two partners are involved namely the donor or reducing agent and the acceptor or oxidizing agent, each of them should be capable of accomodating at least two accessible oxidation states. Superoxide dismutase is one example of such reaction where only one metal center is used for one electron transfer and

no bond is broken in the substrate. Copper-zinc superoxide dismutase has an active site consisting of an imidazole bridged bimetallic center possessing one copper(II) and one zinc(II) ion<sup>165</sup> which has been found in the crystal of eukaryotic cells. This protects the cells from the toxic effects of superoxide ion. This also catalyses the dismutation of superoxide ion by the diffusion controlled one electron redox process shown in scheme 3.1 .

Superoxide dismutase like activity has also been observed with many low



Scheme 3.1

molecular weight copper chelates.<sup>166</sup> The presence of bovine serumalbumine, a plasmatic protein and one of the strongest biological chelator of cupric ion, reduces the activity in most of the cases as bovine serum albumine can mobilize the copper(II) ions from these complexes.

From the foregoing discussion it is clear that there is need of developing biorelated mild, catalytic, efficient methods for the oxidative transformation of aromatic compounds. The glycine is the primary amino acid which forms stable *cis*-bis and *trans*-bis chelate complexes with copper(II)<sup>167</sup>. We set our study to elucidate the reactivity of *cis* and *trans*-bisglycinato copper(II) complexes with activated aromatics under neutral condition in the presence of hydrogen peroxide and also to exploit the material property of the products from these reactions. Hydroxylated products are obtained from phenolic compounds while anilinic compounds were found to oligomerise during the course of the reactions.

### **3.2 Hydroxylation of phenols**

Phenol reacts with hydrogen peroxide in the presence of catalytic amount of *cis*-bis-glycinato copper(II) monohydrate which gives hydroquinone and catechol (equation 3.1). The products of this reaction,

hydroquinone (1), catechol (2) and unreacted phenol were obtained in the form of a stable hydrogen bonded aggregate. The phenolic compounds are known to form aggregates.<sup>168</sup> Aggregation of the catechol, hydroquinone and phenol can be observed from the isolation of these products after purification and also from the <sup>13</sup>C nmr spectra of the unseparated products.

In the case of the products obtained from the reaction of phenol we have recorded the <sup>1</sup>H nmr spectra of the crude product (fig 3.1). The spectra had three sets of hydroxy signals appearing at 8.5, 8.0, 7.8 δ. The phenyl group protons of the three appear in the range of 7.4-6.6 δ. The <sup>13</sup>C{<sup>1</sup>H}

nmr signals of the aggregate of a freshly prepared sample at room temperature (fig 3.2 a) showed lesser number of signals. However, same sample on heating resulted in degradation of the aggregate and gave the  $^{13}\text{C}\{^1\text{H}\}$  nmr signals from each individual entity namely phenol,

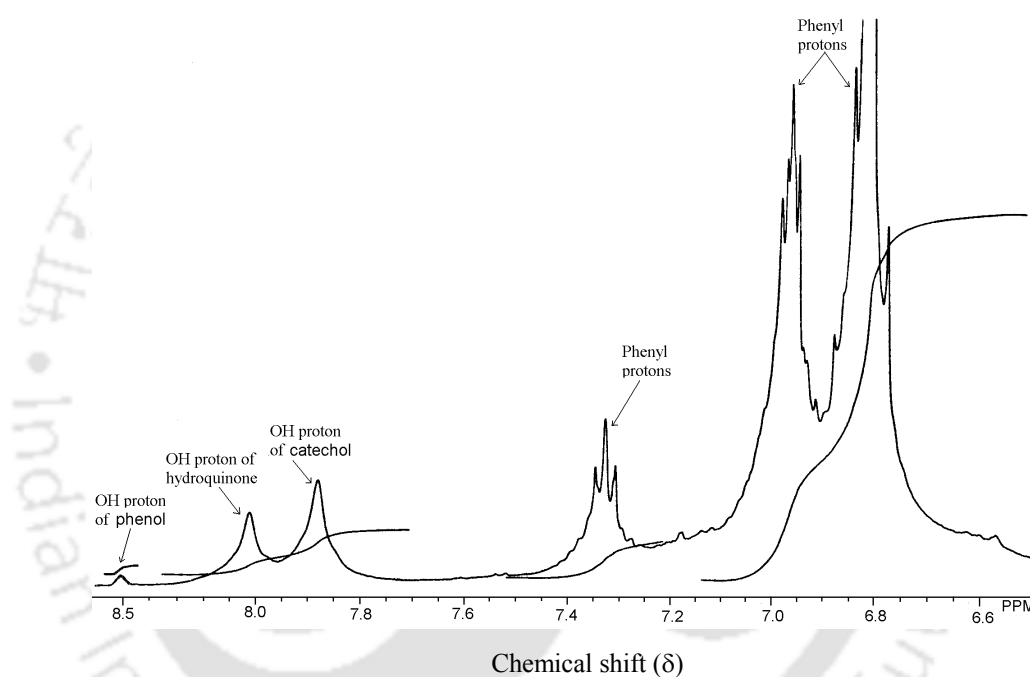


Fig. 3.1 :  $^1\text{H}$  nmr spectra of the product from phenol

catechol and hydroquinone (fig 3.2 b). Hydroquinone have two set of equivalent carbons and gives two signals in the  $^{13}\text{C}\{^1\text{H}\}$  nmr . Catechol gives three signals and phenol gives four signals in  $^{13}\text{C}\{^1\text{H}\}$  nmr. In

fig. 3.2(b) eight peaks are observed. The assignments of the signals are shown in fig 3.2(b). Eight peaks in the  $^{13}\text{C}\{^1\text{H}\}$  nmr instead of nine are obtained due to equivalent chemical shifts. The hydroquinone and catechol from these aggregate could be purified by column chromatography, but the recovery of the compounds were less than 10%. In these reactions further oxidation of hydroxylated compounds to products like *o*-benzoquinone or *p*-benzoquinone as well as ring opening reaction to give dicarboxylic acid was not observed. The yields of hydroxylated derivative were found to be dependant on the catalyst concentration. The results on the yield on

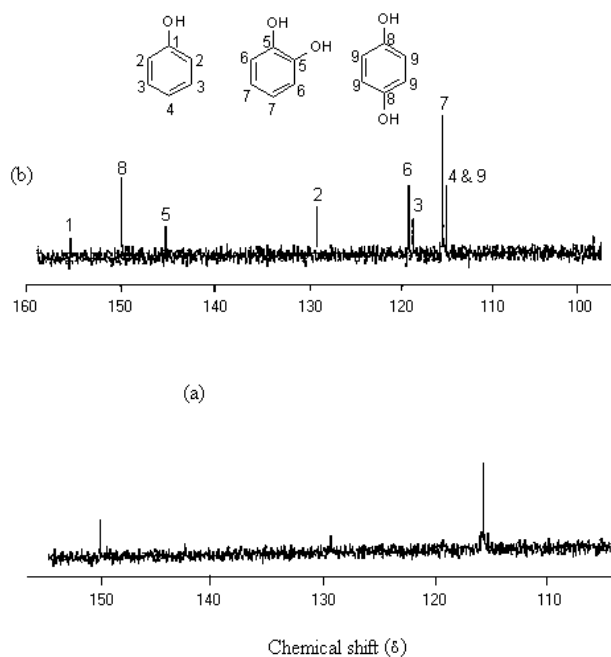


Fig. 3.2  $^{13}\text{C}\{^1\text{H}\}$  nmr spectra of phenol (a) product at room temperature (b) isolated product after heating at  $60^\circ\text{C}$ .

change of catalytic concentration are listed in table 3.1 It also includes comparison on the results of few other well established procedures on similar hydroxylations by other catalytic system.

**Table 3.1**

Name of Catalyst	Phenol (mmol)/ Catalyst (mmol)	hydroquinone : catechol	Phenol conversion
<i>Cis</i> -bis-glycinato Copper(II)	10 mmol / 0.125 mmol	54 : 46	29%
<i>Cis</i> -bis-glycinato Copper(II)	10mmol / 0.23mmol	54 : 46	47.4%

<i>Cis</i> -bis-glycinato Copper(II)	10mmol / 0.38 mmol	54 : 46	44%
Pt(CF <sub>3</sub> )(P-P)(OPh) 62 P-P= diphosphenoethane	6mmol / 0.006 mmol	7 : 55	-
12%	-	84:16	
26%	-	1.4:1	
Titanium silicate <sup>148</sup>	-	1: 1	26.8%
Ketone/acid <sup>146</sup>	-	1:1.5	5%
H <sub>3</sub> PO <sub>4</sub> /HClO <sub>4</sub> <sup>146</sup>	-	1:1.5	5%

The IR spectra of the compound gives a sharp broad signal at 3297cm<sup>-1</sup> due to the hydroxyl group and the O-H deformation band is observed at 1214cm<sup>-1</sup>. The absorption bands appearing at 1618cm<sup>-1</sup> and 1593 cm<sup>-1</sup> can be assigned as due to the stretching vibration of C=C bond of the aromatic nucleus. The C-O bond stretching in this case is observed at 1456cm<sup>-1</sup>. The absorption observed at 1749cm<sup>-1</sup> is due to the overtone of the OH absorption.

The reaction of 2,6-dimethylphenol with the hydrogen peroxide and catalytic amount of *cis*-bis-glycinato copper(II) monohydrate gives hydroxylated compound 1,4-dihydroxy-2,6 dimethylbenzene (equation 3.2) along with 2,6-dimethylbenzoquinone (~5%). The hydroxylated product

1,4-dihydroxy- 2,6-dimethylbenzene was obtained in this case as the major product.

Different cresols were also found to react with hydrogen peroxide in presence of catalytic amount of *cis*-bis-glycinato copper(II) monohydrate. For example, the reaction of *o*-cresol with *cis*-bisglycinato copper(II) in presence of hydrogenperoxide gave 2,5-dihydroxytoluene as the major product.

$^1\text{H}$  nmr spectra of the compound shows a sharp broad signal at 8.3  $\delta$  due to the hydroxyl group and a multiplet is observed at 6.5-7.5  $\delta$  due to the aromatic nucleus. The  $^1\text{H}$  nmr signal for the methyl group is observed at 2.3  $\delta$ . The compounds have  $^{13}\text{C}$  signals at 155.70 and 148.10  $\delta$  which are assigned to the carbons directly attached to the oxygen of the hydroxyl groups. The other four different aromatic carbon atoms give the signals at 114.47, 119.19, 126.46 and 130.48  $\delta$ . The  $^{13}\text{C}$  signal due to the carbon of the methyl group appears at 15.02  $\delta$ . The characteristic IR

absorption for the hydroxyl group is obtained at  $3390\text{cm}^{-1}$  as strong broad signal along with a O-H deformation band at  $1214\text{cm}^{-1}$ . One weak signal is observed at  $2918\text{cm}^{-1}$  due to the absorption caused by the methyl group, The IR absorption due to the aromatic C=C bond stretching is observed at  $1612\text{cm}^{-1}$  and a strong absorption due to the C-O bond stretching is observed at  $1512\text{cm}^{-1}$ .

The major product obtained from the reaction of *p*-cresol with hydrogen peroxide and catalytic amount of *cis*-bis-glycinato copper(II) monohydrate was found to be 3,4-dihydroxytoluene.  $^1\text{H}$  nmr spectra of the compound gives a multiplet at 6.7- 7.6  $\delta$  due to the aromatic nucleus. The -OH protons appears as a sharp broad signal at 7.95  $\delta$ . The multiplet due to the protons of the methyl group appears at 2.4 $\delta$  The  $^{13}\text{C}$   $\{^1\text{H}\}$ nmr spectra of the compound gives six signals due to the six different carbon atoms of the aromatic nucleus. The carbon directly attached to the oxygen atoms of the hydroxyl group gives the  $^{13}\text{C}$  signals at 155.0 and 153.0  $\delta$ . The other four signals appears at 131, 129, 120 and 114.8  $\delta$ . The methyl carbon appears at 19.5  $\delta$ . IR spectrum of the compound gives a strong broad signal at  $3372\text{cm}^{-1}$  which is assigned as due to the hydroxyl groups. One weak

signal is observed at  $2918\text{ cm}^{-1}$  due to the C-H bond stretching of the alkyl group. The O-H deformation band is observed at  $1214\text{ cm}^{-1}$ . Aromatic C=C bond stretching gives the characteristic IR absorption at  $1606\text{ cm}^{-1}$ . The strong IR absorption at  $1510\text{ cm}^{-1}$  is assigned to the C-O bond stretching.

### 3.3 Oligomerisation of aniline and 1,4-phenylenediamine

Reaction of aniline with hydrogen peroxide with catalytic amount of *cis*-bisglycinato copper(II) monohydrate gives polyanilines through C-N bond formation (equation 3.3). Though several side products were formed in the reaction but only the two major components of polyanilines were isolated. The extent of oxidation of the rings to form C=N bonded

compounds in these cases were different. The 400MHz  $^1\text{H}$  NMR of the two major isolated components of polyaniline is shown in fig 3.3. The spectral pattern of two components are quite complicated to draw information about the structure of polyaniline. UV-visible spectrum of polyaniline has a absorption maxima at 440 nm whereas normal leucomeraldine type polyaniline shows the absorption peak at 325nm. This bathochromic shift observed in our case indicates substantial increase of the extent of



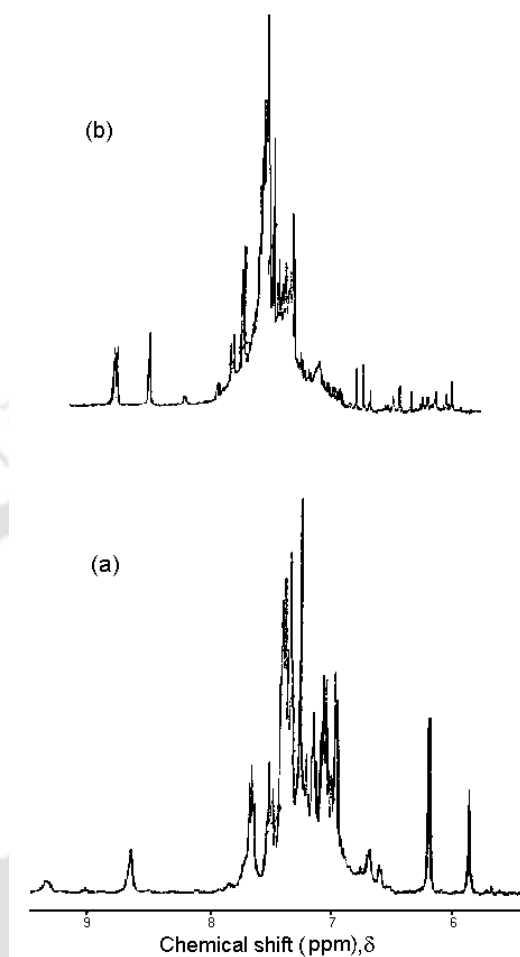


Fig. 3.3 :  $^1\text{H}$  nmr spectra of the two major components of polyaniline pi-conjugation in the polymer. The appearance of a absorption maxima at 440nm can be assigned as due to branched structure of polyaniline from the datas available in literature<sup>169</sup>. The  $^{13}\text{C}$  {  $^1\text{H}$  }nmr spectra can be used as a tool to assign the skeletal structure of a compound. The  $^{13}\text{C}$  {  $^1\text{H}$  }nmr

spectra recorded for the compound indicates the *o*, *p*-branching in the product as well as formation of quinonic end group. The  $^{13}\text{C}$   $\{^1\text{H}\}$  nmr spectra of polyaniline is shown in fig. 3.4.. All the peaks can be assigned with the skeletal structure shown assuming *o*-, *p*- branching in the product polyaniline. The assignments of the peaks are also shown in fig. 3.4.

The GPC measurement for these component showed  $M_n$ ,  $M_w$  values for the two components as 1040, 1250 and 1500, 1900 with the polydispersity values 1.2 and 1.26 respectively. A clear difference in the IR spectra(fig. 3.5) of these two components of polyanilines in the region of  $3300\text{cm}^{-1}$  and also in the region of  $1500\text{-}1700\text{cm}^{-1}$  were observed. Due to C=O, C=N and C=C stretching several strong absorption appear in the  $1500\text{-}1700\text{cm}^{-1}$ . The difference in the two spectra in the region mentioned above is observed in the respective peak intensities as well as peak positions also. This can be understood from the figure itself. It is worth noting that the polyanilines prepared by dehalogenative coupling reactions using nickel complexes as catalyst has a very simple absorption patterns<sup>163b</sup> of the C-NH linkage in this region. This suggests oxidation of the polyanilines to C=N bond leading to pernigraniline type structure during oxidative coupling reactions. The nitrogen contents in the oligomers



were lower than the calculated analytical value of polyaniline having an amino group at one end of the chain. But in both the polyanilines they were close to analysis of a structure having carbonyl as an end group with residual  $\text{Cu}(\text{OH})_2$ . This can occur through an oxidative hydrolysis of the

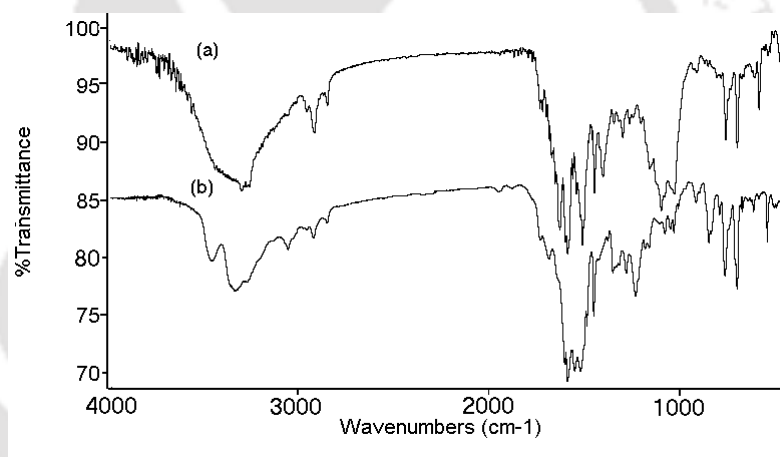


Fig. 3.5 : IR spectra of the two components of polyaniline

$-\text{NH}_2$  group to form  $\text{C}=\text{O}$  group via  $\text{C}=\text{NH}$  bond (path A of scheme 3.2).

Another path can be through a competitive hydroxylation and oxidative polymerisation of aniline (path B of scheme 3.2). The path A is preferred

as we had observed earlier that *p*-aminophenol itself did not oligomerise under similar condition but gave copper(II) containing aggregate.

The preparation of polyaniline by hydrogen peroxide and anilinic compounds are known to catalyse by copper salts such as copper(II) sulphate but the difference of our reaction from the reported one is the mild reaction condition and the performance of the reactions without converting aniline to anilinium salt<sup>163b</sup>.



The 1,4-diaminobenzene oligomerises by *cis*-bis glycinato copper(II) monohydrate in hydrogen peroxide, at ambient temperature in aqueous medium under neutral condition (equation 3.4). The reaction leads

to N-N bonded oligomer as we have observed in the case of cobalt diacetylmonoxime catalysed reaction (section 2.3.4). The proton nmr spectra as well as the  $^{13}\text{C}$  nmr spectra were found to be identical in both the cases indicating that the same type of oligomer is obtained. Therefore no further discussion is made in this regard.

The oligomer has the end group  $-\text{NH}_2$  stretching frequency at  $3333\text{cm}^{-1}$  in contrast to  $-\text{NH}_2$  stretching frequency at  $3432\text{cm}^{-1}$  of the parent 1,4-diaminobenzene. The oligomer has a strong infra-red absorption at  $2665\text{cm}^{-1}$  due to strong intermolecular hydrogen bonding. A strong absorption at  $1545\text{cm}^{-1}$  due to N=N bond stretching is also observed. The extensive hydrogen bonding probably allows to embed copper(II) hydroxide. Formation of interstitial spaces with highly H-bonded systems and inclusion of metal ions in such cavities are well studied<sup>170</sup>. The

aggregation of analogous compound such as benzidine bound to its cationic radical with clay minerals are also documented<sup>171</sup>.

The composition of the different mass fragments obtained in case of the MALDI mass spectra of the oligomer also indicate the presence of both –NH-NH- and –N=N- type of bonding in the oligomer. The MALDI mass spectra of the oligomer has highest m/e value at 1042 suggesting it to oligomerise about ten units of 1,4-diaminobenzene.

The MALDI mass spectra of the oligomer is shown in fig. 3.6. The other mass fragments obtained such as at m/e values 950.04, 843.06, 740.43, 725.54, 634.86, 545.26, 529.23, 434.95 can be assigned as due to the mass fragments as shown in fig. 3.7 below. The highest intensity peak in this case was observed at m/e value 434.95.

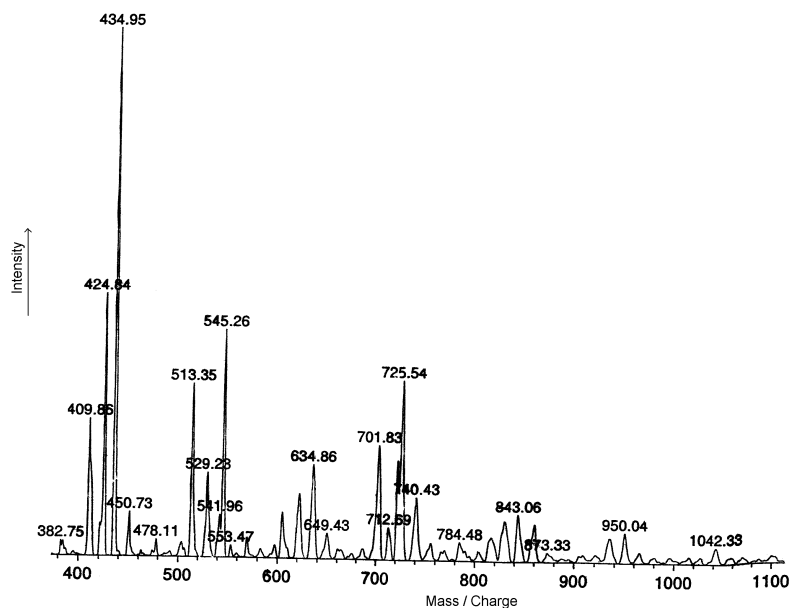
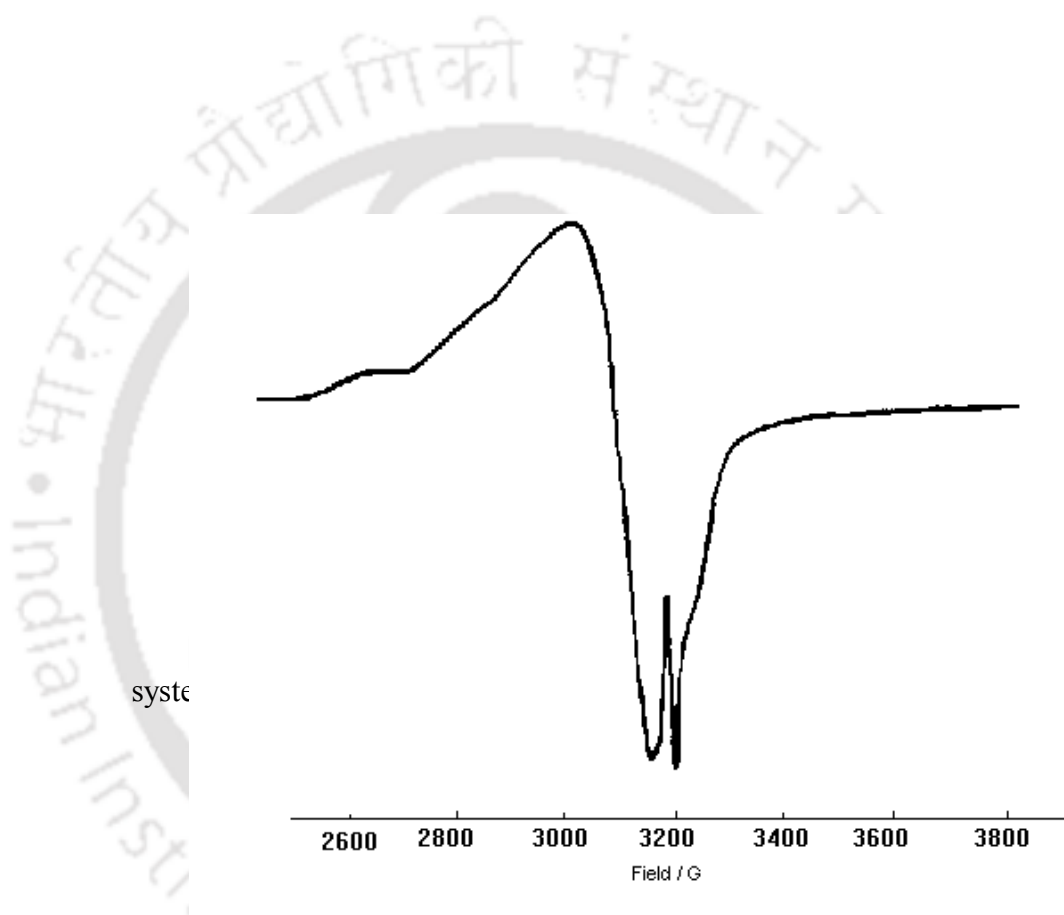


Fig. 3.6 : MALDI mass spectra of oligomer of 1,4-phenylenediamine

In the absence of hydrogen peroxide the 1,4-diaminobenzene interacts with *cis*-bisglycinato copper(II) monohydrate. A stoichiometric mixture of the two has absorption peaks at 435 and 540 nm. On oligomerisation these two absorptions are lost. However, the oligomers possess strong absorption at 473 nm and 332 nm as shown in the case of the oligomer from cobalt diacetylmonoxime catalysed reaction in chapter 2.

This shows the absorptions to be independent of a metal ion present in the



375-450nm<sup>172</sup> in visible spectra. Thus, the absorption at 473 nm is attributed to the formation of radicals at the end group stabilised by metal ion. The polyaniline prepared by copper catalysed reaction has a broad

absorption with usual hyperfine with nitrogen of a distorted octahedral geometry of copper(II) at 3165G and a strong signal due to a radical at 3180G (figure 3.8). These signals are not effected significantly on heating but there is slight dependence on the position of the signals on changing the central field. The oligomers prepared by cobalt catalysed reaction possess only one signal at 3200G due to a radical as shown in chapter 2. The radical probably arises from Cu(II)-O· type of species that may be formed during the oxidative reactions of cis-bis-glycinato copper(II) with hydrogen peroxide. The radicals are possibly stabilised by metal centers embedded in the interstices of the oligomers. The metal stabilised radicals are well documented in the literature<sup>173</sup>, but without a crystal structure it is difficult to draw a three dimensional structure of such metal stabilised

Fig. 3.8 ESR spectra of polyaniline ( Temperature 30<sup>0</sup>C, central field applied 3200G with 1500G sweep width )

radical, additionally the available results can not rule out the possibility of degradation of a Cu<sub>2</sub>O<sub>2</sub> dimeric oxo-bridged species too<sup>174</sup>. The oligomers are stable in neutral medium but degrades in acidic medium to lose it's absorption maximums at 472 nm and 332 nm arising due to a radical and also due to the *trans* N=N bond.

### 3.4 Quinhydron from hydroquinone

The hydroquinone at room temperature on reaction with *cis*-bis glycinato copper(II) monohydrate and hydrogen peroxide did not yield oxidised product. But the reaction of hydroquinone with *t*-butyl hydroperoxide in presence of *cis*-bisglycinato copper(II) monohydrate produces quinhydrone (Equation 3.5). Quinhydrone is the charge transfer

complex of hydroquinone and benzoquinone. The product was characterised by comparing its NMR, IR with authentic sample.

### 3.5 Oxidative reactions of oxime

Oxime is a good protecting group for carbonyl functional group<sup>175</sup>. A selective deprotective methodology is always of demand to regenerate parent carbonyl group. We had observed that oximes can be deoximated to carbonyl compounds by *cis*-bis-glycinato copper(II) monohydrate in the presence of hydrogen peroxide. However, these reactions also led to

carboxylic acid and amides as side products (scheme 3.3). The products formed in the reaction were purified by column chromatography. They were further characterised by recording IR and NMR of the isolated components and by comparison with authentic sample.

### **3.6 UV-Visible study on the reactions of phenol with *cis*-bis glycinato copper(II) monohydrate**

A solution containing phenol with *cis*-bisglycinato copper(II) monohydrate and hydrogen peroxide showed formation of an isosebestic point at 304nm in UV-visible spectroscopy. Due to lack of any well defined

absorption maxima had prevented us from making further kinetic study. However, a solution containing *o*-cresol, *cis*-bis glycinato copper(II) and hydrogen peroxide showed growth of a well defined peak at 412.4 nm. This absorption initially grew to a maximum value and decayed slowly as the hydrogen peroxide got consumed in the reaction (fig. 3.9). The final

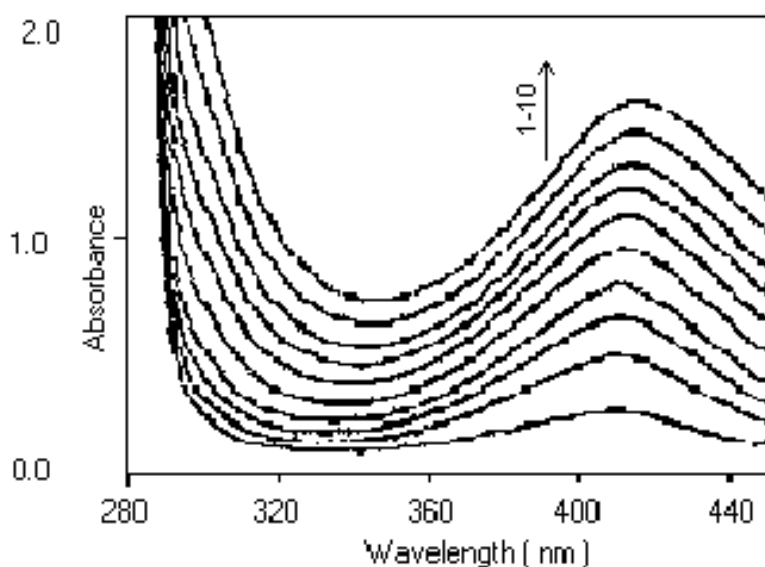


Fig. 3.9 UV-visible spectra of solution containing *o*-cresol ( 0.093 mmol), *cis*-bis-glycinato copper(II) monohydrate (0.0018mmol), Hydrogen peroxide ( 30 %, 100 vol, 5  $\mu$ l ) in water(3ml) at one minute time interval.

products obtained from *o*-cresol did not show the absorption at this wave length. Thus, the origin of the absorbance at 412.4 nm could be from an intermediate species which take part in the reaction. Linear increase in the rate of formation of the intermediate species on increase in concentration of hydrogen peroxide as well as *cis*-bis-glycinato copper(II) monohydrate were observed (fig 3.10). There was a significant difference in the reactivity in *cis*-bis-glycinato copper(II) and *trans*-bis-glycinato copper(II) complex in these hydroxylation reactions. A solution comprising *o*-cresol, *trans*-bis-glycinato copper(II) monohydrate,

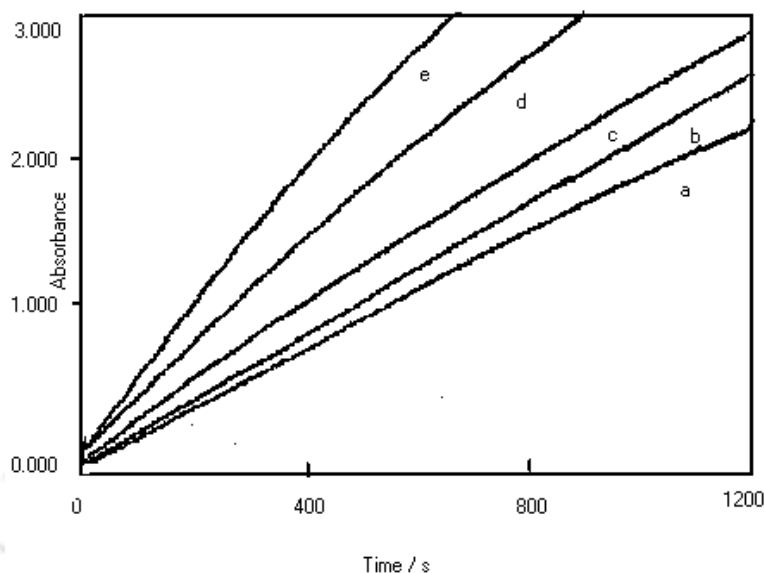


Fig. 3.10: Plot of absorbance vs time at 450nm in case of a-e: *o*-cresol (0.093mmol), *cis*-bis glycinato copper(II) monohydrate (0.0018 mmol) in 3ml water. Hydrogen peroxide (30%, 100vol ) , concentration a = 1 $\mu$ l, b = 2 $\mu$ l, c = 3 $\mu$ l, d = 4 $\mu$ l , e = 5 $\mu$ l

hydrogen peroxide in water upon reaction also showed growth of  $\lambda_{\max}$  at 412.4 nm. All these suggested that both the reactions passed through a similar intermediate. Attempts were made to know about the existence of two different absorptions maximum for intermediates in the reactions of *cis* and *trans* isomer from two independent experiments. The UV-visible spectra of a reaction mixture having both *cis* and *trans* complex together

did not give separate peaks. Taking the rate of increase in the absorption at 412.4 nm as the index of formation of the catalytic species for hydroxylation it was found that the rate of *cis*-bis-glycinato copper(II) monohydrate catalysed reaction was 4.5 times faster than the *trans* counterpart under identical reaction conditions. The rate of a equimolar mixture of *cis* and *trans* isomer was 1.8 times faster than the *trans* isomer. The isomerisation of *trans*-bis-glycinato copper(II) in solution to *cis*-bis-glycinato copper(II) monohydrate is a well known phenomenon<sup>167</sup>. The active center of tyrosinase contains *cis*-histidines as ligand in the active site<sup>176</sup>. The phenoxy linked galactose oxidase<sup>157</sup> also contains *cis*-histidines present in the active site.

### **3.7 Attempted reaction on copper tyrosinato complex**

Tyrosinase is an enzyme that contains copper(II) center and can specifically causes the *ortho* hydroxylation<sup>155</sup>. A complex of tyrosine by the reaction of tyrosine with copper(II) acetate was prepared as shown in equation 3.6. It was obtained as blue solid having composition

(tyro)<sub>2</sub>.Cu.3H<sub>2</sub>O (where tyro is tyrosinato group). The identity of the complex was further ascertained by recording its thermogravimetric analysis. The thermogram is shown in fig. 3.11.

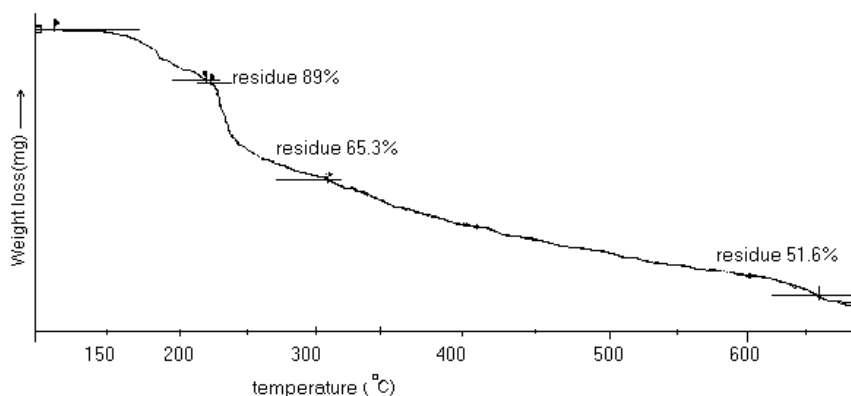


Fig. 3.11 Thermogram of *bis*-tyrosinatocopper(II) trihydrate

The Thermogravimetry giving details of the weight losses upon heating are also shown in scheme 3.4. The IR spectra of the complex shows that the carbonyl frequency for the complex is observed at  $1610\text{cm}^{-1}$  instead of  $1594$  for the parent tyrosine molecule. So is the case with the IR absorption of the hydroxyl group. The -OH absorption frequency is observed at  $3306\text{cm}^{-1}$  instead of  $3210\text{cm}^{-1}$  for the parent molecule. The shifting of

these absorption frequencies to longer wavelength can be attributed as due to the coordination of these groups with the metal center in the complex.

The absorption due to the metal oxygen bond is observed at  $840\text{cm}^{-1}$ . This

compound was found insoluble in most of the conventional solvents including water and thus its reactivity towards hydroxylation reaction could not be explored.

### **3.8 Mechanism of *cis*-bis glycinato copper(II) catalysed oxidative reactions:**

The interaction between hydrogen peroxide and copper(II) has been investigated with greater scientific interest as this provides an efficient combination for oxidation of numerous organic substrates. In alkaline medium the interaction of copper(II) salts with hydrogen peroxide usually yields an unstable brown precipitate. Such precipitate obtained from the interaction between hydrogen peroxide and copper acetate was claimed to afford  $[\text{Cu}(\text{OH})_2(\text{OOH})(\text{OAc})_2]$  on the basis of copper content of the air dried product.<sup>177</sup> The same compound after sufficient vacuum drying yields a raw formula of  $\text{CuO}_2\text{H}$ <sup>178</sup>. The possible intervention of superoxide  $\text{O}_2^-$  had also been taken into account due to its decomposition to  $\text{O}_2$  and  $\text{H}_2\text{O}_2$ .<sup>179</sup> Catalytic decomposition of hydrogen peroxide by copper(II) complexes, particularly with phenanthroline and imidazole ligands were found to generate  $\text{Cu}(\text{I})\text{O}_2\text{Cu}(\text{I})$  superoxide ion as intermediate<sup>180</sup>. The copper(I) by the reaction with  $\text{O}_2$  and  $\text{H}_2\text{O}_2$  regenerates copper(II). Generation of peroxodicopper(II)  $[-\text{Cu}(\text{II})-\text{O}-\text{O}-\text{Cu}(\text{II})-]$  structure from the reaction of copper(II) and  $\text{H}_2\text{O}_2$  was also observed.<sup>181,182</sup>

The activation of dioxygen molecule for coordination to the metal containing active site is a fundamental step involved in these reactions. Binding involves electron transfer from the reduced metal site to the oxygen molecule accompanying with a decrease in the O-O bond order<sup>182</sup>. Reductive cleavage of the O<sub>2</sub> molecule in metalloenzyme catalyzed oxidation of organic substrates and oxidase reactions involving the conversion of dioxygen to water is a basic phenomena.<sup>182</sup> Extensive research on metal dioxygen adducts have been carried out with a particular reference to the adduct characterized from the reaction of dioxygen with Cu<sup>I</sup> precursor and product formed was characterized in detail. The study indicated the generation of [Cu<sub>2</sub>O<sub>2</sub>]<sup>n+</sup> core in which the two oxygen atom lie between the two copper center with different thermal and geometric

parameters.<sup>181</sup> This can be a  $[\text{Cu}_2(-\text{O})_2]^{n+}$  (A) or  $[\text{Cu}_2(-\text{O}_2)]^{n+}$  (B) core in which the O-O bond is retained. This type of adduct receives much attention as an intermediate in hydroxylation reactions carried out by copper oxygenase such as tyrosinase and methane monooxygenase.<sup>183</sup> The core(B) has the ability to interconvert to (A) prior to activation of the substrate C-H bond and evidence in support of the core (A) to hydroxylate arene rings are available.<sup>184</sup> Another binding mode for the copper core is also documented where the copper ions are bridged by peroxide in a *cis*  $\mu$ -1,2 configuration (C) with an additional bridge<sup>185</sup>, most likely hydroxide<sup>186</sup>. The structure formed is also influenced by the nature of the

ligand.<sup>187</sup> Generation of dimeric oxo-bridged copper core having nitrogen ligands as the surrounding ligands is also established<sup>155,173,188</sup>.

We have observed that the catalytic system of *cis*-bis glycinato copper(II) can cause hydroxylation of phenol but the reaction was not specific and both *ortho* and *para* dihydroxy phenols were obtained. In order to explain products of *cis*-bis-glycinato copper(II) monohydrate catalysed reactions described in the this chapter a possible reaction mechanism is proposed (scheme 3.5 ).

Similar mechanism was also used in biological systems to explain reactivity of copper(II)bipyridine complex towards oxidation reaction<sup>189</sup>. The *cis*- alignment of the two oxygen atoms of the catalyst possibly provides favourable environment for the reactant molecules such as phenol and hydrogen peroxide. This in turn leads to the formation of metal peroxo intermediate or metal hydroxo species as shown in the scheme 3.5 and these intermediate species are believed to be responsible for the formation of hydroxylated products as shown in the scheme 3.5. This might be one of the reason of the slower reaction rate in case of *trans*-bis-glycinatocopper(II) complex. Although the oxo-bridged Cu<sub>2</sub>O<sub>2</sub> core of copper catalyst are involved in many biologically related systems,

we prefer to use a peroxy species as our reactions did not proceed with molecular oxygen in the presence of oxygen at room temperature. The



copper(II) dimeric cores usually binds with oxygen in reversible manner. We have also observed radical species in the aggregate of hydroquinone as well as in polyaniline and poly 1,4-phenylenediamine. The radicals are

believed to be  $\text{Cu}^{\text{II}}\text{-O}\cdot$  analogous to the one (A) suggested in the scheme 3.5.

### 3.9 Electrical and thermal properties of hydroquinone aggregate, polyanilines and related compounds:

We had observed that *cis*-bis-glycinato copper(II) monohydrate along with hydrogen peroxide at ambient condition does not oligomerise hydroquinone. It is also a well known fact that hydroquinone has aggregated structure and it can form a large number of aggregates such as  $\alpha, \beta, \gamma$  forms and also clathrates with different organic molecules<sup>174</sup>.

We have found that hydroquinone on reaction with hydrogen peroxide in the presence of a catalytic amount of *cis* bisglycinato copper(II) monohydrate gives a hydroquinone aggregate, through an exothermic reaction. The aggregate is soluble in solvents such as acetone and acetonitrile. On the basis of elemental analysis of the compound and copper estimation of copper the adduct is found to be  $[\text{C}_6\text{H}_6\text{O}_2 \cdot \text{H}_2\text{O}]_{11} [(\text{C}_2\text{H}_4\text{O}_2\text{N})(\text{C}_6\text{H}_4\text{O}_2)(\text{H}_2\text{O})\text{Cu}]$

The IR spectrum shows a broad and sharp signal at  $3297\text{cm}^{-1}$  due to O-H stretching. The characteristic absorption due to *p*-substituted aromatic ring is observed at  $1593, 1357\text{ cm}^{-1}$ . The absorption at  $1090\text{ cm}^{-1}$  is

assigned to C-O bond stretching. The aromatic C=C stretching frequency appears at  $1618\text{cm}^{-1}$ .

The  $^1\text{H}$  nmr spectra of the product gives two sharp signals. One observed at  $8.6\ \delta$  due to the two hydroxyl protons and the other at  $6.5\ \delta$  due to the aromatic protons. This further supports the fact that the product is an aggregate of hydroquinone. The -OH signal of the DMSO- $\text{d}_6$  solvent gets significantly enhanced at  $3.1\delta$  as compared to a signal arising from the dissolved water in the solvent used. As expected the  $^{13}\text{C}\{^1\text{H}\}$  nmr spectra also gives two signals at  $116,150\ \delta$  only. The  $^{13}\text{C}$  signal at  $150\ \delta$  is due to the carbons directly attached to the hydroxyl groups and the one at  $116\delta$  is due to the other set of four equivalent carbons.

The  $M_n$  and  $M_w$  in DMF for the product was found to be 3350 and 3362 respectively from GPC record of the product(fig 3 .12) The role of hydrogen peroxide in this reaction appears to facilitate formation of a strong hydrogen bonding network during its decomposition to water and

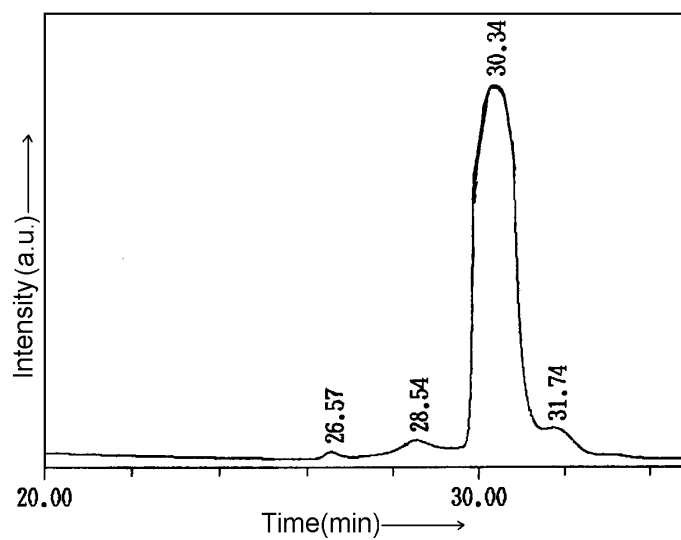


Fig. 3.12 : GPC of hydroquinone aggregate

oxygen and anchor the copper(II) ion to the aggregate.

The esr studies carried out on the aggregate reveals the presence of copper(II) center in the aggregate(fig. 3.13). The temperature dependent

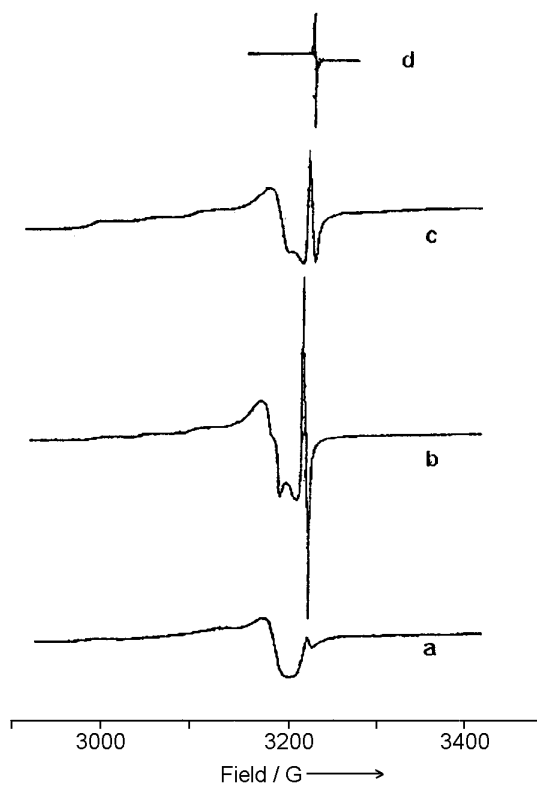


Fig. 3.13 ESR spectra of hydroquinone aggregate (a) at 30<sup>0</sup>C (b) at 180<sup>0</sup>C (c) at 40<sup>0</sup>C after cooling (d) dpph as standard ( central field applied is 3200G with 1500G sweep width)

esr studies of the aggregate shows that the sample has a signal typical of copper(II) ion in a distorted octahedral environment at room temperature.

The original esr signal at 3200G changes on heating and give rises to new signals at 3180G and 3220G suggesting a tetragonal distortion in the copper center. A new signal at 3240G appears on heating the sample that resembles the radical generated by copper(II) ion from ascorbate<sup>190</sup>. The signal does not have the hyperfine structure as anticipated for a semiquinone type of radical which suggests that this could be a free electron in the matrix generated from the copper center and could be a phenomenon occurring due to a structural change where the  $t_{2g}$  set of orbitals energy are enhanced and participate in partially losing the electron to the matrix through lateral overlap. The esr spectra at two different temperature are shown in fig. 3.13 (a) & (b). The sharp signal appearing in a similar position to the standard diphenyl picryl hydrazil signal does not disappear on cooling but weakens it's intensity with time. The two signals which appeared on heating disappear to give one signal [fig.3.13(c)]. This observation indicates that the electron/s generated in the matrix get localised on the metal center on cooling.

The electrical resistance offered by thin films prepared from the hydroquinone aggregate containing copper hydroxide/ hydroperoxides were studied. The variation of resistance versus temperature in the range of 30-200<sup>0</sup>C had a normal Gaussian shape(fig. 3.14).

The resistivity plot shown above indicates that the normalised resistivity increases up to a temperature of 107°C and beyond that temperature the resistivity decreases. Material prepared from a homogeneous mixture of hydroquinone and *Cis*-bis-glycinatocopper(II) monohydrate in acetonitrile and subsequent removal of solvent, can also show a similar property, where

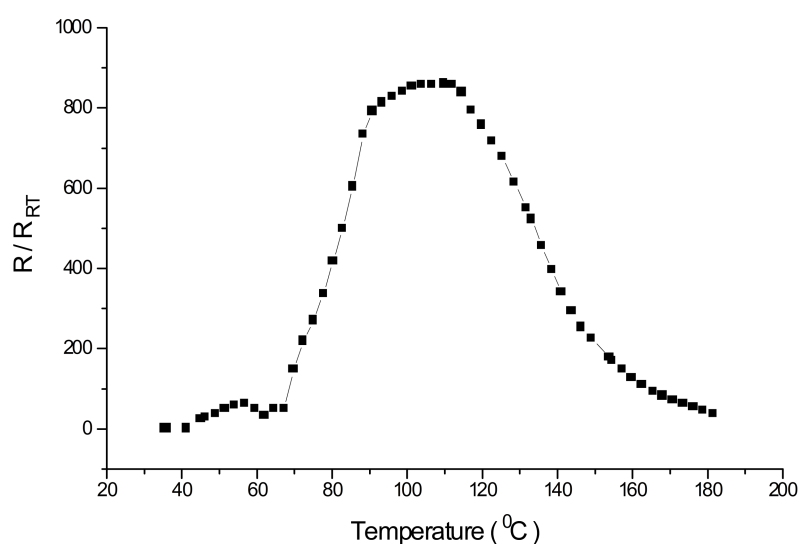


Fig. 3.14: Plot of resistance( R ) normalised to resistance at room temperature ( R<sub>RT</sub> ) vs temperature of hydroquinone aggregate

there is a sharp 6.5 fold rise in the resistivity from 60-80°C and the resistance falls beyond 80°C. The profile thus obtained has a different

shape compared to the profile obtained from the aggregate prepared by *cis*-bis-glycinato copper(II) monohydrate and hydrogen peroxide with hydroquinone.

Polyanilines synthesised above from the reaction of aniline with hydrogen peroxide in the presence *cis*-bis-glycinato copper(II) monohydrate have interesting electrical properties. The films prepared from each of them had a resistance profile which increased with temperature to a maximum value and then decreases beyond that temperature. The plot of resistance normalised to room temperature resistance vs temperature of polyaniline are shown in fig. 3.15(a). As mentioned there are two major fraction of polyaniline having difference in molecular weight. Both shows the same trend in change in resistance. Therefore only variation of resistance of one sample is shown. Similar observation was obtained for the oligomer of 1,4-phenylenediamine is also shown in fig. 3.15(b).

The quinhydrone forms stacked structure in solid state<sup>191</sup>. Thus the quinhydrone increases slowly in the range 30-100<sup>0</sup>C and then the resistivity drops down ten fold in the range 100<sup>0</sup>C to 160<sup>0</sup>C [fig. 3.16(a)]. To understand the effect of copper(II) ion on the electrical properties of quinhydrone, *cis*-bis-glycinato copper(II) monohydrate was doped in the

quinhydrone by dissolving quinhydrone and *cis*-bis-glycinato copper(II) monohydrate (10:1 molar ratio) in acetonitrile.

So the resistance of quinhydrone vs temperature were measured in absence and presence of copper complexes. The resistance vs temperature of the sample was measured of a film made from this solution. The observation recorded in this case is shown in [figure 3.16(b)].



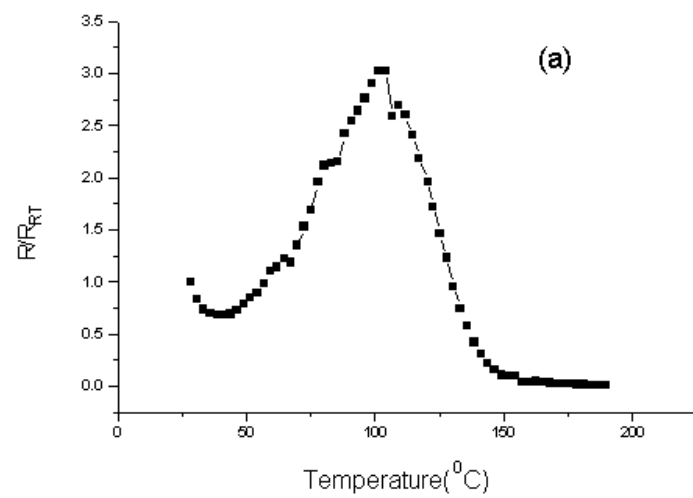
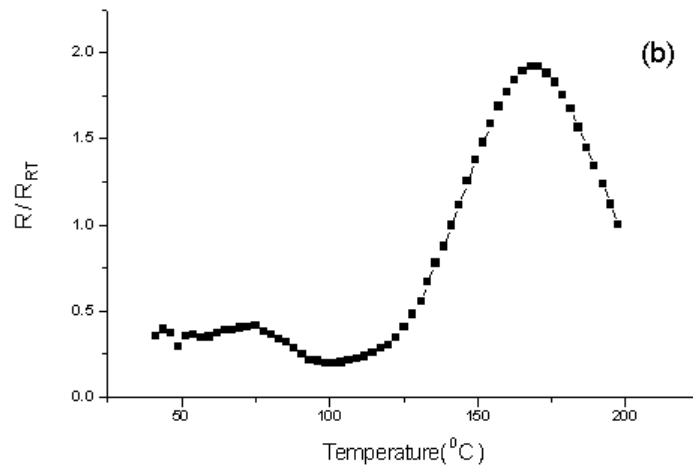


Fig. 3.15 : Plot of resistance(  $R$  ) normalised to resistance at room temperature (  $R_{RT}$  ) vs temperature of (a) polyaniline (b) oligomer of 1,4-phenylene diamine

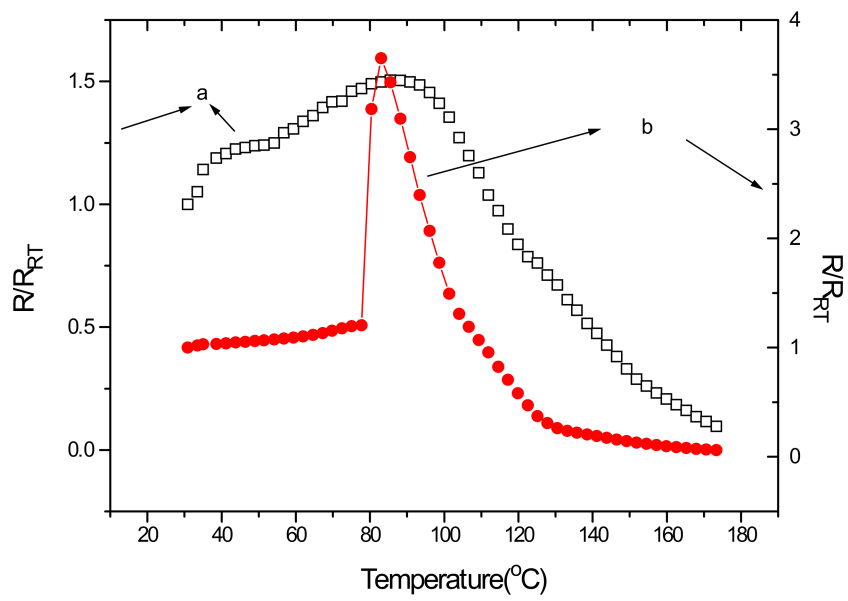


Fig. 3.16

This temperature dependence of resistivity profile are interesting because of the possibility of using these to devise thermoelectric switch. These profiles can be explained in terms of proton conductivity arising from extensive hydrogen bonding in the system. Such hydrogen bonding gets disrupted upon heating and consequently the proton conductivity decreases. Above a particular temperature the proton conductivity becomes less significant and the conductivity arising from the delocalisation of the  $\pi$ -electrons in the system become predominant and the resistivity therefore decreases beyond that particular temperature.

Thermal measurements carried out on samples of polyaniline indicates that the polymer is unstable beyond 180<sup>0</sup>C. The thermogram of polyaniline shows substantial weight loss at that temperature. The compound losses 45% of its original weight in between the temperature range 180-250<sup>0</sup>C. 23% of residue left after heating to a temperature of 650<sup>0</sup>C. This instability of polyaniline is reflected in the DSC trace also. The DSC trace of the polymer shows that it exhibits exothermic behaviour beyond 180<sup>0</sup>C. The thermogram and DSC profile of polyaniline are shown in fig. 3.17.

Between the temperature range 200-580<sup>0</sup>C the compound losses 92% of its original weight and only 8% residue is left after heating to a temperature of 650<sup>0</sup>C. The DSC profile of the oligomer shows continuous exothermic behaviour beyond 50<sup>0</sup>C and the rate of heat desorption increases beyond 200<sup>0</sup>C indicating that an internal structural change occurs in between the temperature range 200-580<sup>0</sup>C. In both the cases the compounds does not show any melting point in their respective DSC profile in between 30-350<sup>0</sup>C.

The thermogram of the hydroquinone aggregate shows that the weight loss of the aggregate takes place in two stages. Between 160-250<sup>0</sup>C the weight loss calculated was 53% while beyond 250<sup>0</sup>C the weight loss is continuous and finally the compound left with only 7% residue. Nevertheless the compound is unstable beyond 160<sup>0</sup>C. In

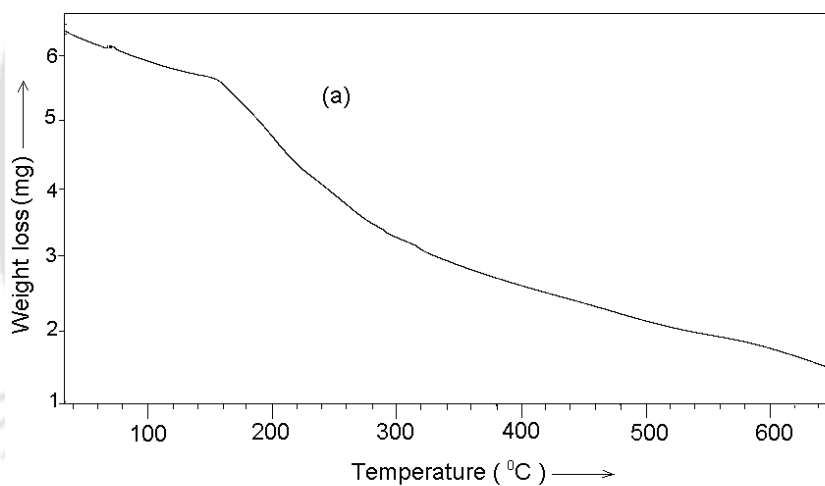
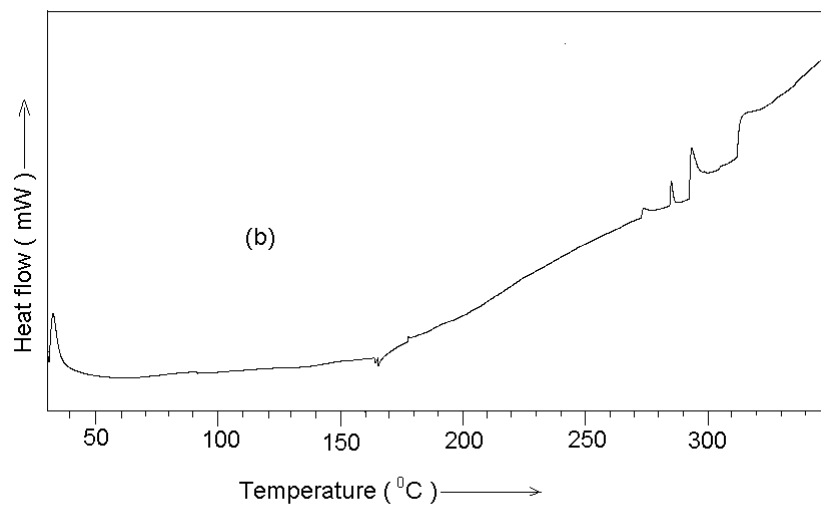
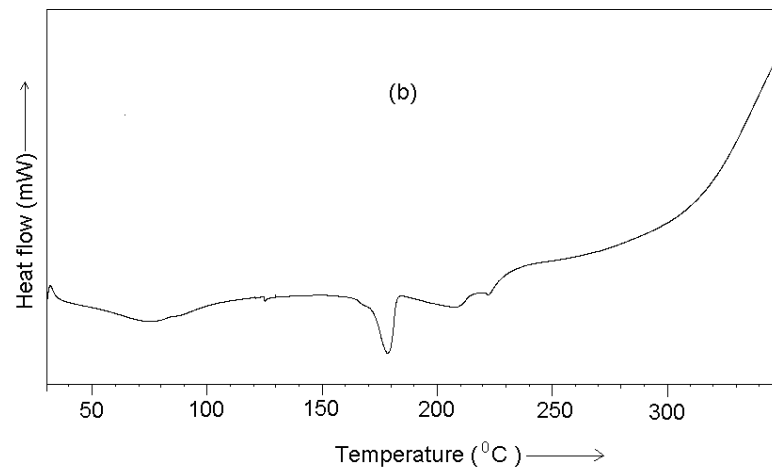


Fig. 3.17 (a) Thermogram of polyaniline (under nitrogen atmosphere)

(b) DSC profile of polyaniline ( heating rate  $5^{\circ}\text{C} / \text{min}$  )

the DSC profile of the aggregate there is a sharp endothermic peak at



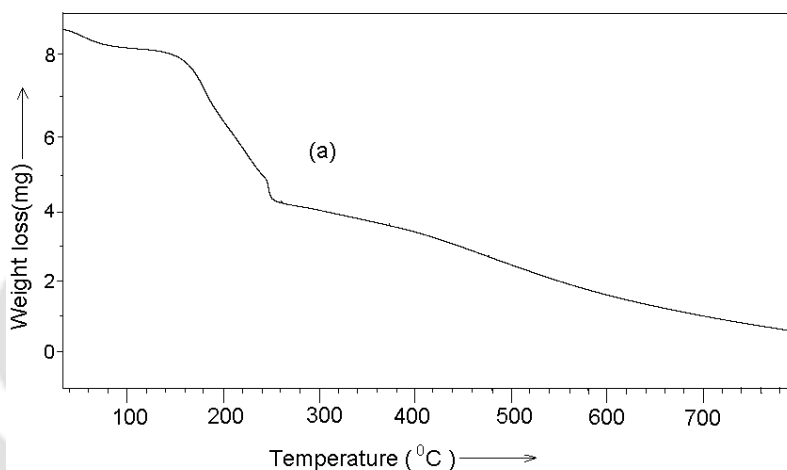
160°C. This observation indicates that the aggregate might break at

Fig. 3.18 (a) Thermogram of hydroquinone aggregate

(b) DSC of hydroquinone aggregate(heating rate  $5^{\circ}\text{C} / \text{min}$ )

that temperature and the endothermic peak observed may correspond to sublimation of hydroquinone. The thermogram and the DSC profile for hydroquinone aggregate are shown in fig. 3.18(a) & (b) respectively.

### 3.10 Comparison of copper(II) and cobalt(II) catalysed oxidation



reactions

Although both the copper(II) and cobalt(II) catalysed reactions

causes oxidative transformations of aromatic compounds, both have their characteristic features.

a) Copper(II) catalysed reactions took place in milder conditions relative to cobalt catalysed reactions.

b) Copper(II) catalysed reactions gives hydroxylated phenols from reactions of phenolic compounds without selectivity on a unsubstituted phenol. The cobalt catalysed reactions of phenols led to oligomerisation of phenols through C-O bond formations and were very specific when cresol derivatives were used.

c) In the reaction of 2,6-dimethylphenol the cobalt complex led to oligomerisation via C-O and C-C bond formation whereas similar reactions by *cis* bis glycinato copper(II) gave the quinone as well as dihydroxy derivative.

d) In the case of cobalt dionemoxime catalysed reactions benzylic activation is predominant, whereas this is not true for *cis*- bis glycinatocopper(II) catalysed reaction.

e) In the case of aniline the C-N bonded oligomers having linear structure was observed to be prominent in cobalt catalysed reaction but

in the case of copper catalysed reactions *o*, *p* coupled product having end group as carbonyl was found to be prominent.

f) The cobalt system was found to be very effective for oxidation of benzyl alcohol under mild condition but in the case of copper this reaction was less predominant.

### 3.11 Experimental

Discussion about the general instrumental/analytical techniques followed has already been done in chapter 2(section 2.7). Therefore further discussion in this regard will not be made here. The copper estimation was done by standard iodometric procedure by adding potassium iodide and titrating the liberated iodine with sodium thiosulphate solution. Sodium thiosulphate solution was standardised by iodometric titrations by using potassium dichromate solution as the primary standard.

The reagents used for the synthesis such as copper(II) sulphate pentahydrate, copper(II) acetate monohydrate, glycine were of analytical grade and were procured from E.Merck and Qualigen(Glaxo). The solvents used during the synthesis were purified by the procedure as mentioned in chapter 2 (section 2.7). *p*-Tolyl

benzaldoxime was synthesised by the standard procedure. For this hydroxylamine hydrochloride (1g) and sodium acetate (2g) was dissolved in water (10ml). *p*-Tolyl benzaldehyde (0.5g) was added to this solution with shaking. The mixture was then allowed to stir for few minutes and allowed to stand. Then the mixture was warmed on a water bath for 10 minute and cooled. The product oxime was then filtered off and washed with cold water (2x20ml) and recrystallised from ethanol. Melting point 79<sup>0</sup>C (reported 80<sup>0</sup>C)

*p*-Tolyl benzaldimine was synthesised by condensation of aniline with *p*-tolylaldehyde by standard procedure (m.p. of *p*-tolyl benzaldimine 169<sup>0</sup>C found 169<sup>0</sup>C)

The *cis*-bis-glycinato copper(II) monohydrate and *trans*-bis-glycinato copper(II) monohydrate were prepared by published procedure<sup>167</sup>. The kinetic studies were carried out by mixing requisite amount of *cis*-bis glycinato copper(II) monohydrate and phenolic compound in water or acetonitrile followed by addition of hydrogen peroxide to the reaction mixture in quartz cell (cap. 3cm<sup>3</sup>) and carrying out the time and wavelength scan of the solutions at room temperature(25<sup>0</sup>C). In the reaction where *o*-cresol was used as one of

the reactant the kinetic at 450nm were recorded in time scan mode with variation of concentration of *cis*-bis-glycinato copper(II) monohydrate and hydrogen peroxide to make the study uniform.

#### **Preparation of *cis*-bis-glycinato copper(II) monohydrate:**

Copper(II) sulphate pentahydrate ( 3.0g, 12.0 mmol) was dissolved in 17 ml of hydrochloric acid(1M). Glycine (1.5g, 20.0 mmol) was added to this solution with stirring and the resulting solution was warmed over an water bath for one hour. To this solution solid sodium hydrogen carbonate was added until the precipitation was complete. The precipitate was then filtered and then recrystallised from hot water. The resulting product was dried in an oven. IR (KBr) : 3280(b,s), 2992(m,s), 1600(s), 1388(s), 1328(s), 1156(s), 1063(s), 917(s). UV-visible,  $\lambda_{\max} = 630\text{nm}$ .

#### **Preparation of *trans*-bis-glycinato copper(II) monohydrate**

A homogeneous mixture of copper(II) acetate monohydrate and glycine were mixed together in 1: 2 molar ratio in a pastel amd mortar and ground into paste and left for 3hrs at room temperature. The product was washed with ethanol and diethyl ether ether to obtain the *trans*-bisglycinato copper(II) monohydrate<sup>167</sup>.

### **Preparation of bis-tyrosinato copper(II) trihydrate**

Copper acetate monohydrate ( 1g, 5 mmol) was dissolved in 10 ml of hydrochloric acid(1M). Tyrosine (0.9g, 5 mmol) was added to this solution and the resulting solution was warmed on an waterbath at 100<sup>0</sup>C for one hour. A clear solution was obtained. The solution was then cooled and then neutralised with sodium bicarbonate solution (1 M, 10 ml). Light blue coloured solid was obtained. The solid product obtained was then filtered and washed with water and finally dried in an oven. Elemental analysis: Calculated for the composition C<sub>18</sub>H<sub>20</sub>N<sub>2</sub>O<sub>6</sub>.Cu:3H<sub>2</sub>O, C, 45.2 ; H, 5.44 ; found C, 45.7 ; H, 4.05 ; N, 5.52. N, 5.86. IR (KBr) 3300(b,s), 3150(m), 1610(s), 1580(s), 1510(s), 1400(s), 1245(s), 1096(s), 840(m).

### ***Cis*-bisglycinato copper(II) monohydrate catalysed reaction of phenol with hydrogen peroxide**

To a mixture of *cis*-bisglycinato copper(II) monohydrate ( 50 mg, 0.225 mmol) and phenol (473 mg 5.32 mmol) in a round bottom flask hydrogen peroxide(1cm<sup>3</sup>, 30%) was added and the mixture was allowed to stirred at room temperature. A white paste

obtained was slowly turned brown and the colour intensified with time. After 24 hrs of continuous stirring the reaction mixture was washed several times with petroleum ether (4 X 20cm<sup>3</sup>) to obtain a paste and this paste was washed with water (1cm<sup>3</sup>) and dried in evacuated desiccator to obtain black solid. Yield 51%. IR (film) 3297(s), 2930(s), 1749(s), 1618(s), 1593(s), 1456(s), 1357(s), 1214(s), 1090(s), 835(s), 741(s)cm<sup>-1</sup>. <sup>1</sup>H nmr (DMSO-d<sub>6</sub>) 8.5(s), 8.0(s), 7.8(s), 6.8(m), 7.0(m) and 7.35(m) δ. <sup>13</sup>C{<sup>1</sup>H} nmr (DMSO-d<sub>6</sub>) 115, 116, 119, 120, 129, 145, 150 and 155 δ. The crude mixture thus obtained was passed through a silica gel column with hexane ethyl acetate mixture (15 % ethyl acetate in hexane) as eluent. The products hydroquinone, catechol were further characterised by recording their nmr, IR and comparing melting point with authentic sample.

#### **Reaction of cresols**

A mixture of cresol ( 540mg, 5mmol) , hydrogen peroxide (1cm<sup>3</sup>, 30%) and *cis*-bisglycinato copper(II) monohydrate (50mg, 0.225 mmol) was stirred at room temperature for six hours. The solvent was removed under reduced pressure. The products were purified by column chromatography by using hexane and ethyl acetate mixture as

eluent with silica gel as column material. The analytical and spectroscopic data obtained for different cresols are given below.

**(a) Product of *o*-cresol**

Yield of 2,5-dihydroxy toluene 98%.  $^1\text{H}$  nmr (acetone- $\text{d}_6$ , 400 MHz ) 2.2-2.4(m, 3H), 6.5-7.5(m, 3H), 8.3(broad s, 1H)  $\delta$ ;  
 $^{13}\text{C}$   $\{^1\text{H}\}$ nmr (acetone- $\text{d}_6$ ) 15.02, 114.47, 119.19, 126.46 130.48 , 148.10 and 155.70  $\delta$ ; IR (neat) 3390 (bs), 2918(w), 1730(m),1612 (s), 1512(s), 1214(s), 810(s). Elemental analysis, found C, 67.29; H, 5.93 calculated for  $\text{C}_7\text{H}_8\text{O}_2$ ; C, 67.74 H, 6.4.

**(b) Product of *p*-cresol**

Yield of 3,4-dihydroxy toluene 37 %. IR (neat) 3372(bs), 2918 (w), 1736(m), 1606(s), 1510(s), 1214(s), 816(s).  $^1\text{H}$  nmr (dms $o$ - $\text{d}_6$ , 400MHz ) 2.2-2.6 (m, 3H) , 6.7-7.6 (m, 3H) , 7.95 ( broad s, 2H )  $\delta$ .  $^{13}\text{C}$  $\{^1\text{H}\}$  nmr (acetone- $\text{d}_6$  , 400 MHz ) 19.5, 114.7, 119.62, 126, 129.36, 131.78 and 134.3  $\delta$ . Elemental analysis: found C, 67.26 H, 5.70 calculated for  $\text{C}_7\text{H}_8\text{O}_2$ ; C, 67.74 H, 6.4

### Reaction of 2,6- dimethylphenol

To a mixture of 2,6-dimethylphenol (0.610g, 5mmol) and *cis*-bis-glycinato copper(II) monohydrate (50mg, 0.225 mmol) hydrogen peroxide (1cm<sup>3</sup>, 30%) was added. The resulting mixture was stirred at 70<sup>0</sup>C on a water bath for 4hrs. The pasty mass obtained was washed with petroleum ether(3x25ml) and then with dichloromethane ( 2x25 ml). Finally the product was dried under vacuum to obtain a solid product. The product was further purified by column chromatography to obtain 2,6-dimethyl benzoquinone(5%) and 1,4-dihydroxy 2,6-dimethylbenzene(31%). The compounds were characterised by recording nmr, IR, and comparing with authentic sample. The analytical data of 1,4-dihydroxy-2,6-dimethylbenzene. IR (KBr) 3472(bs), 2919(s), 1719(s), 1659(s), 1600(s), 1480(s), 1200(s), 1029(s), 886(m) cm<sup>-1</sup>. <sup>1</sup>H nmr (DMSO-d<sub>6</sub>) 7.9(s, 2H), 7.2(s, 2H), 2.6(s, 6H) δ. <sup>13</sup>C{<sup>1</sup>H} nmr 16.5, 115, 130 and 139 δ. The side product 2,6-dimethyl benzoquinone was obtained as light yellow solid having m.p. 71-73<sup>0</sup>C (reported 71-73<sup>0</sup>C).

## Reactions of aniline

A well stirred reaction mixture containing aniline (930mg, 10mmol) *cis*-bis glycinatocopper(II) monohydrate (50 mg, 0.225mmol) and hydrogen peroxide (1 cm<sup>3</sup>, 30%) was stirred at room temperature for 4hrs. The reaction mixture turned black. On concentration of the reaction mixture under vacuum at room temperature gave black paste. The paste was washed with petroleum ether (2X15cm<sup>3</sup>) (60-80<sup>0</sup>C). The residue (368mg, 40%) thus obtained was purified by column chromatography to two major components of polyaniline **A** and **B** in ratio (2:1.6).

The analytical and spectral data of polyaniline **A**; Anal. found C, 73.97, H, 5.38, N, 10.87 anal. calcd for [(-C<sub>6</sub>H<sub>4</sub>N-)<sub>5</sub>(-C<sub>6</sub>H<sub>4</sub>O) 0.4{Cu(OH)<sub>2</sub>}]<sub>n</sub> C, 73.02, H, 4.62, N, 11.35. <sup>1</sup>H nmr (CDCl<sub>3</sub>) 5.8(s), 6.8(d, J=8Hz), 6.6-7.8(m), 8.7(s), 9.4(s) δ; IR (neat film) 3341(bs), 3072(m), 2931(m), 1641(s), 1601(s), 1507(s), 1447(s), 1393(m), 1299(m), 761(s), 694(s) cm<sup>-1</sup>. MALDI mass, (m/e) 1438 to 2134

The analytical and spectral data of polyaniline **B**; Anal. found C, 65.5, H, 4.95, N, 11.86 calcd for [(-C<sub>6</sub>H<sub>4</sub>N-)<sub>5</sub>

$(-C_6H_4O)Cu(OH)_2]_n$  C, 65.27, H, 4.35, N, 10.15  $^1H$  nmr  
( $CDCl_3$ ) 6.8-7.8(m), 8.4(s), 8.7(s)  $\delta$ .  $^{13}C\{^1H\}$  nmr( $CDCl_3$ ) 181,  
154, 149, 144.5, 138, 129.5, 129, 125, 124, 122.5 and 120  $\delta$ . IR (neat  
film) 3308(bs), 2925(s), 2851(m), 1689(s), 1608(s), 1541(s), 1501(s),  
1313(s), 762(s), 702(s)  $cm^{-1}$ . MALDI mass, (m/e) 1491-2503.

#### Reactions of 1,4-diamino benzene:

To a well stirred solution of 1,4-diaminobenzene (653mg, 6mmol), *cis*-bisglycinato copper(II) monohydrate (50mg, 0.23mmol) in water ( $1cm^3$ ) hydrogen peroxide (30%, 100Vol,  $1cm^3$ ) was added in portion and the reaction mixture was stirred continuously for 6 hrs over a water bath at  $30^{\circ}C$ . The black solution was cooled and water was removed under reduced pressure. The paste obtained was washed with cold water ( $2 \times 10cm^3$ ) followed by washing with a mixed solvent of ethylacetate (10%) in petroleum ether ( $10cm^3$ ) to obtain a black powder. Yield 292mg. Elemental anal calcd. for  $[(C_6H_4ON)(-C_6H_4N_2-)]_{12}(C_6H_6N_2)]_2Cu(OH)_2$ ; C, 60.54, H, 3.75, N, 22.83 found C, 59.79, H, 5.16, N, 21.57.  $^1H$  NMR ( $CDCl_3$ ) 7.5(s,

0.1H), 6.6 (s, 8H), 6.0(s, 3H), 5.7(s, 1H), 5.0(s, 3H)  $^{13}\text{C}\{^1\text{H}\}$  NMR (CDCl<sub>3</sub>) 153.31, 148.26, 144.86, 140.02, 122.23, 114.32, 90.63. IR(KBr) 3332(w), 2691(s), 1603(s), 1542(s), 1500(s), 1272(m), 1163(m), 832(s). MALDI mass(m/e) 1470.5, 1327.1, 1220.1, 1103.7, 1042.3, 950.0, 859.9, 843.0, 740.4, 725.5, 701.8, 634.8, 545.3, 513.4, 434.9, 424.8, 409.8.

### Preparation of hydroquinone aggregate

To a solution of *cis*-bis glycinatocopper(II) monohydrate (20mg, 0.1mmol), finely ground hydroquinone (660mg, 6mmol) in water(1ml) in a flask, hydrogen peroxide was added (1ml, 30%). An exothermic reaction took place to give a dark brown colour. The colour intensified with time and the reaction mixture was allowed to stir for 2 hrs. The solvent was removed under reduced pressure and the residue was washed with petroleum ether (4 X 20ml) to obtain a black solid. Yield 90 %. Elemental anal found C, 53.24, H, 4.3, N, 0.81, Cu 3.82, calc. for [C<sub>6</sub>H<sub>6</sub>O<sub>2</sub>.H<sub>2</sub>O]<sub>11</sub> [(C<sub>2</sub>H<sub>4</sub>O<sub>2</sub>N)(C<sub>6</sub>H<sub>5</sub>O<sub>2</sub>)(H<sub>2</sub>O))Cu]

C, 53.06, H, 4.42, N, 0.83 Cu, 3.79. The  $^1\text{H}$  nmr (DMSO-d<sub>6</sub>)

6.5 (s, 4H), 8.6(s, 2H)  $\delta$   $^{13}\text{C}\{^1\text{H}\}$  nmr (DMSO-d<sub>6</sub>) 116,150  $\delta$ . GPC

(DMF)  $M_n$  3350,  $M_w$  3362; IR (neat film) 3297 (bs), 1729(m), 1618(s), 1593(s), 1357(s), 1214(s), 1090(s), 835(s), 742 (s)  $\text{cm}^{-1}$ .

### Quinhydrone from hydroquinone

*Cis*-bis glycinato copper(II) monohydrate (20mg, 0.1mmol) and finely ground hydroquinone (660mg, 6mmol), *t*-butyl hydroperoxide (1ml, 70%) were mixed together in a flask and stirred at room temperature. The colour intensified with time and the reaction mixture was allowed to stir for 2 hrs. The reaction mixture is extracted with dichloromethane (2X 100ml) and concentrated to obtain the quinhydrone (540 mg). The sample was characterised by comparing its nmr, IR with an authentic sample. Elemental anal found C, 66.12 H, 4.54, calcd for  $(\text{C}_6\text{H}_6\text{O}_2)(\text{C}_6\text{H}_4\text{O}_2)$  C, 66.06, H, 4.59.

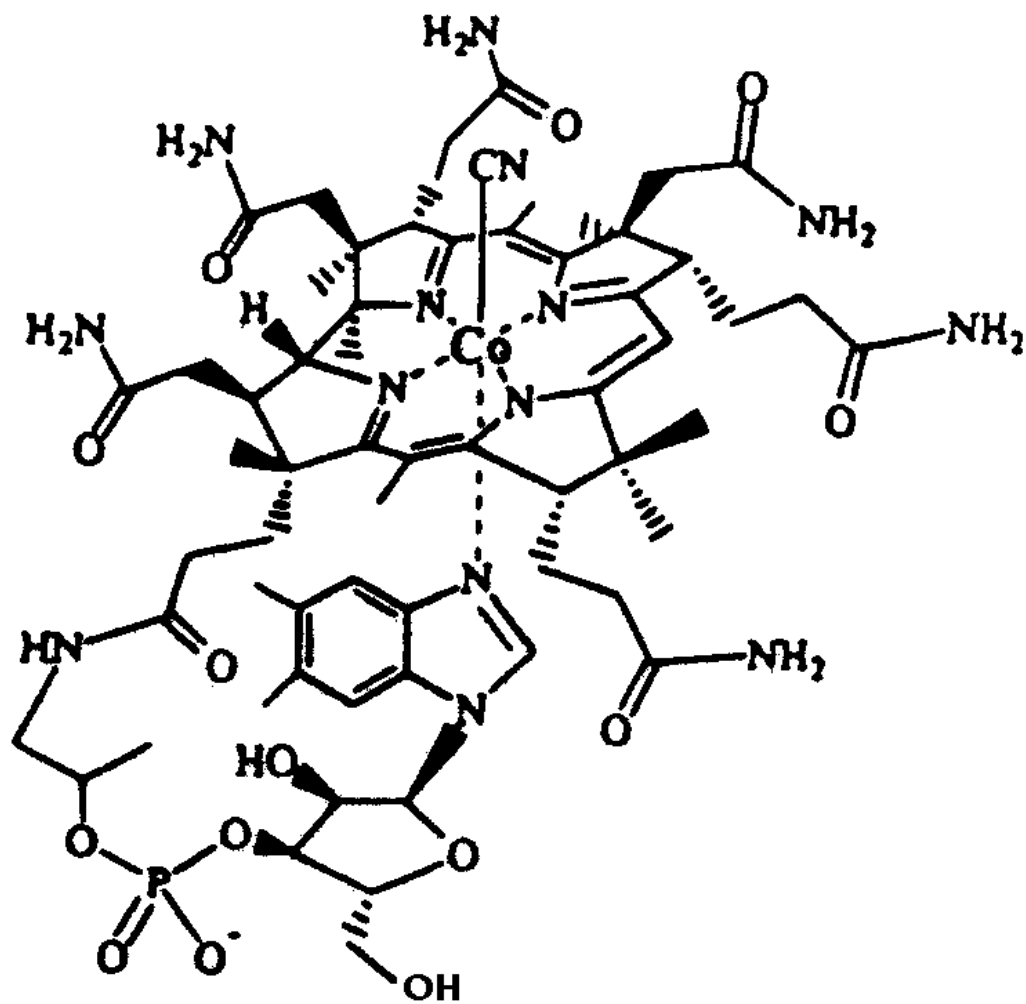
### Reaction of oxime

A mixture of oxime (0.810g, in case of *p*-methyl benzaldoxime 6mmol) and *cis* bis glycinatocopper(II) monohydrate (50mg, 0.23mmol) was taken in a round bottom flask in acetonitrile (5ml). Hydrogen peroxide (30%, 100vol,  $1\text{cm}^3$ ) was added to this solution and the resulting mixture was allowed to stir at room temperature for 6 hrs. The solvent from the reaction mixture was removed under reduced pressure and the product obtained was then

washed with petroleum ether (3x25 ml). Finally the product was dried over vacuum. The product then was purified through liquid chromatography. The yield of different isolated products were as follows: in case of the reaction of *p*-methyl benzaldoxime the products were *p*-methylbenzoic acid 62 % (m.p. 178<sup>0</sup>C), *p*-methyl benzaldehyde 12 % and *p*-methyl benzamide 5.6 % (m.p.159<sup>0</sup>C). The products were further characterised by recording nmr, IR and mass spectra.

Similarly, *p*-tolyl benzaldimine(1.17g in; 6mmol ) was mixed with *cis*-bis-glycinato copper(II) monohydrate(50mg, 0.23mmol) in a round bottom flask in acetonitrile(5 ml ). Hydrogenperoxide (30%, 100Vol, 1cm<sup>3</sup>) was added to this solution and the reaction mixture was stirred at room temperature for 6 hours. The solvent was removed under reduced pressure and the product was washed with petroleum ether as mentioned above. The products of the reaction were purified and isolated by column chromatography. The products were characterised by recording nmr, IR and melting point and then comparing with authentic sample. The yields of different isolated products were as follows: benzoic acid 76% and benzaldehyde 6 %.





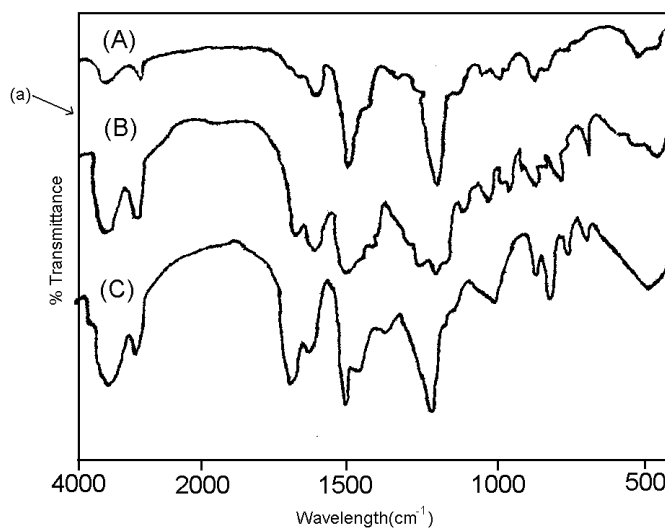
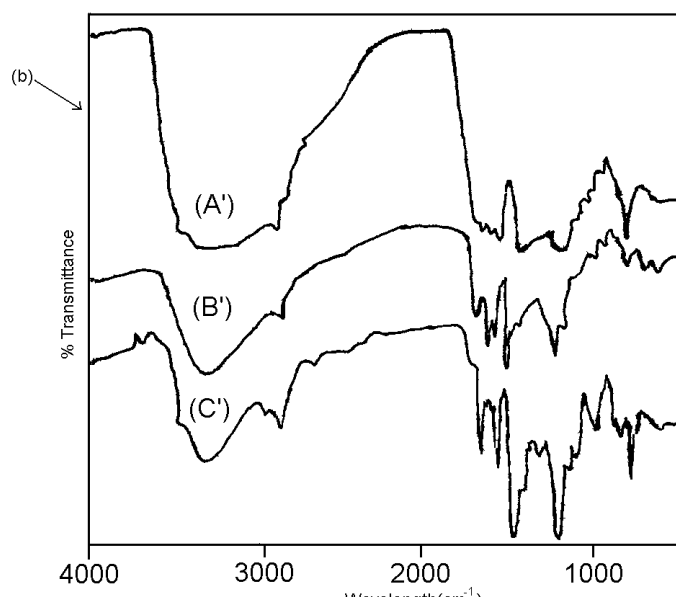
Vitamin B<sub>12</sub>

Fig. 2.1









phenylene ether) (C) poly (p-methyl phenylene ether) obtained by SBP catalysed reaction of three different cresols . (b) IR spectra of (A') poly (*o*-methyl phenylene ether) (B') poly(*m*-methyl phenylene ether) (C') poly (p-methyl phenylene ether) obtained by 2.V catalysed reactions of three different cresols.



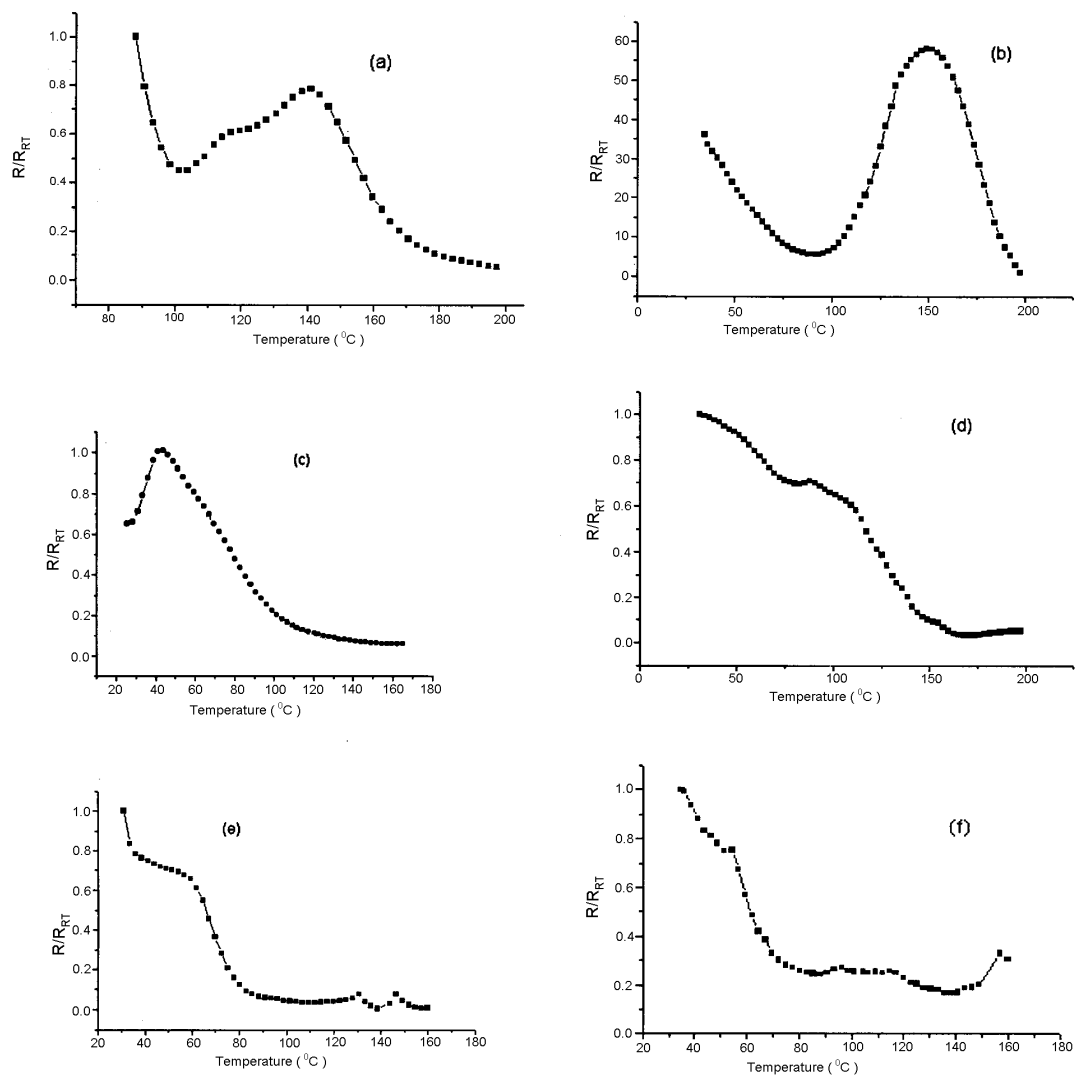


Fig. 2.39 : Resistance vs temperature profile of (a) poly (*o*-methyl phenylene ether)(b) oligomer 1,4-phenylenediamine (c) polyphenylene

ether (d) poly (*m*-methyl phenylene ether) (e) poly (*p*-methyl phenylene ether ) (f) polyaniline prepared by catalytic reaction of **2.V**



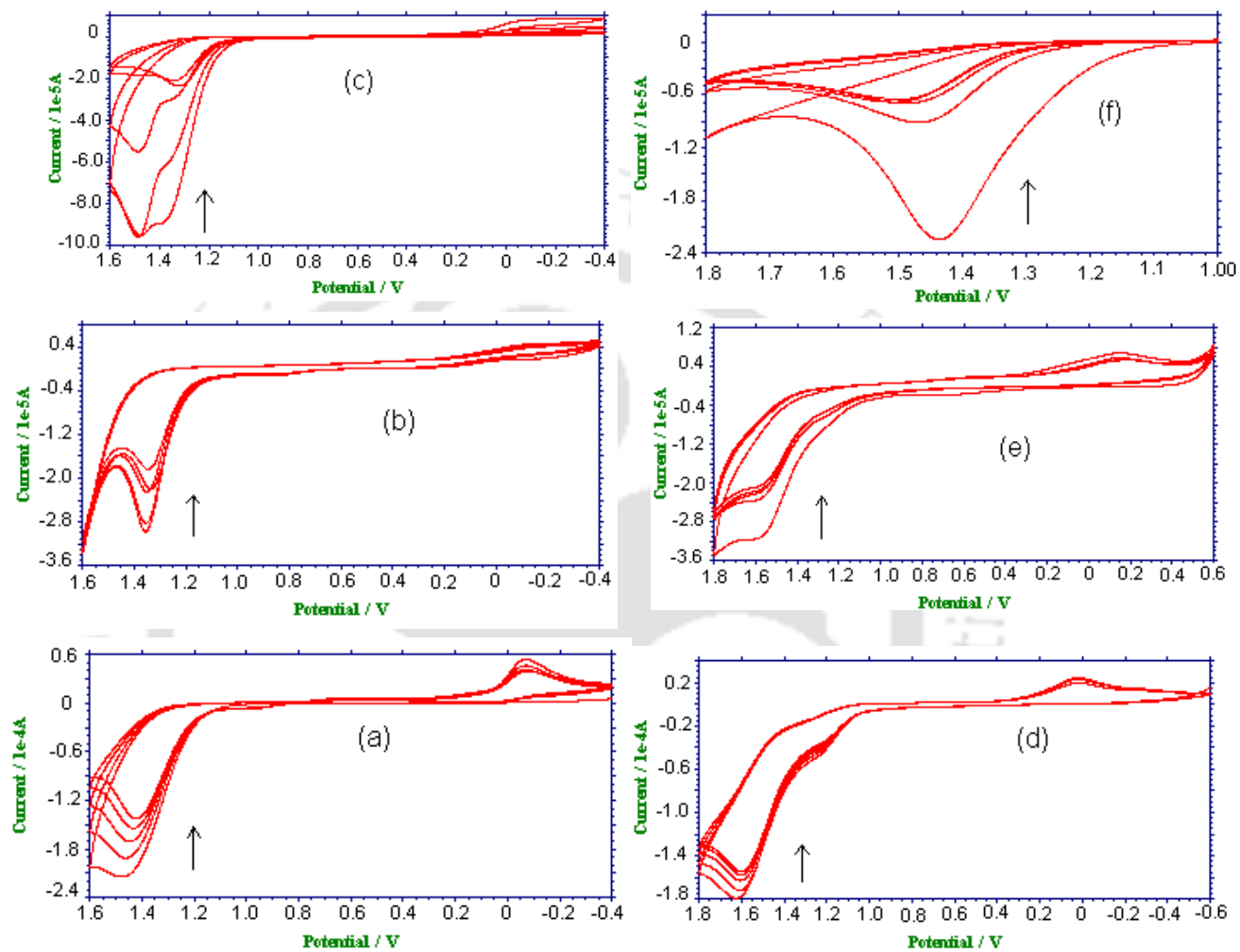


Fig. 2.40 : Scan dependency of the cyclic voltamogram of (a) *o*-cresol (b) *m*-cresol (c) *p*-cresol (d) poly (*o*-methyl phenylene ether) (e) poly (*m*-methyl phenylene ether) (f) poly (*p*-methyl phenylene ether)

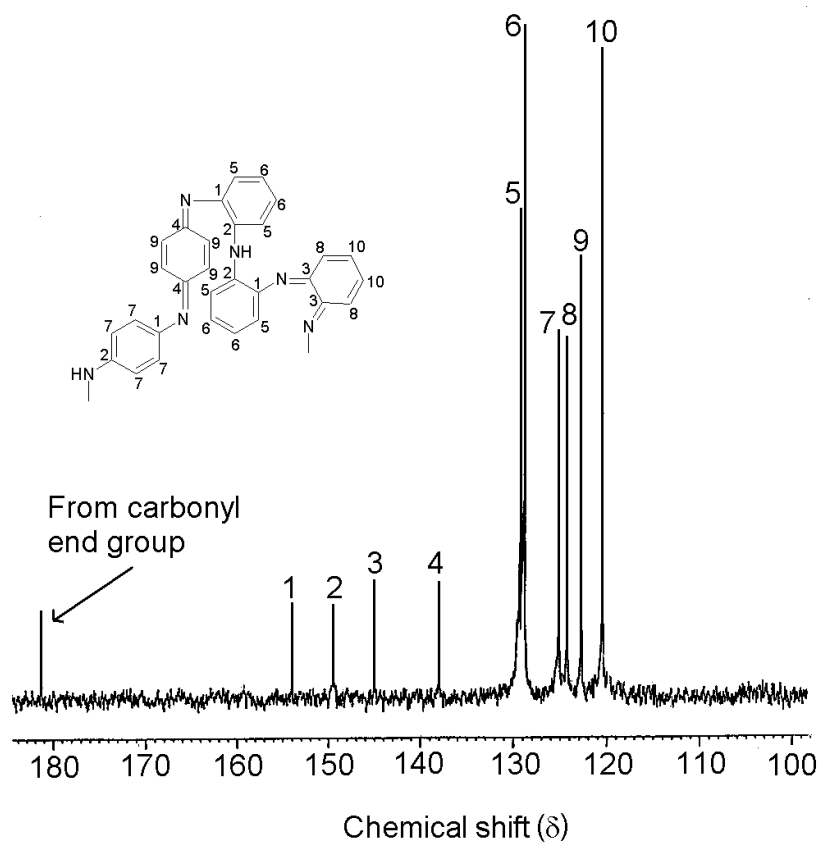


Fig. 3.4  $^{13}\text{C}\{^1\text{H}\}$  nmr spectra of polyaniline

## Research Publications

1. Recycling of oxygen liberated from decomposition of hydrogen peroxide during cobalt(II) catalysed oxidation of benzylalcohol  
A. Puzari, L. Nath, J. B. Baruah, *Indian J. Chem.* **37A** (1998) 723
2. Thermoelectric switch from anilinic compounds  
A. Puzari, J.G. Handique, A. Purkayastha, J. B. Baruah, A. Srinivasan, *Indian J. Chem.* **38A** (1999) 521
3. Cobalt(II) diacetylmonoxime complex catalysed oxidative coupling reaction of few aromatic compounds  
A. Puzari, J. B. Baruah, *J. Mol. Catal.* **153** (2000) 1
4. Hydroquinone aggregates as thermoelectric switch  
A. Puzari, A. Srinivasan, J. B. Baruah, *React. Funct. Polym.* **44** (2000) 201
5. Copper(II) catalysed reactions of activated aromatics  
A. Puzari, J. B. Baruah, *J. Org. Chem.* **65** (2000) 2344
6. Synthesis, characterization and physicochemical properties of polyphenols prepared by Cobalt(II) catalysed oxidative polymerisation  
A. Puzari, J. B. Baruah, *React. Funct. Polym.* **46** (2000) 701
7. Oxidative oligomerisation of 1,4-diaminobenzene by Copper and Cobalt catalyst  
A. Puzari, J. B. Baruah, *React. Funct. Polym.* **47** (2001) 147

## References:

1. *Inorganic Chemistry* by J. E. Huheey, E. A. Keiter, R. L. Keiter; 4<sup>th</sup> edition, Harper Collins, New York, 1993
2. *Organic Chemistry* by I.L.Finar ; Vol.II, 25<sup>th</sup> edition, ELBS, London, 1986
3. *Metal-Catalyzed Oxidation of Organic Compounds* by RA. Sheldon, J.K. Kochi; Academic Press, New York, 1981
4. *Physical Chemistry* by I. N. Levine, 4<sup>th</sup> edition, Mcgraw- Hill, New-York. 1995
5. *Phase Transfer Catalysis* by E.V.Dehmlow, S.S. Dehmlow ; 3<sup>rd</sup> edition, VCH, New-York 1993
6. *Catalysis of Organic Reactions by Supported Inorganic Reagents* by J. H. Clark , VCH, New-York, 1994
7. J. Muzart, *Chem. Rev.* **92** (1992) 113
8. *Activation of saturated hydrocarbons by transition metal complexes* by A.E. Shilov, D. Reidel Publishing Co., Lancaster 1984
9. *Principles of organic synthesis* by R.O.C.Norman, J.M.Coxon, 3<sup>rd</sup> edition, Oxford University press, Oxford, 1995

10. *Organic chemistry*, by P.Y. Bruice, 2<sup>nd</sup> edition; Prentice-Hall International, 1998
11. R.F. Moreira, P.B. When, D.Saes ; *Angew. Chem. Int. Ed. Engl.* **39** (2000) 1618
12. (a) W.Zhang, J.L. Loebach., S.R. Wilson; E.N. Jacobsen ; *J. Am. Chem. Soc.* **112** (1990) 2801 (b) E. N. Jacobsen in *Catalytic Asymmetric synthesis*, I.Ojima, ed. VCH, New-York, 1993
13. (a) D.A. Annis, E.N. Jacobson ; *J. Am. Chem. Soc.* **121** (1999) 4147 (b) S. Peukert, E.N. Jacobsen, *Org. Lett.* **1** (1999) 1245
14. S. Ogunwumi, T. Bein, *J. Chem Soc. Chem. Commun.* (1997) 901
15. S.R. Thomas; K.D. Janda, *J. Am. Chem. Soc.* **122** (2000) 6929
16. H. B. Kagan in *Catalytic asymmetric synthesis*, I. Ojima, ed. pp203, VCH, New-York, 1993
17. T. Katsuki, K.B. Sharpless, *J. Am. Chem. Soc.* **102** (1980) 5974
18. (a) W. Zhang, J. L. Loebach, S. R. Wilson, E. N. Jacobsen, *J. Am. Chem. Soc.* **112** (1990) 2801 (b) E. N. Jacobsen in *Catalytic asymmetric synthesis*, I. Ojima, ed. Chapter 4.2, VCH, New York, 1993,
19. H. J. H. Fenton, *J. Am. Chem. Soc.* **65** (1894) 899

20. (a) C. Walling, *Acc. Chem. Res.* **8** (1975) 125 (b) H. E. de la Mare, J. K. Kochi, F. F. Rust, *J. Am. Chem. Soc.* **85** (1963) 1437
21. D. H. R. Barton, J. Boivin, M. Gastinger, J. Morzycki, S. Motherwell, W. B. Motherwell, N. Ozabalik, K. M. Schwartzentruber ; *J. Chem. Soc. Perkin Trans. I* (1986) 947
22. (a) K. B. Sharpless, W. Amberg, M. Beler, H. Chen, J. Hartung, Y. Kawanami, D. Lubben, E. Manoury, Y. Ogino, T. Shibata, T. Ukita ; *J. Org. Chem.* **56** (1991) 4585. (b) I. Marko, E. M. Jacobsen, W. S. Mungall, G. Sohrodev, K. B. Sharpless, *J. Am. Chem. Soc.* **110** (1988) 1968 (c) J. S. M. Wai, I. Marko, J. S. Srengsen, M. G. Finn, E. N. Jacobsen, K. B. Sharpless, *J. Am. Chem. Soc.* **111** (1989) 1123. (d) K. Tomioka, T. Nakajima, K. Koga, *Tetrahedron Lett.* **31** (1990) 1741
23. H. C. Kolb, M. S. Vannieuwehze, K. B. Sharpless, *Chem. Rev.* **94** (1994) 2483
24. (a) O. Reiser, *Angew. Chem. Int. Ed. Engl.* **35** (12) (1996) 1308 (b) K. L. Reddy, K. B. Sharpless, *J. Am. Chem. Soc.*, **120** (1998) 1207
25. A. Stutz, *Angew. Chem. Int. Ed. Engl.* **26** (1987) 320
26. (a) O. P. Dhingra in *Oxidation in Organic Chemistry*, W. S. Trahanovsky, ed. Vol. 5, Part D, Chapt.3, p 207, Academic Press,

- New-York, 1982 (b) *Glycopeptide antibiotics*, R. Nagarajan ed. Marcel Dekker : New-York 1994.
27. K. Sonogashira in *Comprehensive organic synthesis*, B M. Trost, ed. Vol.3, p551, Pergamon Press, New York, 1991
28. A. S. Hay, *J. Org. Chem.*, **27** (1962) 3320,
29. G. M. Whitesides, C. P. Casey, *J. Am. Chem. Soc.* **88** (1966) 4541
30. (a) *Organometallic mechanisms and catalysis* by J. K. Kochi, Academic press, New York, 1987 (b) *Paladium reagents in organic syntheses* by R. F. Heck, Academic press, New York, 1985 (c); *Organotransition metal Chemistry, Application to organic syntheses* by S. G. Davies; Pergamon Press, Oxford, 1982
31. Y. Ito, M. Inoue, M. Murakami, *Tetrahedron Lett.* **29** (1988) 5379,
32. H. Konishi, C. Matsumura, T. Okano, J. Kiji, *J. Organomet. Chem.* **364** (1989) 245
33. Q. Liu, D. J. Barton, *Tetrahedron Lett.* **38** (1997) 4371
34. R. Rossi, A. Carpita, C. Bigelli, *Tetrahedron Lett.* **26** (1985) 523
35. Y. Hatanka, T. Hiyama, *J. Org. Chem.* **53** (1988) 920
36. Y. Nishihara, K. Ikegashira, K. Hirabayashi, J. Ando, A. Mori, T. Hiyama *J. Org. Chem.* **65** (2000) 1780

37. I. Malner, C. J. Sih, *Tetrahedron Lett.* **41** (2000) 1907
38. B. M. Chaudhuri, P. N. Reddy, *J. Chem. Soc., Chem. Commun.* (1993) 405
39. *Principles and applications of organotransition metal chemistry* by J. P. Collman, L. S. Hegedus, University Science, Mill Valey, 1980
40. C. Blom, G. Schingloft, K. Weickhardt, *Angew. Chem. Int. Ed. Engl.* **33** (1994) 1843
41. *Bioinorganic chemistry* by I. Bertini, H.B. Gray, S.J. Lippard, J.S. Valentine, Viva books pvt. Ltd. New Delhi, 1998
42. *Basic inorganic chemistry* by F. A. Cotton, G. Wilkinson 5<sup>th</sup> edition, John Wiley, New-York, 1988
43. J. S. Dordick, M. A. Marletta, A. M. Kilbanov, *Biotechnol. Bioeng.* **30** (1987) 31
44. W. Liu, J. Kumar, S. Tripathy, K. J. Senecal, L. Samuelson, *J. Am. Chem. Soc.* **121** (1999) 71
45. J. A. Halfen, B. A. Jazdzewski, S. Mahapatra, L. M. Berreau, E. C. Wilkinson, L. Que Jr. W. B. Tolman ; *J. Am. Chem. Soc.* **119** (1997) 8217

46. (a) J. W. Whittaker in *Metalloenzymes involving amino acid residue and related radicals* H. Sigel, A. Sigel, eds. Vol. 30, p315, Marcel Dekker, New York, 1994 (b) P. F. Knowles, N. Ito in *Perspectives in bio-inorganic chemistry*, Vol.2, p207, Jai Press Ltd., London, 1994 (c) N. Ito, S. E. V. Phillips, C. Stevens, Z. B. Ogel, M. J. McPherson, J. N. Keen, K. D. S. Yadav, P. F. Knowles, *Nature* **350** (1991) 87 (d) N. Ito, S. E. V. Phillips, C. Stevens, Z. B. Ogel, M. J. McPherson, J. N. Keen, K. D. S. Yadav, P. F. Knowles, *Faraday. Discuss.* **93** (1992) 75 (e) N. Ito, S. E. V. Phillips, K. D. S. Yadav, P. F. Knowles, *J. Mol. Biol.* **238** (1994) 794.
47. *Bioinorganic catalysis* by J. Reedijk, p30, Marcel Dekker, New York, 1993
48. *Dioxygen activation and homogeneous catalytic oxidation* by L. I. Simandi, Elsevier, Amsterdam, 1991
49. D. Mansui in *Coordination chemistry of metalloenzymes in hydrolytic and Oxidative process* I. Bertini, R. S. Drago, C. Luchina, eds. p243, Reidel, Dordrecht, 1982

50. J.E. Lyons, C-Y. Hsu in *Biological and inorganic copper chemistry*, K.D. Karlin, J. Zubieta eds. vol 2, Adenine, Guilderland, New-york, 1986
51. K. D. Karlin, Y. Gultneh, T. Nickolson, J. Zubieta, *Inorg. Chem.* **24** (1985) 3725
52. S. E. W. Williams, C. A. James, S. Vrice, M. Saraste, P. Lappalainen, J. Van der Oost, M. Fabian, G. Palmer, W. H. Woodruff, *J. Am. Chem. Soc.*, **118** (1996) 3986
53. E. I. Solomon, U. M. Sundaram, T. E. Machonkin, *Chem. Rev.* **96** (1996) 2563
54. E. Pidcock, S. Debeer, H. V. Obias, B. Hedman, K. O. Hodgson, K. D. Karlin, E. I. Solomon, *J. Am. Chem. Soc.* **121** (1999) 1870
55. M. G. M. Tromp, G. Olafsson, B. E. Krenn, R. Wever, *Biochim. Biophys. Acta.* 1040, 192.
56. *Biopolymers* by M. Hofrichter, A. Steinbuchel, Vol I, p153, Wiley-VCH, New-York, 2001
57. E. De Boer, H. Plat, M. G. M. Tromp, R. Wever, M. C. Franssen, H. C. Van der plas, E. M. Meijer, H. E. Schoemaker, *Biotechnol. Bioeng.*, **30** (1987)607

58. R. F. Moreira, P. M. When, D. Sames, *Angew. Chem. Int. Ed. Engl.* **39** (2000) 1618
59. K. B. Sharpless, T. R. Verhoeven, *Aldrichimica Acta* **12** (1979) 63
60. D.H.R. Barton, B. Hu, *Tetrahedron* . **52** (1996) 10313
61. (a) F. Haber and J.J. Weiss, *Proc. Roy. Soc. London, Ser. A.*, **147** (1934) 332 (b) J. H. Merz and W. A. Waters, *Discuss. Faraday Soc.* **2** (1947) 179
62. A. Marsella, S. Agapakis, F. Pinna, G. Strukul, *Organometallics* **11** (1992) 3578
63. K.D. Karlin, J.C. Hayes, Y. Gultneh, R.W. Cruse, J.W. McKown, J.P. Hutchinson, J.Zubieta, *J. Am. Chem Soc.* **106** (1984) 2121
64. M. E. Snook and G. A. Hamilton, *J. Am. Chem. Soc.*, **96** (1974) 960
65. J. M. Thomas, R. Raja, G. Sankar, R. G. Bell, *Nature*, **398** (1999) 227
66. R. Raja, J. M. Thomas, *J. Chem Soc. Chem. Commun.* (1998) 1841
67. R. E. White, M. J. Coon, *Annu. Rev. Biochem.*, **49** (1980) 315
68. E. J. Mckenna, M. J. Coon, *J. Biol. Chem.* **245** (1970) 3882

69. D. H. R. Barton, D. Doller in *Dioxygen Activation and Homogeneous Catalytic Oxidation*, L.I. Simandi ed. Elsevier Science, Amsterdam, 1991
70. I. Tabushi, T. Nakajima, K. Seto; *Tetrahedron Lett.* **21** (1980) 2565
71. D. E. Williams, S. E. Hale, R.T. Okita and B. S. Silermasters, *J. Biol. Chem.* **259** (1984) 14600
72. (a) J. J. Grovers, S. Krichnan, G. E. Averil and T. E. Nemo, *Adv. Chem. Ser.* **191** (1980) 277 (b) I. Tabushi, N. Koga, *Adv. Chem. Ser.* **191** (1980) 291.
73. *Highlights of Organic Chemistry* by W. J. L. Noble, p 878, Marcel Dekker, New-York, 1974
74. M. Hartmann, S. Earnst, *Angew. Chem. Int. Ed. Engl.* **39** (2000) 888
75. M. Enomoto, T. Aida, *J. Am. Chem. Soc.* **121** (1999) 874
76. N. N. Murthy, M. Mahroof-Tahir, K. D. Karlin, *J. Am. Chem. Soc.*, **115** (1993) 10433
77. *Modern methods of organic synthesis* by W. Carruthers; 3<sup>rd</sup> edition, Cambridge University press, Oxford 1987
78. H. Mimoun, M. Mercedes, P. Machirant, I. S. deRoch, *J. Am. Chem. Soc.* **100** (1978) 5437

79. F. Igersheim and H. Mimoun, *J. Chem. Soc., Chem. Commun.* (1978) 559
80. (a) A. Onopchenko, J. G. D. Schulz, *J. Org. Chem.* **38** (1978) 909  
(b) A. Onopchenko, J. G. D. Schulz, *J. Org. Chem.* **38** (1978) 3729
81. (a) K. Bowden, T. G. Heilbron, E. R. H. Jones, B. C. L. Weedon, *J. Chem. Soc.* (1946) 39 (b) A. Bowers, T. G. Halsall, E. R. H. Jones, A. J. Lemin, *J. Chem. Soc.* (1953) 2548.
82. (a) J.C. Collins, W. W. Hess, F. J. Frank, *Tetrahedron Lett.*, (1968) 3363 (b) R. Ratcliffe, R. Rodehorst, *J. Org. Chem.* **35** (1970) 4000 (c) K.B. Sharpless, K. Akashi, *J. Am. Chem. Soc.* **97** (1975) 5927.
83. E. J. Corey, A. Suggs ; *Tetrahedron Lett.* (1975) 2647.
84. A. Riahi, F. Henin, J. Muzart, *Tetrahedron Lett.* **40** (1999) 2303
85. W. Adam, F. G. Gelacha, C. R. Saha-Moller, V. R. Stegmann ; *J. Org. Chem.* **65** (2000) 1915
86. *Methods for the oxidation of organic compounds, alcohols, alcohol derivatives, alkyl halides, carbonyl compounds, hydroxyarenes and aminoarenes* by A. H. Haines, Chapter 2, Academic Press, London, 1988

87. S. Campestrini, G. D. Furia, G. Modena, F. Novelle in *Dioxygen activation and homogeneous catalytic oxidation*, p375, Elsevier, Amsterdam, 1991
88. S. Itoh, M. Taki, H. Nakao, P.L. Holland, W. B. Tolman, L. Que. Jr., and S. Fukuzumi, *Angew. Chem. Int. Ed. Engl.*, **39** (2000) 398
89. B. D. Scott, K. T. Carron, C. A. Norlund, P. A. Goodson, A. K. Powel, *Organometallics* **13** (1994) 1355
90. E. G. Samsel, J. K. Kochi, *Inorg. Chem.* **25** (1986) 2450
91. D. A. Peaks, M. L. Gross, D. P. Ridge, *J. Am. Cem. Soc.* **106** (1984) 4307
92. M. Anton, N. Clos, G. Muller, *J. Organomet. Chem.* **267** (1984) 213
93. J. K. Kochi, *Pure Appl. Chem.* **4** (1971) 377
94. R. A. Sheldon, J. K. Kochi, *Adv. Catal.* **25** (1976) 272
95. C. M. Park, D. G. Micklewright, *U. S. Patent*, **4 (053)** (1977) 506
96. (a) G. Centi, F. Trifiro, J. R. Ebner, V. M. Franchetti, *Chem. Rev.* **88** (1988) 55 (b) B. K. Hodnett, *Catal. Rev. Sci.* **27** (1985) 373
97. (a) M. Hartmann, L. Kevan, *Chem. Rev.* **99** (1999) 635 (b) J. B. Thomas, G. N. Greaves, G. Sankar, P. A. Wright, J. Chen, A. T. Dent, L. Marchese, *Angew. Chem. Int. Ed. Engl.* **33** (1994) 1871

98. W. B. Tolman, *Acc. Chem. Res.* **30** (1997) 227
99. C. X. Zhang, H. S. Liang, E. Kim, Q. F. Gan, Z. Tyeklar, K. C. Lam, A. L. Rheingold, S. Koderli, A. D. Zuberbuhler, K. D. Karlin ; *J. Chem. Soc., Chem. Commun.* (2000) 631
100. S. Olivero, J. P. Rolland E. Dunaoh, *Organometallics* **19** (2000) 2798
101. R. W. Denny, A. Nickon, *Org. React.*, 20 (1973)133
102. T. Matura, A. Horinaka, H. Yoshida, Y. Butsugan, *Tetrahedron*, **27** (1971) 3095.
103. G. O. Schenck, K. Gollnick, G. Buchwald, S. Schroeter, G. Ohloft ; *Ann. Chem.* **93** (1964) 674.
104. *Excited states in organic chemistry* by J. A. Barltop, J. D. Cole, John Wiley, New York, 1978
105. A. I. Scott, *Tetrahedron* **50** (1994) 13315
106. L. G. Mirzilli in *Bioinorganic Catalysis* Ed. J. Reedjik, p 227, Marcel Dekker, New-York, 1993
107. *B<sub>12</sub>*, D. Dolphin ed. vol 1 and 2, Wiley Interscience, New York, 1982

108. L. Walder, G. Rytz, K. Meier, R. Scheffold, *Helv. Chem. Acta.* **61** (1978) 3018
109. *Electroorganic Synthesis* by T. Shono, Academic Press, New-York, 1991
110. (a) G. Pattenden *Chem. Soc. Rev.* **17** (1988) 361 (b) *Dioxygen activation and homogeneous catalytic oxidation* L.I. Shimandi ed. Elsevier, New York, 1991 (c) D.E Cabelli. in *Peroxyl radicals*, Z.B. Alfassi, ed., Wiley, New York, 1997
111. J. Iqbal, B. Bhatia, N. K. Nayyar, *Chem. Rev.* **94** (1994) 519
112. N. Bresciani-Pahor, M. Forcolin, L. G. Marzilli, L. Randaccio, M. F. Summers, P. J. Toscano, *Coord. Chem. Rev.* **63** (1985) 1
113. M. Yamada, K. Araki, S. Shiraishi, *J. Chem. Soc. Perkin Trans.1*, (1990) 2687
114. W. C. Hamilton, *Acta Crystallogr.* **14** (1961) 95
115. A. Chakravorty, *Coord. Chem. Rev.* **13** (1974) 1
116. C. R. H. I. de Joug, H. J. Hageman, G. Hoentgen, W. J. Mijs ; *Org. Synth. Coll. Vol VI* (1998) 412

117. (a) Y. Mashiko, *Jpn Kokai, Tokyo Koho JP* **08**, 208, 813, (1995) (b) M. Ayyagari, J. A. Hkkara, D. L. Kaplan, *Mater. Sci. Eng.* **CC4** (1996) 169
118. (a) A. S. Hay, *Encycl. Polymer. Sci., Technol.*, **10** (1962) 92 (b) H. Nishide, T. Minakata, E. Tsuchida, S. Yamada, *Macromol. Chem.* **183** (1982) 1989 (c) E. Tsuchida, H. Nishide, T. Maekawa, *J. Macromol. Sci. Chem.* **A21** (1984) 1081
119. A. I. Scott, *Quart. Rev.* **19** (1965) 1
120. *Plastic materials* by J.A. Brydson, Newnes-Butterworths, London. 1975
121. '*Frontier Orbitals and Organic Chemical Reactions*' by I. Fleming, Wiley London, 1976, pp195-
122. *Desk references of functional polymers: synthesis and application*, R. Arshady, ed., American Chemical Society, Washington, DC, 1997
123. K. Funabiki, M. Nakamura, M. Tsuriyam, *Netsukokasei Jushi*, **2** (1981) 220
124. T. Matsunaga, H. Daisuka, T. Nakajima, T. Kawagoe, *Polym. Adv. Technol.* **1** (1990) 33

125. E. J. Tsuchida, K. Yamamoto, in *Bioinorganic Catalysis*, J. Reedjik, ed. p29, Marcel Dekker , New-York, 1993
126. Y. Wei, C. Yang and T. Ding, *Tetrahedron Lett.*, **37** (1996) 731
127. S-B Kim, K. Harada, T. Yamamoto, *Macromolecules* **31** (1998) 988
128. A. G. Mac Diarmid, S.L. Mu, M. L. D. Somasiri, W. Wa, *Mol. Cryst. Liq. Cryst.*, **121** (1985) 187
129. D-K. Moon, K. Osakada, T. Maruyama, K. Kubota, T. Yamamoto, *Macromolecules* **26** (1993) 6992
130. A. Mederos, S. Dominguez, R. Hernandez-Molina, J. Sanchiz, F. Brito, *Coord. Chem. Rev.* **193** (1999) 913
131. B. Armitage, P.A. Klekotka, E. Oblinger, D.F. O'Brien, *J. Am. Chem. Soc.* **115** (1993) 7920.
132. D. H. R. Barton, D.R. Hill, B. Hu ; *Tetrahedron Lett.* **38** (1997) 1711
133. A. E. Martell, R.J. Motekaitis, *J. Am. Chem. Soc.* **110** (1988) 8059
134. F. A. Chavez, P. K. Mascharak, *Acc. Chem. Res.* **33** (2000) 539
135. J. Iqbal, B. Bhatia, N. K. Nayyar ; *Chem. Rev.* **94** ( 1994) 519
136. A.E. Martell, *Pure and Appl. Chem.* **60** (1988) 1325

137. F. A. Chavez, P. K. Mascharak, *Acc. Chem. Res.*, **33** (2000) 539
138. F. A. Chavez, C. V. Nguyen, M. M. Olmstead, P. K. Mascharak, *Inorg. Chem.* **35** (1996) 6282
139. F. A. Chavez, J. M. Rowland, M. M. Olmstead, P. K. Mascharak, *J. Am. Chem. Soc.* **120** (1998) 9015
140. C. Giannotti, C. Fontain, A. Chiaroni, C. Riche, *J. Organomet. Chem.* **113** (1976) 57
141. A. Chiaroni, C. Pascard-Billy, *Bull Soc. Chim. Fr.* (1973) 781
142. L. Saussine, E. Brazi, A. Robine, H. Momoun, J. Fischer, R. Weiss, *J. Am. Chem. Soc.* **107** (1985) 3534
143. H. C. Tung, D. T. Sawyer, *J. Am. Chem. Soc.* **112** (1990) 8214
144. H. Gampp, A.D. Zuberbuhler in *Metal ions in biological systems*, H. Sigel, ed. Merceel Dekker, New York, **12** (1981) 133
145. (a) H-J. Kruger, *Angew. Chem. Int Ed. Eng.* **38** (1999) 1433 (b) H. Higashimura, K. Fujisawa, Y. Moro-oka, M. Kubota, A. Shiga, A. Terahara, H. Uyama, S. Kobayashi, *J. Am. Chem. Soc.* **120** (1998) 8529.
146. *Ulmanns encyclopedia of industrial chemical technology*, M.J. Grayson ed., 3<sup>rd</sup> edition, Wiley and Sons, New York 1988

147. F. Garnier, *Angew. Chem. Int. Ed. Engl.* **28** (1989) 513
148. J. Sudhakar Reddy, S. Sivasankar, P. Ratanaswamy, *J. Molecular Catal.* **71** (1992) 373
149. *Introduction to magnetochemistry* by A. Earnshaw, Academic Press, New-York, 1968
150. J. A. Riddick, W. B. Bunger in *Organic solvents-techniques in organic chemistry*, A. Weissberger, ed., vol. 2, Wiley Interscience, New-York, 1970
151. *Vogel's textbook of practical organic chemistry*, Revised by B. S. Furniss, A. J. Hannaford, P. W. G. Smith, A. R. Tatchell, ELBS, London, 1996
152. *Experimental inorganic chemistry* by W. G. Palmer, p530, Cambridge Press, Cambridge, 1954
- 153.(a) K.A.Magnus, H.Ton-That, J.E.Carpenter, *Chem. Rev.* **94** (1994) 727 (b) E.I. Solomon, V.M.Sundaran, T.E.Machonkin, *Chem Rev.* **96** (1996) 2563 (c) D.W.Margernum, W.M.Scheper, M.R. McDonald, F.C. Frederick, L.Wang, H.D.Lee in *Bioorganic chemistry of copper*, K.D. Karlin, Z.Tyeklar, eds. Chapman and Hall, New York, 1993 (d) D.W.Margerum, in *Oxidase and related redox systems*, T.E. King,

- H.S.Mason, M. Morrison, eds., p 193 Pergamon press, Oxford, 1982 (e)
- N. Ito, S.E.V. Phillips, L. Stevens, Z.B. Ogel, P.F. Knowles, *Nature* **350** (1991) 87 (f) A.Sokolowski, J Muller., T.Weyhermuller, R.Schept, P.Hildebrandt, K.Hildenbrand, E.Brothe, K.Weigenhardt, *J. Am. Chem. Soc.* **119** (1997) 8889 (g) P. J.Baesjou, W.L.Driessen, G. Challa, J.Reedijk, *J. Am. Chem. Soc.* **119** (1997) 12590 (h) H. Steinhagen, G.Helmchen ; *Angew. Chem. Int Ed. Eng.* **35** (1998) 2339
154. (a) Z Tyklar, K.D.Karlin, *Acc. Chem. Res.* **22** (1989) 241 (b) H.Steinhagen, G.Helmchen ; *Angew. Chem. Int. Ed. Eng.* **35** (1996) 2339
155. E. Pidcock, S.Debeer, H.V.Obias, B.Hedman, K.O.Hodgson, K.D.Karlin, E.I.Solomon, *J. Am. Chem. Soc.* **121** (1999) 1870
156. E.Lamour, S.Routier, J-L.Bernier, J-P.Catteau, C.Bailly, H.Vezin, *J. Am. Chem. Soc.* **121** (1999) 1862
157. (a) Y.Wang, J.L. Dubois, B.Heman, K.O.Hodgson, T.P.D.Stack, *Science* **279** (1998) 537 (b) P. Chaudhuri, M.Hess, U.Florke, K. Wieghardt , *Angew. Chem. Int. Ed. Eng.* **37** (1998) 2217 (c) H. J. Kruger, *Angew. Chem. Int. Ed. Eng.* **38** (1999) 1433

158. H. J. Kruger, *Angew. Chem. Int. ed. Eng.* **38** (1999) 627.
159. (a) N. Ito, S. E. V. Phillips, C. Stevens, Z. B. Ogel, M. J. Mcpherson, J. N. Keen, K. D. S. Yadav, P. F. Knowles, *Nature* **350** (1991) 87 b) N. Ito, S. E. V. Phillips, K. D. S. Yadav, P. F. Knowles, *J. Mol. Biol.* **238** (1994) 794
- 160(a) A.S.Hay, H.S.Balchand, G.F.Endrer, J.E.Eustance, *J.Am. Chem. Soc.*, **81** (1959) 6335 (b) A. J.Schoten, D.Noordergraaf, A.P.Jekel, G.Challa, *J. Mol. Catal.* **5** (1979) 5331
161. K.D.Karlin, Y. Gultneh, in *Progress in inorganic chemistry*, S. J. P. Lippard ed. John Wiley, New York, **35** (1987) 219
- 162 (a) O.Reinaud, P,Capdevielle M.Maumy; *J. Chem. Soc. Chem Commun.* (1990) 566 (b) P.Capdivielle, D.Sparfel, J. B Lafort, N.K.Cuong, M Maumy, *J. Chem. Soc. Chem. Commun.* (1990) 565
- 163 (a) A.G. MacDiarmid, J.C.Chian, M.Halporn, W.S.Huang, S.L Mu., N.L.Somasiri, W.Wu, S.I.Yaniger, *Mol. Cryst. Liq. Cryst.* **121** (1985)
173. (b) S-B Kim, K.Harada, T. Yamamoto, *Macromolecules* **31** (1998) 988 (c) D.C. Trivedi, *Bull. Mater Sci.* **22** (1999) 447

164. J. L. Pierre, *Chem. Soc. Rev.* **29** (2000) 251
165. A. Tainer, E. D. Getzoff, J. S. Richardson, D. C. Richardson, *Nature*, **306** (1983) 284
166. J. R. Sorenson, *Prog. Med. Chem.* **26** (1989) 437
167. Xin X-Q, Zheng L-M, *J. Phys. Chem. Solid*, **58** (1997) 951
168. (a) D.D. McNicol in *Inclusion compounds*, J.L. Atwood, J.E.D.Davies eds., vol 2, pp1-45, Academic Press, London 1984
169. K. S. Alva, J. Kumar, K. A. Marx, S. K. Tripathy ; *Macromolecules*, **30** (1997) 4024
170. E Tsuchida, K.Yamamoto, in *Bioinorganic catalysis*, J.Reedjik, ed., pp 29-87, Mercel Dekker, New York, 1993
171. K.Yamamoto, H.Nishida, E.Tscusida, *J. Chem. Soc. Jpn.* (1986) 152
172. (a) J.A. Halfen, S.Mahapatra, E.C.Wilkinson, S. Kareli, V.G. Young, L.Que Jr. A.D. Zuberbuehler, W.B. Tolman, *Science* **271** (1996) 1397(b) S. Mahapatra, J.A. Halfen, E.C. Wilkinson, G. Pan , V.G.Young,

- C.J.Cramer, L. Que Jr., W.B.Tolman, *J. Am. Chem. Soc.* **118** (1996) 11555 (c) E.Pidcock, H.V. Obias, M. Abe, H.C.Liang, K.D. Karlin, E.I. Solomon, *J. Am. Chem. Soc.* **121** (1999) 1299
173. H Gampp., A.D. Zuberbuhler in *Metal ions in biological Systems*, H. Sigel, ed. Mercel Dekker, New York, **12** (1981) 133
174. D.D. McNicol in *Inclusion Compounds*, J.L. Atwood, J.E.D.Davies, eds. vol 2, pp1-45, Academic Press, London 1984.
175. V. Y. Kukushkin, A. J. L. Pombeiro ; *Coord. Chem. Rev.* **181** (1999) 147
176. (a) A.Oikawa, *Biochemistry, Jpn*, **48** (1976) 872. (b) G.A. Swan, *J. Chem. Soc. Perkin 2* (1977) 1346
177. E-I. Ochiai, *Inorg. Nucl. Chem. Lett.* **9** (1973) 987
178. P. Capdevielle, M. Maumy, *Tetrahedron Lett.*, **31** (1990) 3891
179. D. T. Sawyer, J. S. Valentine, *Acc. Chem. Res.*, **14** (1981) 393
180. T. M. Florence, J. L. Stauber, K. J. Mann, *J. Inorg. Biochem.* **24** (1985) 243

181. Z. Tyeklar, K. D. Karlin, *Acc. Chem. Res.* **22** (1989) 241
182. W. B. Tolman, *Acc. Chem. Res.* **30** (1997) 227
183. (a) E. I. Solomon, U. M. Sundaram, T. E. Machonkin, *Chem. Rev.*, **96** (1996) 2563 (b) A. Sanchez-Ferrer, J. N. Rodriguez-Lopez, F. Garcia-Canovas, F. Garcia-Carmona, *Biochim. Biophys. Acta*, **12** (1995) 1. (c) H. H. T. Nguyen, S. J. Elliot, J. H. K. Yip, S. I. Chan, *J. Biol. Chem.*, **273** (1998) 7957
184. P. L. Holland, K. R. Rodgers, W. B. Tolman, *Angew. Chem. Int. Ed. Eng.* **38** (1999) 1139
185. (a) E. I. Solomon, K. W. Penfield, D. E. Wilcox, *Structure and Bonding* **53** (1983) 1 (b) E. I. Solomon, *Pure and Appl. Chem.* **55** (1983) 1069 (c) E. I. Solomon, in *Copper proteins*, T. G. Spiro, ed. p 41, Wiley, New York, 1981
186. A. Volbeda, W. G. J. Hol, *J. Mol. Biol.* **209** (1989) 249.
187. (a) C. J. Cramer, B. A. Smith, W. B. Tolman, *J. Am. Chem. Soc.* **118** (1996) 11283 (b) X. Y. Liu, A. A. Palacios, J. J. Novoa, S. Alvarez ;

*Inorg. Chem.* **37** (1998) 1202 (c) A. Berces, *Inorg. Chem.* **36** (1997)  
4831

188. (a) E.I. Solomon, M.J. Baldwin, P.K. Ross, F. Tuczek, in *Dioxygen activation and homogeneous catalytic oxidation*, , L.I. Shimandi, ed., pp357-365, Elsevier, Amsterdam 1991

189. M. A. Halcrow, *Angew. Chem. Int. Ed. Engl.* **40** (2001) 346

190. M. Scarpa, F. Vianello, L. Signor, L. Zennaro, A. Rigo, *Inorg. Chem.* **35** (1996) 5201

191. T. Sakurai, *Acta. Cryst.* **19** (1965) 320

192. J.C. Ma, D.A. Dougherty, *Chem. Rev.* **97** (1997) 1303

